INFORMATION TO USERS

This manuscript has been reproduced from the microfilm master. UMI films the text directly from the original or copy submitted. Thus, some thesis and dissertation copies are in typewriter face, while others may be from any type of computer printer.

The quality of this reproduction is dependent upon the quality of the copy submitted. Broken or indistinct print, colored or poor quality illustrations and photographs, print bleedthrough, substandard margins, and improper alignment can adversely affect reproduction.

In the unlikely event that the author did not send UMI a complete manuscript and there are missing pages, these will be noted. Also, if unauthorized copyright material had to be removed, a note will indicate the deletion.

Oversize materials (e.g., maps, drawings, charts) are reproduced by sectioning the original, beginning at the upper left-hand corner and continuing from left to right in equal sections with small overlaps. Each original is also photographed in one exposure and is included in reduced form at the back of the book.

Photographs included in the original manuscript have been reproduced xerographically in this copy. Higher quality 6" x 9" black and white photographic prints are available for any photographs or illustrations appearing in this copy for an additional charge. Contact UMI directly to order.

UMI

A Bell & Howell Information Company
300 North Zeeb Road, Ann Arbor MI 48106-1346 USA
313/761-4700 800/521-0600

DETAILED PERFORMANCE ANALYSIS AND FEASIBLITY ASSESSMENT OF SELF-HEALING LOCAL EXCHANGE RING NETWORKS BASED ON WDM TECHNOLOGY

by

Jin-Yi Pan

A dissertation submitted to the Graduate Faculty in Engineering in partial fulfillment of the requirements for the degree of Doctor of Philosophy, The City University of New York

1997

This manuscript has been read and accepted for the Graduate Faculty in Engineering in satisfaction of the dissertation requirement for the degree of Doctor of Philosophy.

01-06-97
Date

Chair of Examining Committee (Signature)

1/6/97
Date

Executive Officer (Signature)

Prof. Mohamed Ali (EE. Dept. CCNY)

Prof. Leonid Roytman (EE. Dept. CCNY)

Prof. Ibrahim Habib (EE. Dept. CCNY)

Prof. Roger Dorsinville (EE. Dept. CCNY)

Dr. Chinlon Lin (Bellcore)

Supervisory Committee

ABSTRACT

DETAILED PERFORMANCE
ANALYSIS AND FEASIBLITY
ASSESSMENT OF SELF-HEALING
LOCAL EXCHANGE RING
NETWORKS BASED ON WDM
TECHNOLOGY

by

Jin-Yi Pan

Mentor: Prof. M. Ali

Co-Mentor: Dr. Aly Elrefaie

The thesis is a complete component and system level analysis and feasibility study of self-healing local exchange ring networks based on wavelength division multiplexing (WDM) technology. Two type WDM ring have been studied: two-fiber uni-directional path-switched and line-switched ring, four-fiber bi-directional line-switched ring. The scalability, survivability of the WDM optical high-capacity ring networks have been investigated, analyzed and optimized through the computer simulation and modeling. The optimization of critical elements necessary for the implementation of such a optical ring network have been fully investigated. A 21-node uni-directional path switched self-healing ring with an aggregate capacity of 210 Gbit/s (assuming 10 G/s SONET ADMs are used) has been designed without using any external device to

balance the gain flatness. An 11-node full mesh connection bi-directional line switched self-healing ring with an aggregate capacity of 825 Gbit/s has also been designed and assessed. The signals quality has also been assessed in each node for either drop and pass according to the unique wavelength assignment. The average signal to noise ratio of better than 25 dB with a gain variation less than 5 dB have been achieved without use any external gain variation devices.

Key words: WDM, EDFA, SONET, Self-Healing Ring (SHR)

ACKNOWLEDGMENTS

I wish to thank Prof. M. Ali, Dr. Aly Elrefaie to be my mentors in the City College of New York and in Bellcore. I am grateful to many people in Bellcore whose expertise and helpful in many areas to make this thesis possible. Especially I would like to thank Dr. Chinlon Lin for his many valuable advice and guidance. I am also grateful to my wife Yanling that without her fully support and patience it wouldn't be possible to finish this thesis.

Table of Contents

LIST OF TABLES

LIST OF FIGURES

GLOSSARY

ADM	Add and Drop Multiplex
APS	Automatic Protection Switching
ASE	Amplified Spontaneous Emission
ATM	Asynchronous Transfer Mode
B-ISDN	Broadband Integrated Services Digital Network
BLSR	Bi-Directional Line Switched Ring
CO	Central Office
CW	Continous Wave
DEMUX	Demultiplexer
DS	Digital Signal
DXC	Digital Cross Connect
EDF	Erbium Doped Fiber
EDFA	Erbium Doped Fiber Amplifier
ISDN	Integrated Services Digital Network
ITU	International Telecommunication Union
ITU-T	Telecommunication Standization Section of ITU
LPS	Line Protection Switching
MUX	Multiplexer
MZ	Mach Zehnder

OC	Opical Carrier
PPS	Path Protection Switching
Rx	Receiver
SDH	Synchronous Digital Hirachy
SHR	Self Healing Ring
SNR	Singal-to-Noise Ratio
SONET	Synchronous Optical Network
STS	Synchronous Transport Signal
Tx	Transmitter
ULSR	Uni-Directional Line Switched Ring
UPSR	Uni-Directional Path Switched Ring
WADM	Wavelength Add and Drop Multiplexer
WDM	Wavelength Division Multiplex
WIXS	Wavelength Interchange Cross Connect
WR	Wavelength Router
WSXC	Wavelength Selective Cross Connect
WTM	Wavelength Terminal Multiplexer

Chapter 1

INTRODUCTION

1.1 INTRODUCTION

Driven by the emerging explosion of information exchange and the prospect of introducing broadband integrated services digital network (B-ISDN) to the mass business and residential customers, the capacity requirements of future transport networks will be demanding. Various estimate predict an increase in the traffic demands by the turn of the century by a factor of 10 or more and the traffic demands in 10 years by a factor of 100 or more. In today's information infrastructure, the increased transport capacity requirements of telecommunication networks are met by the use of fiber-optics as a single-channel, point-to-point transmission links.

Optical communications was introduced as a concept no more than 20 years ago, when it became possible to reduce the attenuation in silica glass to a few dB per kilometer. Since then, optoelectronics and silica fibers have been the subjects of a large-scale world-wide research and product development. As a result, optical communications is today established as one of the most promising technologies within the area of local and long-distance communication systems. As the January of 1994, there are more than 54 million kilometers of optical fiber being deployed in the terrestrial system worldwide. This number is increased by 20% or more each year. The first generation of optical communication system was long-haul point-to-point system, with electronic regenerators to overcome the transmission loss. To provide the survivability and network control and management, the multipoint-

to-multipoint network with redundancy system and self-healing SONET ring with electronic add/drop multiplexers (ADM) and speed of up to 10 Gb/s was introduced later. To upgrade such an infrastructure, a core transport network is required to handle both narrow-band and broadband services together in an efficient manner. This calls for not only high-capacity channels but also transport channels with sufficient granularity to handle signals at all levels in the network. Electronics switching systems are seen to have a capacity limit in the region of a few tens of Gbit/sec. While it will no doubt be possible to increase this limit through further development of high-speed electronic technology, there will be an increased price to pay.

By carefully layering of a future transport network, it may be possible to minimize cost by introducing a new optical network layer based on multiwavelength optical communication technology in the transport hierarchy, with optical switching controlled in an appropriate way through a network management system. Such an optical layer [1] can smoothly evolve with the existing system and form a common underlying network for different overlying networks and could be made transparent to data rate and format, and would be particularly suitable for bulk transport of high-bandwidth signal services.

The prospects for creating such multiwavelength optical networks that are transparent to signal format and bit rate are being investigated in several consortia activities and research programs around the world [2-5]. The principal goal for these programs is to create the possibility of a "future proof" network in which the optical signals flowing through the network are uninterrupted by electronics from source to destination, and in which the character of the individual signals is determined by the terminal equipment which is attached to the network at the source and destination.

The envisioned multilayer network architecture satisfies these objectives by combining optical wavelength division-multiplexing (WDM) with synchronous optical networking (SONET) and asynchronous-transfer mode (ATM) networking. The principal feature of this network structure is that the optical transport layer, comprising the wavelength/space cross-connect switches (OXCs), allows large blocks of capacity to be routed around the network without the need for optoelectronic conversion and processing,. The end-user services are supported by a layer of SONET and ATM electronic switches, which, in turn, are supported by the transparent optical WDM network layer.

Figure 1.1 shows the envisioned multilayer network architecture. As shown in the Fig. 1.1, the optical network layer is segmented into local-exchange networks, that is the focus of this thesis, and a long distance network. Note that the WDM networking layer is conceptually the same for both applications.

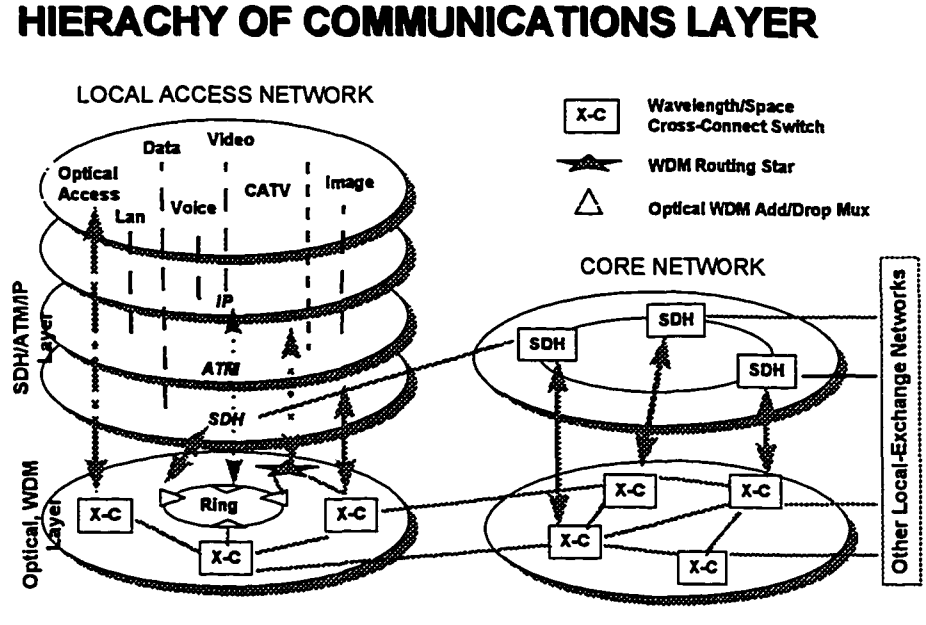

Figure 1.1 Multilayer Network Architecture

However, the local-exchange network will, in general, comprise more variety of network architectures such as broadcast stars, fixed wavelength routing, ring, and mesh-interconnected topologies. In the long-distance network, the distances between WDM cross-connect switches is longer and the network architecture is more homogenous, consisting of a mesh of large WDM cross-connect switches.

One of the most important network architectures in the future local access sub-network is the WDM self-healing ring (SHR) which can be upgraded from the existing SONET/SDH SHR. Therefore, this thesis will focus on the performance and feasibility of the WDM SHR. The advantages of the WDM SHR are network flexibility [1,6], reliability , scalability, transparency and cost-effectiveness[7] .

Reliability is one of the most important concern in the telecommunication industry. A general rule of thumb for any network is that automatic protection switching should be done (ideally) at the lowest possible layer (the layer closest to the physical hardware). At the lowest layer, the data streams have the highest aggregation. The WDM ring architecture with the protection path can recover automatically from a variety of individual faults, including the most common failures such as electronic multiplexer failure and fiber cuts. As shown in Figure 1.1, the WDM ring network can provide a common physical transport layer for a variety of existing and emerging client layers (e. g. SONET, non-SONET backbone digital video, GHz analog signal). Most of the client transport applications, in particular the predominant SONET applications, inherently provide various levels of redundancy and protection. Introducing optical protection will result in double redundancy and reduce the complexity of the client layer protection schemes.

In the WDM ring network, the network size is limited by the number of available wavelengths. Within the limitation of the number of available

wavelengths, which is determined in practice by the erbium-doped fiber amplifier (EDFA) bandwidth as discussed later, the network size can be increased by carefully adding and assigning the wavelengths. If the number of wavelength is eventually limited, the level of scalability can be achieved in multi-hop networks by using WDM cross-connect switches without losing the transparency.

1.2 THESIS STATEMENT

This thesis investigates self-healing ring networks that utilize WDM technology, all-optical Add-and-Drop Multiplexers (ADMs) and all-optical protection ring using EDFAs [8] and optical switches, to provide survivable transport in the local-exchange network layer. Specifically, we analyze two WDM schemes of self-healing ring [9] architectures: 2-fiber uni-directional path-switched and line-switched [10] rings and 4-fiber bi-directional line switched rings [11]. Both types of WDM ring can be designed to be consistent with present SONET standards, allowing graceful upgrades from electronic SONET rings to WDM SONET rings [12, 13].

The overall objective is to investigate and analyze, through computer simulation and modeling, the performance of all the critical elements necessary for the implementation of high-capacity, scalable, and survivable WDM optical ring networks. We propose to implement a flexible, powerful computer modeling tool for design, optimizing and evaluating the end-and-end performance of both uni-directional and bi-directional ring architectures. We compare the maximum number of nodes and the maximum aggregate capacity for the two architectures and their physical limitations.

The uni-directional ring requires two fibers, one working and one protection, and is an open ring with all optical signal originating and terminating at a single

hub office, with one wavelength dropped and added at each office in between. For the 2-fiber uni-directional path-switched ring (UPSR), transmission on both fiber ring is identical except for the direction of propagation; the receiver is a standard SONET UPSR ADMs which is equipped with an electrical selector to choose a better signal from the two paths, and the counter-propagating signals can facilitate network survivability during a cable cut. The 2-fiber uni-directional line-switched ring (ULSR) uses the optical switches and automatic protection switching capability of the standard unidirectional SONET ADMs to provide the survivability. The bi-directional line-switched ring (BLSR) uses four fibers together with a new capability for automatic protection using optical switching and bi-directional SONET ADMs. In BLSR, there are two working and two protection fibers, each working ring is a closed optical ring since only a few wavelengths are dropped and added at any particular office, while most of the signals pass through the individual offices without being dropped.

Within the working ring, a set of WDM signals traverse a cascade of fiber amplifiers, with the number of offices, geographic size, and capacity typically determined by the number of WDM channels that can be supported. The amplifiers' non-flat gain spectra and the filters' inter-channel spacing will impose size and capacity limits that depend on the specific drop-and-add arrangement of the network. We will investigate the size and capacity limits for both uni-directional and bi-directional ring architectures.

Since the use of EDFA cascade represents the key technology which enables the realization of the WDM ring networks, the main thrust of this thesis is to develop an understanding of the various technological difficulties which face EDFA and EDFA cascades with multiwavelength handling capabilities. Two related fundamental problems will be addressed:

(1) Spectral gain non-uniformity or "gain equalization" and the EDFA usable bandwidth limitation due to the non-uniformity. This is one of the major remaining problems facing multiwavelength lightwave networks with fiber-amplifier cascades. When wavelength-multiplexed signals traverse a single amplifier, the individual channels experience various gains determined by the spectroscopy of the gain medium, the fiber length, and the signal and pump power levels. In a single amplifier, these spectral gain variations are generally modest, but they accumulate from stage to stage in a cascade, rapidly growing too large to allow adequate signal-to-noise performance at the less-favored signal wavelengths.

(2) Noise accumulation in high data rate WDM repeater chains. The main objective is to ensure sufficient gain flatness to permit amplifiers to be cascaded while maintaining acceptable signal-to-noise ratio (SNR) at all wavelengths. The SNR and the gain flatness in the cascaded EDFA are directly related due to the signals competing for pump power.

Different approaches to equalize (flatten) the passband of individual and cascaded EDFA for the WDM ring network applications have been examined:

(i) An analytic analysis suggested that the wavelength allocation which agreed to the ITU-T standard grid can be optimized based on the EDFA intrinsic emission and absorption cross section at a specific EDF length. Therefore, the passband which the wavelength allocated have the intrinsic flat characteristics.

(ii) A simple optimization analysis was also suggested to relate the individual amplifier performance parameters to the overall performance of an amplifier cascade for best overall system performance without having to resort to expensive external equalization methods. This work showed that 980-nm pumping, together with the optimum choice of the amplifier

length at the optimized wavelength allocation, provides adequate performance for 15 nodes bi-directional mesh-connect WDM self-healing ring without using external gain equalization devices.

(iii) If the optimized intrinsic EDFA characteristics can not guarantee the required SNR and gain variations, this study showed that the EDFA parameters have to be optimized to simplify the practical implementation of the external gain equalizer. Using this approach, the effective of several passive equalization techniques have been examined to exploit the entire optical bandwidth of the amplifiers. The results of this approach showed effective gain equalization over most of the entire useful EDFA gain bandwidth.

However, many other active and passive components are also very important for achieving the optimum performance of the WDM self-healing ring networks. This thesis only focus on the WDM self-healing ring architectures design and their performance analysis based on the optimized EDFAs.

Chapter 2

WDM NETWORK TOPOLOGIES

2.1 NETWORK TOPOLGIES INTRODUCTION

We can divide communication systems, from the topological viewpoint, into three general classes, as shown in Figure 2.1-2.3. These systems interconnect node or called office in the terms of telecommunication, which in general could be switches, terminals, computers, workstations, telephones, etc.

Figure 2.1 is a single point-to-point link, either unidirectional (simplex) or bi-directional (duplex). A transmitter at one end sends messages to a receiver at the other, and there are only two parties on the network. In the figure 5 is indicated a one-to-many situation, which we shall arbitrarily call a multipoint network. Now there are N parties, but they are not all equal. One of them (node 1) can send to a subset of all the other N-1 directly, and N-1 nodes have to send messages to each other through node 1, which is called hub. Another special case of a multipoint is the broadcast situation in which the one station can send to all N-1 others. These two topologies, the point-to-point and the multipoint are subsets of the network indicated in the figure 6, a system which each of the N nodes can reach each of the others. To be maximally useful, the network must provide this any-to-any connectivity (mesh connectivity), rather than a situation in which some nodes can communicates with only a subset of the N-1 others, etc.

An interesting thing seems to be happening now in the world of fiber optical communication. The preoccupation with the single long-distance link (trunk system) is shifting to one with multipoint and networks [7, 8, 11]. The driving application for multipoint system seems to be local fiber to the home or office, while that for networks is the "local area" or "metropolitan area" broadband access network. With the development of WDM technology, the concept of

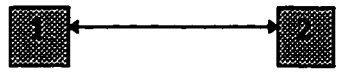

Figure 2.1: Point-to-Point

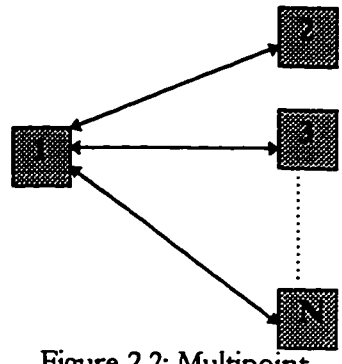

Figure 2.2: Multipoint

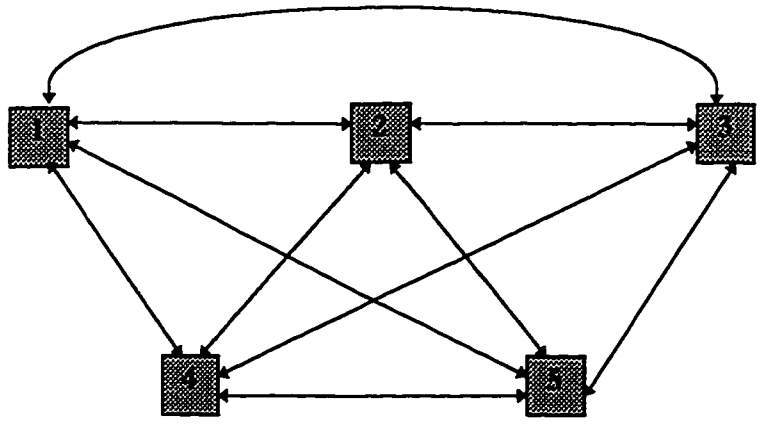

Figure 2.3: Network

networks are extended to many varity of versions. Virtually, in the WDM, each wavelength can set up a channel or a link. Therefore, a one point to multipoint star topology or a mesh connectivity of multipoint-to-multipoint can be on the same ring structure with different wavelength assignment. The following we are going to discuss the general WDM network which can be category as sub-network and inter-network. A sub-network is the network that has the direct interface with clients. It forms the lowest tier of the network hierarchy. An inter-network is the network that links the sub-networks.

2.2 WDM SUB-NETWORK ARCHITECTURES

2.2.1 Point-to-Point WDM

A point-to-point WDM architecture is shown in Figure 2.4. The architecture shows only one direction with two fibers, one for working and one for protection. This is done for the sake of clarity. A similar arrangement exists for the other direction. The working fibers must be on diverse facilities from the protection fibers. Figure 2.4 also shows an example of 1+1 electrical client layer protection. It is also possible to consider 1:N protection schemes which use shared protection. However, we do not consider this in any more detail here.

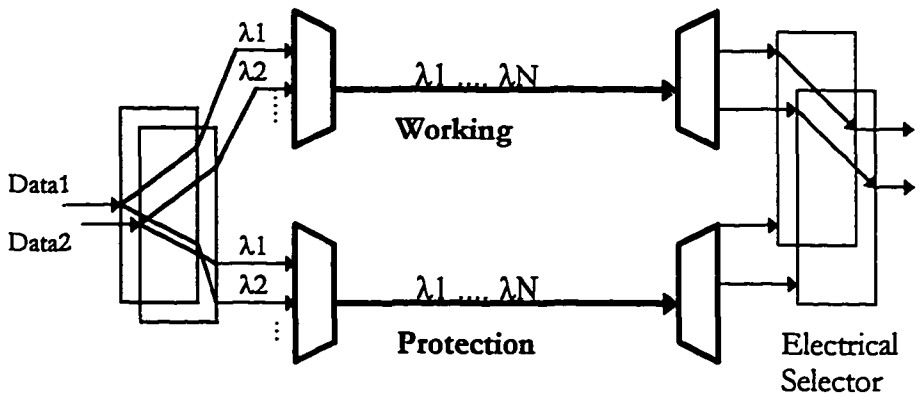

Figure 2.4

2.2. 2 WDM Ring Networks

We define two ring architectures, 2-fiber and 4-fiber.

2-Fiber WDM Ring Architecture

Figure 2.5 shows a 2-fiber WDM ring architecture [10]. This architecture uses 2-fiber WADMs (Wavelength Add-Drop Multiplexers) which drop and add wavelengths from the 2-fiber ring. It is possible that the WADMs are equipped to provide an optical drop and continue function on a per-wavelength basis. A pair of fibers between different offices are required to be on diverse facilities.

The WADMs may or may not have optical protection switching capabilities. When the WADMs come with optical layer protection, care must be taken in wavelength assignment and routing. More detail on this issue will be provided in the the next section. Some electrical interfaces have built in protection capabilities. In the next section, the network protection will be discussed with various options for the electrical layer and the WDM layer protection using 2-fiber rings.

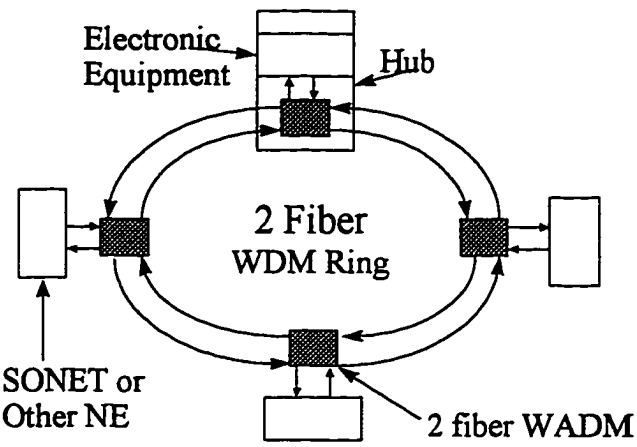

Figure 2.5: 2-Fiber Ring Network

4-Fiber WDM Ring Architecture

Figure 2.6 shows a 4-fiber WDM ring architecture [14], [15]. This architecture uses 4-fiber WADMs (Wavelength Add-Drop Multiplexers) which drop and add wavelengths froms the 4-fiber ring. The 4-fiber ring is expected to have a larger capacity than a 2-fiber ring. Once again, it is possible that the ADMs provide a per-wavelength optical drop-and-continue function. Pairs of fibers between different offices are required to be on diverse facilities. The 4-fiber ring has optical WADMs and optical protection switching capabilities. For the 4-fiber ring with optical protection switching the protection fibers will be discussed later.

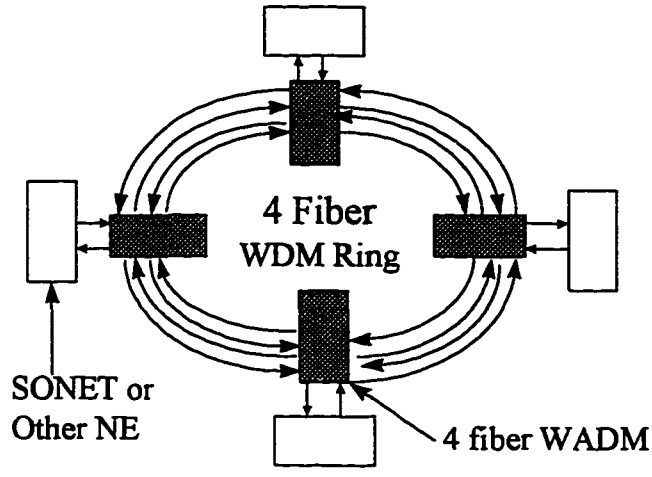

Figure 2.6: 4-fiber ring

2.2.3 WDM Bus or Chain Networks

A bus or chain architecture would simply be an "unfolded" ring. In this case, the optical WADMs are configured in a cascade of point-to-point fiber connections. For economic reasons, the fibers between the two WADMs may not be diversely routed. It is useful for cases in which demands need not be protected, or cases in which it is infeasible to protect demands through route diversity. For example a carrier might determine that broadcast video, which is a CATV-like application, need not be protected because it's competition. The carrier might decide to compete based on other factors. In such a case, a chain (it would need to be a drop-and-continue chain) may be less expensive than a ring. Or there may be a few central offices without enough physical connectivity for route diversity. That is another situation in which a chain would be a useful architecture.

2.2.4 WDM Star

Figure 2.7 shows a single WDM star and a dual WDM star. The WDM star can be a wavelength router (WR), a Wavelength Selective Cross-connect (WSXC) or a Wavelength Interchanging Cross-Connect (WIXC). The dual WDM star

architecture offers network protection capabilities by essentially duplicating both transmitters and diverse fibers. The WDM star can also be a broadcast star. The transmitters on such a broadcast network can use either fixed or tunable lasers that transmit only at one wavelength at any given time, More details on broadcast star architectures can be found in the Lambdanet [16], Rainbow [17] and the All-Optical Networks projects [18]. Hence, WDM broadcast stars are considered as stand-alone architectures that can be used for applications like video broadcast.

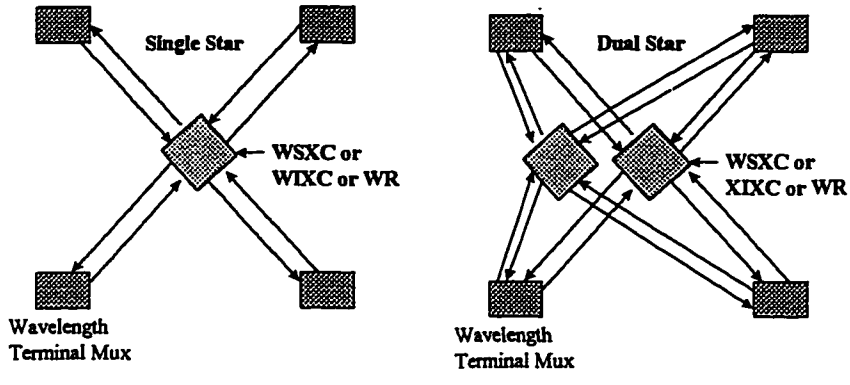

Figure 2.7: Star Networks

2.2.5 WDM Mesh

Figure 2.8 shows a full mesh network that uses WSXCs (Wavelength Selective Cross-Connects) or WIXCs (Wavelength Interchanging Cross-Connects). This type of an architecture might be useful in cases where high capacity full mesh connectivity is required between offices. In this case, mesh type reconfiguration algorithms will be needed to provide optical protection. However, more work is needed to determine the requirements placed on the WDM cross-connects for such networks to provide automatic protection switching (e.g. within 50 msecs as in SONET). Traditionally, cross-connect mesh type networks provide reconfiguration or rerouting from faults in the range of seconds to minutes. Of

course, another option is to use client (electrical) layer protection schemes in conjunction with mesh type architectures. This can substantially reduce the requirements placed on cross-connect reconfiguration.

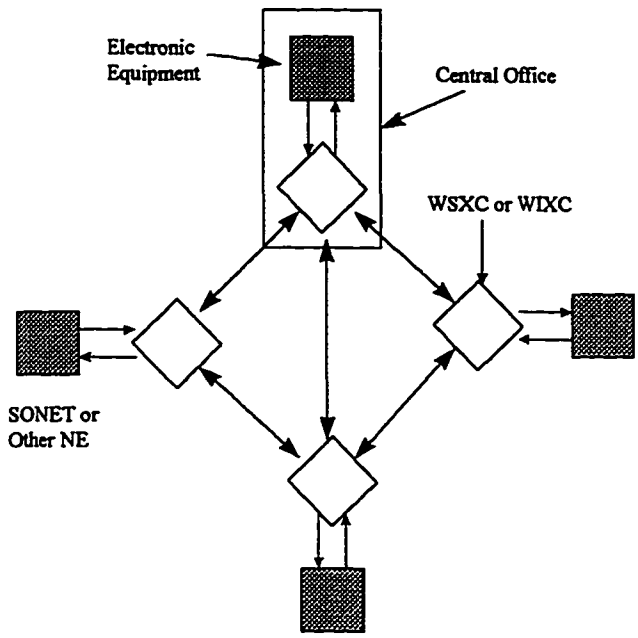

Figure 2.8: Mesh Connection

2.3 WDM INTER-NETWORK ARCHITECTURES

In this section, architectures for the interconnection of sub-networks of WDM are listed. The overall architecture proposed here is essentially two-tier. For some client applications, WDM sub-networks can be interconnected via the client layer (e.g. using SOMET Digital Cross-Connects). Such interconnection might remove many of the cascaded physical layer constraints. However, this approach is not consistent with offering end-to-end optical access. Here we consider interconnection of sub-networks at the optical multiwavelength layer.

2.3.1 Dual-Hub Dual-WDM-Point-to-Point Interconnection

Figure 2.9 shows dual-hub 2-fiber WDM ring sub-networks interconnected by a dual-WDM-point-to-point architecture. It is called dual-hub dual-WDM-

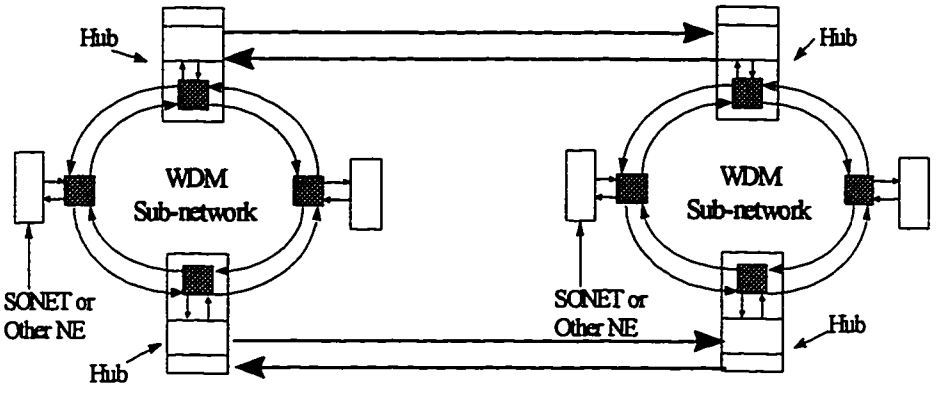

Figure 2.9: Dual-Hub WDM Point-To-Point Inter-Network

point-to-point interconnection architecture. Each sub-network can be a 2-fiber or 4-fiber ring with dual interconnecting hubs (for redundancy) that carry traffic between the rings. Each hub has a WSXC or a WIXC. The hubs are shown to be on opposite sides of the WDM sub-network rings; however, the hubs could also be adjacent nodes. The two hubs use different inter-network point-to-point systems to carry traffic into and out of the sub-networks. Two 2-fiber inter-network point-to-point systems are shown in the figure. These two systems should be on diverse facilities.

The sub-network architectures could be any combination of the candidates defined in the previous section. For example, when interconnecting WDM star sub-networks the dual stars become hub cross-connects. When interconnecting mesh sub-networks, any two WSXCs or WIXCs on each mesh can become hub cross-connects.

2.3.2 Dual-Hub Dual-WDM-Ring Interconnection

Figure 2.10 shows a longer term view of interconnection among WDM sub-networks. In this case, dual-hub 2-fiber WDM ring sub-networks are interconnected by a dual-ring architecture. This is called a dual-hub dual-ring

interconnection architecture. Each sub-network ring can be 2-fiber or 4-fiber with dual interconnection hubs (WIXC or WSXC). The hubs are shown to be

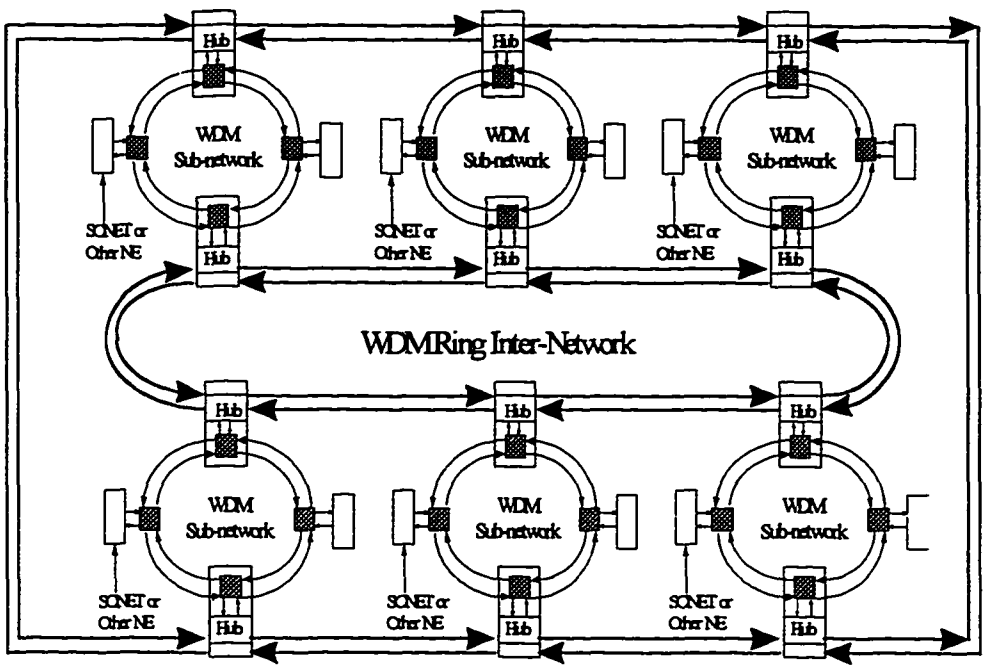

Figure 10: Dual-Hub Dual-WDM-Ring Inter-network

on opposite sides of the WDM sub-network rings; however, the hubs could also be adjacent nodes. The two hubs use different inter-network rings to carry traffic into and out of the sub-networks. Two 2-fiber inter-network rings are shown in the figure. These two rings should be on diverse facilities.

The sub-network architectures could be any combination of the candidates defined in the previous section. For example, when interconnecting WDM star sub-networks by the WDM ring the dual stars become hub cross-connects. When interconnecting mesh sub-networks by the WDM ring any two WSXCs or WIXCs on each mesh can become hub cross-connects.

2.3.3 Dual-Hub Dual-WDM-Star Interconnection

Figure 2.11 shows dual-hub WDM ring sub-networks interconnected by a Dud-WDM-star architecture. This is called a dual-hub dual-WDM-star interconnection architecture. The two hubs use different inter-network stars to carry traffic between the sub-networks using the WDM star. The fiber pairs interconnecting the two hubs to the two star cross-connects should be on diverse facilities.

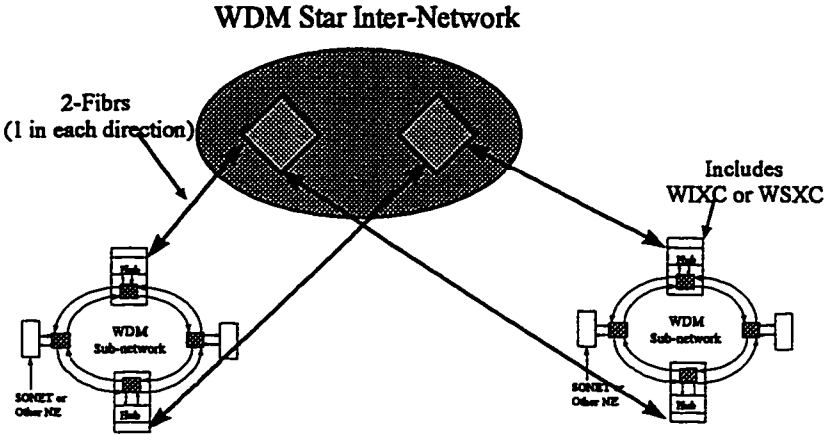

Figure 2.11: WDM Star Inter-Network

The sub-network architectures could be any combination of the candidates defined in the previous section. For example, when interconnecting WDM dual star sub-networks by the dual WDM star the dual stars at the sub-network become the hub cross-connects. When interconnecting mesh sub-networks by the dual WDM star, any two WSXCs or WIXCs on each mesh can become hub cross-connects.

2.3.4 Dual-Hub Dual-WDM-Mesh Interconnection

Figure 2.12 shows dual-hub WDM ring sub-networks interconnected by a dual-mesh interconnection architecture, This is called a dual-hub dual- WDM-Mesh interconnection architecture. Each sub-network ring can be 2-fiber or 4-fiber with dual hubs for redundancy that carry traffic into and out of them. Each hub is a WSXC or a WIXC.

Dual-Hub Dual-WDM-Mesh Inter-Network

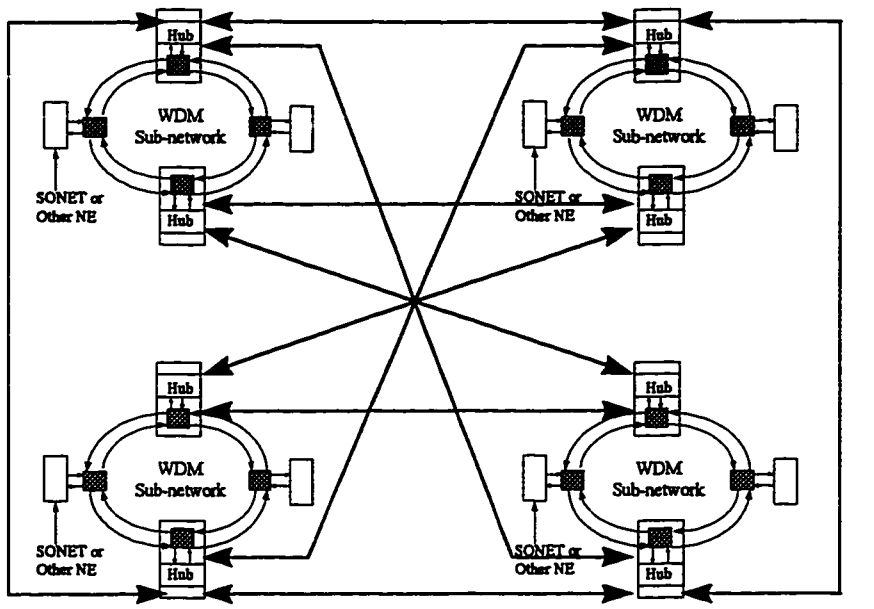

Figure 2.12: Dual-Hub Dual-WDM-Mesh Inter-Network

The hubs are shown to be on opposite sides of the WDM sub-network rings. However, the hubs could also be adjacent nodes. The two hubs use different inter-network cross-connects (WSXCs or WIXCs) to carry traffic into and out of the sub-networks. Two inter-network meshes (outer and inner) are shown in the figure. These two meshes should be on diverse facilities relative to each other. Although the figure shows full mesh connectivity, in general, this can be any arbitrary mesh.

The sub-network architectures could be any combination of the candidates defined in the previous section. For example, when interconnecting WDM dual star sub-networks by the dual-WDM-mesh the dual stars at the sub-network become the hub cross-connects. When interconnecting mesh sub-networks by the dud-WDM-mesh any two WSXCs or WIXCs on each mesh sub-network can become hub cross-connects.

Chapter 3

WDM SELF-HEALING-RING NETWORK ARCHITECTURES

3.1 INTRODUCTION

Since late 80's, the telecommunication carriers have spent billions of dollars to deploy the fiber optical transmission system to meet the increasing demand of capacity. Not long after they built these optical communications system, the capacities immediately reached their limits. Now, the carriers face the problems of how to upgrade these system to meet the exponential increasing capacity demand cost-effectively. The goal of this thesis is trying to solve this problem. The new high capacity network must be based on the legacy system, so an overview of the existing optical communication system is necessary.

The existing optical communications systems are mostly Synchronous Optical Network (SONET by North America standard) or Synchronous Digital Hierarchy (SDH by ITU standard). SONET synchronous multiplexing refers to combining (multiplexing) low speed digital signals (DS-1 of 1.544 Mb/s, CEPT-1 of 2.048 Mb/s, DS-1C of 3.152 Mb/s, DS-2 of 6.312 Mb/s, and DS-3 of 44.736 Mb/s) into a high speed signal format that allow easy extraction of the low speed constituents from the high speed line. Where the DS-1, DS-1C, DS-2 and DS-3 etc. are the pre-existing asynchronous hierarchy system before SONET. SONET transport these signals (called payload) in a synchronous fashion over fiber transmission systems. DS-1, CEPT-1, DS-1C, and DS-2 are mapped into the SONET signal using a structure called a virtual tributary. The DS-3 signal is mapped directly into a standard synchronous transport signal (STS) STS-1. These tributary signals along with line, section and path overhead form the STS-1. The SONET signal architecture is formed by a byte

interleaved multiplexing scheme. Through the extensive use of pointers, both asynchronous and synchronous payloads can be carried by the OC-N (Optical Carrier). Payloads can be readily added or dropped from the carrier by a network element called the Add Drop Multiplexer (ADM). The SONET ADM is intended for multiplexing signals as low as 1.544 Mb/s and as high as 2.5 Gb/s. There are mostly two network architectures for SONET, linear Add/Drop and ring. Linear Add/Drop is basically a bus topology which rapidly superseded the initial deployment of simple point-to-point system. SONET/SDH rings, relying upon ADMs with unidirectional or bi-directional transport, are of two principal types, as discussed previously: unidirectional path-switched rings (UPSRs) or line-switched rings [ULSR] [19] and bi-directional line-switched rings (BLSRs) [19]. Additionally, these ring architectures are themselves dependent upon basic automatic protection. The basic protection is consisted of equipment protection and facility protection. Equipment protection is supported by providing spare equipment-often referred to as a "hot-standby" or "protection" equipment. Facility protection can be can be classified as either 1+1, where every working facility has a dedicated protection facility, or M:N, where M protection entities are shared among N working entities.

3.1.1 AUTOMATIC PROTECTION SWITCHING

The facility protection usually have a automatic protection switching (APS) to switch from failure working entity to the protection entity. Two basic types of automatic protection switching come into play in these system: path-protection switching (PPS) and line-protection switching (LPS).

PPS, as the name refers, protects the path level as the low-speed input to ADMs. Referred to as (1+1)-protection, traffic transmitted by the ADMs is duplicated and sent out over two independent fibers, the working and protection pair. When a failure occurs, the receiver compares the quality of the

dual-fiber input signals and selects the best. Figure 3.1 shows such a ADM with PPS.

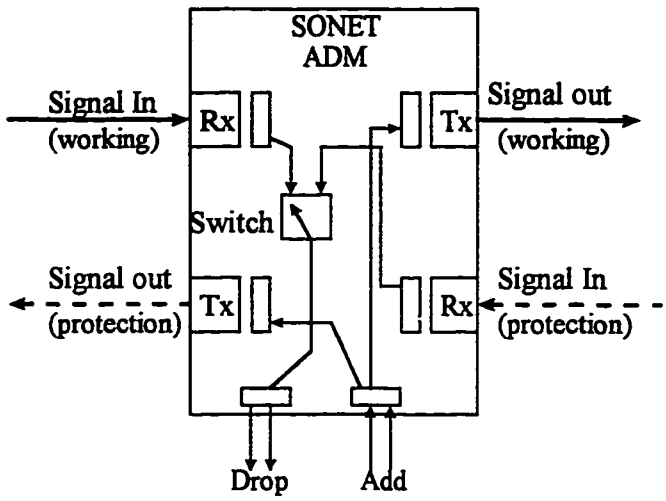

Figure 3.1: ADM with path-protection swtching

In LPS, line-layer switching requires that the fiber trunk interconnecting two nodal ADMs be duplicated, with working and protection transmit/receiver pairs. In the event of disrupted or degraded signal quality such as fiber cut, trunk traffic is switched to the protection pair. Figure 3.2 shows such a LPS.

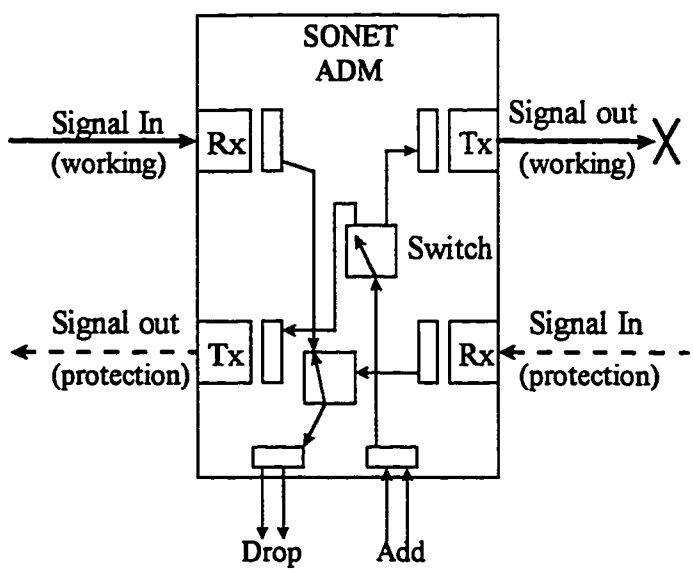

Figure 3.2: ADM with line-protection swtching

3.1.2 UPSR AND BLSR

The unidirectional path-switched rings (UPSR) protects traffic on the basis of individual path quality. Two fibers connect each adjacent pair of nodes and the nodes are connected in a ring configuration. One fiber is used for working traffic, while the other is dedicated to protection. SONET Path protection is provided as follows: the SONET Path is permanently bridged at the Transmitter (Tx) end to both outgoing fibers (see figure 3.1), as this is electrical level protection, the Receiver (Rx) end continuously compares the incoming signals at the SONET Path layer and selects the better of the two. The UPSR is a 1+1 unidirectional architecture—each end operates independently, and no APS channel is required. Figure 3.3 is showing such a UPSR.

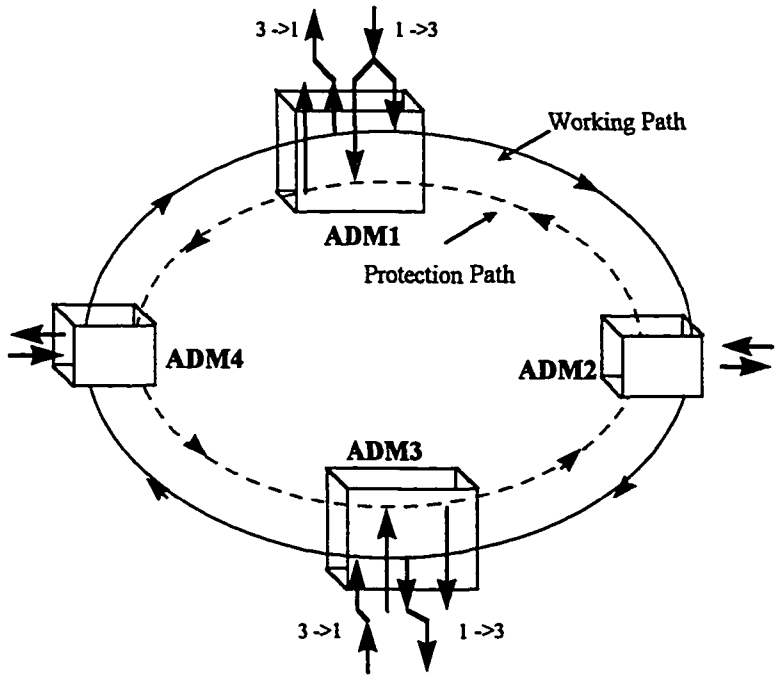

Figure 3.3: 2-fiber Unidirectional SHR

The bi-directional line-switched rings (BLSR) is an especially robust form of ring network using LPS in conjunction with bi-directional transmission. It is electrical SONET Line-layer shared protection. Two types of BLSRs have been

defined –2-fiber and 4-fiber. In the 2-fiber ULSR, like the UPSR, two fibers connect each adjacent pair of nodes and the nodes are connected in a ring configuration. Half the signal bandwidth on each fiber is reserved for protection. In 4-fiber BLSR, four fibers connect each adjacent pair of nodes, and the nodes are connected in a ring configuration. The additional two in each direction allow the capacity of one fiber pair to be used for working traffic, while the other fiber pair is dedicated to protection of the working traffic. Figure 3.3 illustrates the 4-fiber BLSR in the failure-free state.

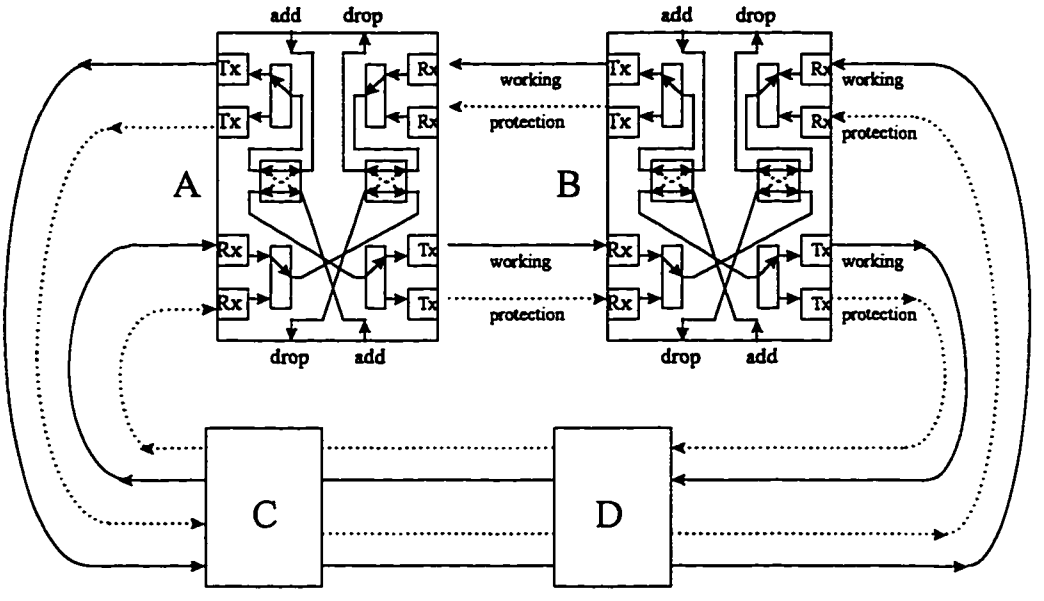

Figure 3.4: 4-Fiber BLSR – Failure Free

If only working line is lost, the short path APS communication between nodes is maintained, and the nodes can coordinate a protection switch. Figure 3.5 shows a span switch, which is used for short path restoration. A span switch is coordinated for 1+1 electrical facility protection.

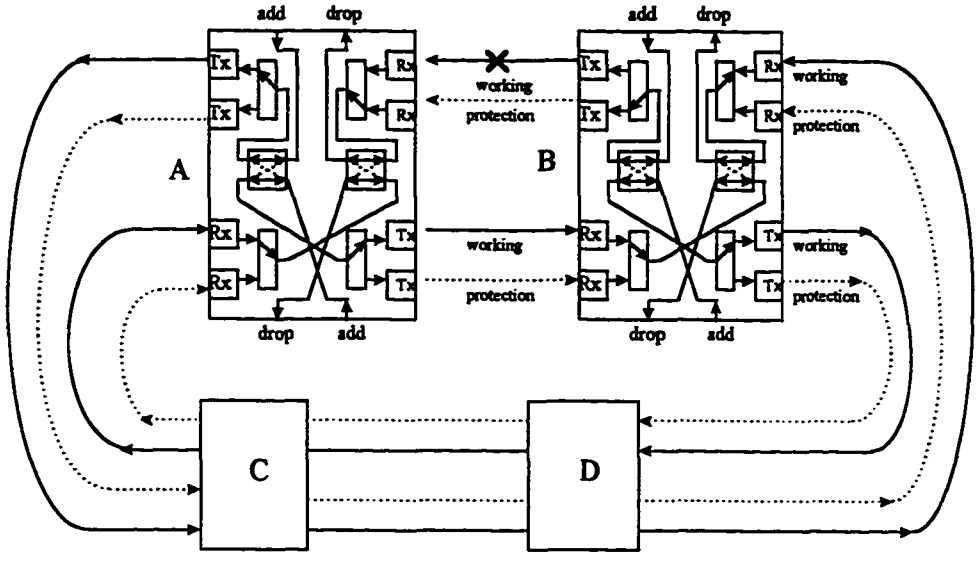

Figure 3.5: 4-Fiber BLSR -- Failure State (Span Switch)

If both the working and protection fibers are cut, as shown between nodes A and B in Figure 3.6, the short path APS communication path between nodes A and B is severed.

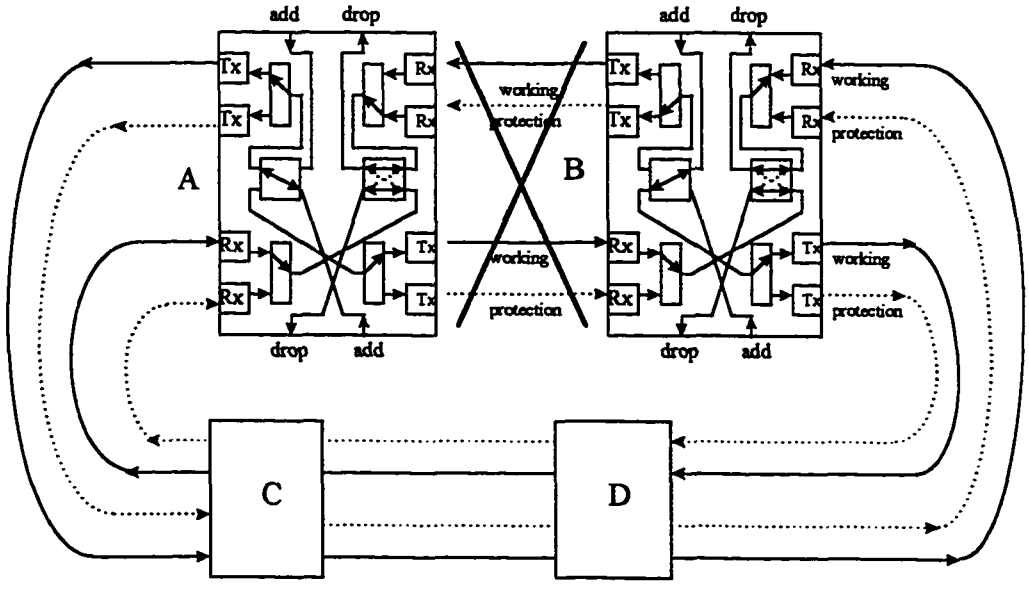

Figure 3.6: 4-Fiber BLSR -- Failure State (Ring Switch)

Unlike the linear architecture, where a failure on all fibers between two nodes leads to loss of service, the 4-fiber BLSR architecture supports a long path ring protection switch in addition to the short path span protection switch – see figure 3.6. Advantages of the 4-fiber over 2-fiber BLSR architecture include: a) the 4-fiber BLSR can carry twice as much working traffic and twice as much extra traffic as the 2-fiber BLSR. b) the 4-fiber BLSR supports both span switching and ring switching, and hence can simultaneously protect (using span switches) up to N simultaneous working line failure between nodes on a N-node 4-fiber BLSR. These ring structures are all called Self-Healing-Rings (SHR).

3.2 WDM 2-FIBER ARCHITECTURES

SONET Self-Healing-Ring has brought the network reliability and redundancy to a new level. But with the exponential capacity increase, the SONET SHR is very expensive to upgrade. There are two ways to increase the capacity of SONET ring before the WDM technology. One is increase the electronic devices' speed, e.g. from 2.5 Gb/s to 10 Gb/s or 20 Gb/s. Another way is to deploy new SONET rings. Both are extremely expensive. Also, the conventional SONET ring lacks of flexibility for capacity upgrade. If any user (node) on the ring want to change, e.g. increasing the capacity, changes have to be done on all the other nodes around the ring as well if the total capacity is used up by the existing nodes, because all the signals have to be dropped at any node and re-transmited. By using the WDM and photonic switching in the transport network, one can route the entire multi-gigabit/sec wavelength channel without breaking into the data streams. In this way, it is possible to increase the capacity, flexibility and reliability of the total network.

A WDM 2-fiber unidirectional ring actually is almost like multi-SONET 2-fiber SHR coexisting in the 2-fiber optical self-healing ring. A physical optical ring can be divided into either a logic star, a logic ring or even a mesh connection.

A logic ring network requires that all the optical signals be dropped at all the nodes and passed on the shortest route between transmitter and receiver. The advantage is that one can increase the capacity by a factor of N where N is the number of multiplexed wavelengths.

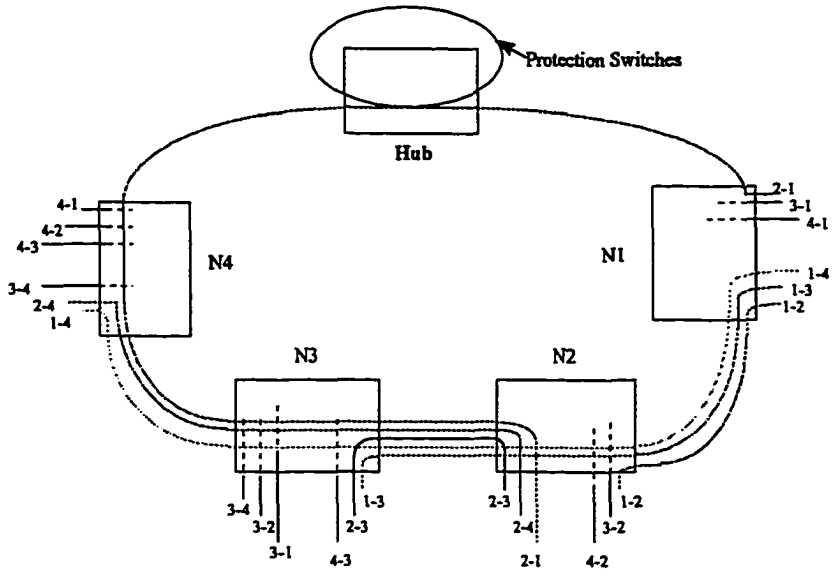

Figure 3.7: Mesh Connectivity Uni-Directional WDM Ring

A full mesh connection 2-fiber uni-directional ring is not practical because it requires too many wavelengths. In this architecture, each node has to directly communicate to the rest of the nodes on the direction of the flow (either clockwise or counter-clockwise). Each nodes talk back to the nodes in front of the circle by using the same wavelength received from that node and through the central-office hub. Figure 3.7 illustrates the wavelength assignment for a mesh connected 2-fiber WDM uni-directional ring. For N-node mesh-ring network, each node will send out N-1 wavelengths (channels) and receive N-1 wavelengths. It can be obviously seen that the total number of wavelength W needed for an N nodes mesh-ring is:

$$W = \sum_{i=1}^{N-1}(N-i) = \frac{N(N-1)}{2} \qquad (3.1)$$

Therefore, for an 8-node mesh-ring, the total wavelength needed is 28. The total number of wavelength is restricted by the optical active components such as EDFA, Optical Multiplexer (MUX) and Demultiplexer (DEMUX), Lasers etc. which will be discussed in detail later.

In considering the compatibility of conventional networks and using the wavelength effectively, the logical star is the most attractive solution for the 2-fiber uni-directional SHR [20] [21]. The logic star 2-fiber uni-directional SHR consists of a central-office and N local nodes (local offices) which are interconnected by N wavelengths. All transmission are either originating or terminating at the hub. The communications between nodes must go through the hub. Thereby, a logical star composing of a number of separate point-to-point wavelength connections by allocating separate wavelength channel to each local node is established. Hence, changes in one node can be made without impact on the others, unlike the conventional SONET that all the nodes have to make the same changes. This architecture is optimized for a network with centralized traffic pattern, such as those that arise when advanced switching features are localized in a hub office serving multiple local offices. Erbium-Doped Fiber Amplifiers are used in between the local offices to recover the loss of transmission and network element such as MUX and DEMUX (See Figure 3.8). There are two fibers on the ring, one working fiber and one protection fiber. Under normal conditions, the signals are sent on the working path. When working fiber is cut, the traffic can be routed via the protection path to the designated terminal.

The SHR is managed from a control terminal. The node intelligence is sufficient for handling configuration and signaling to the control computer on e.g. alarm conditions. Each node is capable of creating alarm signals serving as a basis for switching decisions necessarily made after a fiber break. A fraction of the signal is drawn off at the monitoring points near each node. Both the

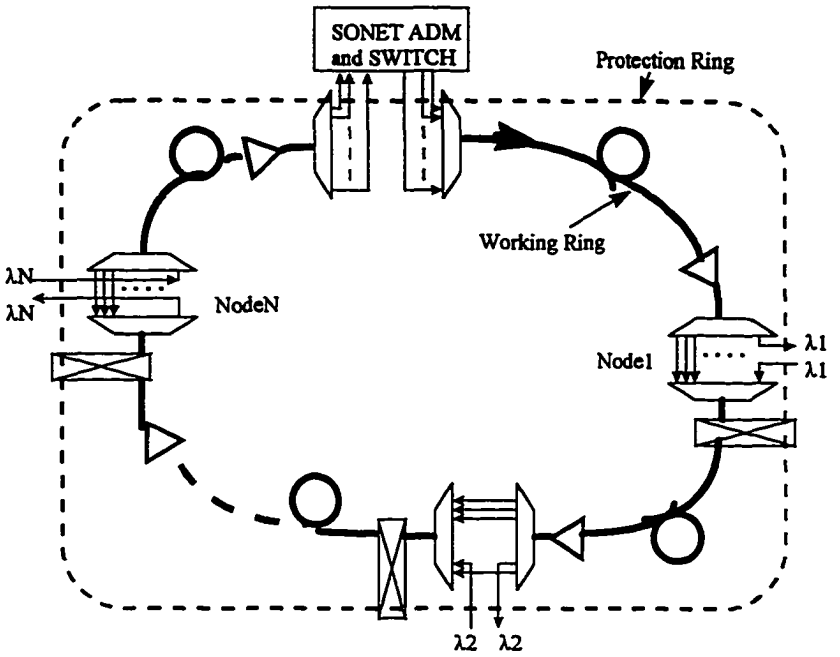

Figure 3.8: 2-Fiber Star Uni-Directional SHR

working ring and protection ring are supervised by a monitoring point. Figure 3.9 illustrates the functional block diagram of inside of a node.

The SHR is now configured so the nodes always fold the ring to safeguard the facility of the ring independently from both fibers or just one cut. If the fiber break occurs between two nodes then the node before the broken fiber switches the signals to the protection ring. There the signals just bypass all the other nodes including the hub, until the signal return to the other side of the fiber break, then the last node loops back the signals to the Optical ADM.

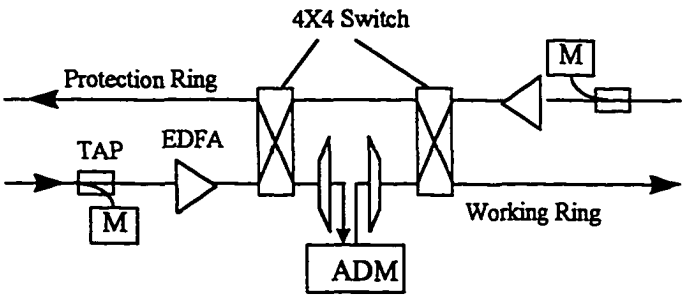

Figure 3.9: Configuration of SHR node

Figure 3.10 illustrates a ring under such a configuration. As one can see from Figure 3.10, the WDM signals in the case of fiber break have to pass through all the EDFAs on the protection path. Therefore, the network performance and the size of the node are not only decided by the number of wavelengths we can use but also limited by the signal quality after passing through cascade of EDFAs, which is limited by EDFA's ASE and non-flat gain profile. Even with the ring operating under the normal condition (no fiber cut), WDM signals pass through different number of EDFAs before being dropped at the hub. Therefore, signal originated at different node with different wavelength will experience different gain and gain variation. For example, the signal added at node one will pass the most number of EDFAs and signal added at node N will pass the least number of EDFA. These are many of the factors which will affect the size and performance of 2-fiber SHR. How to cope with these factor and reach maximum number of nodes or best SNR will be fully discussed later.

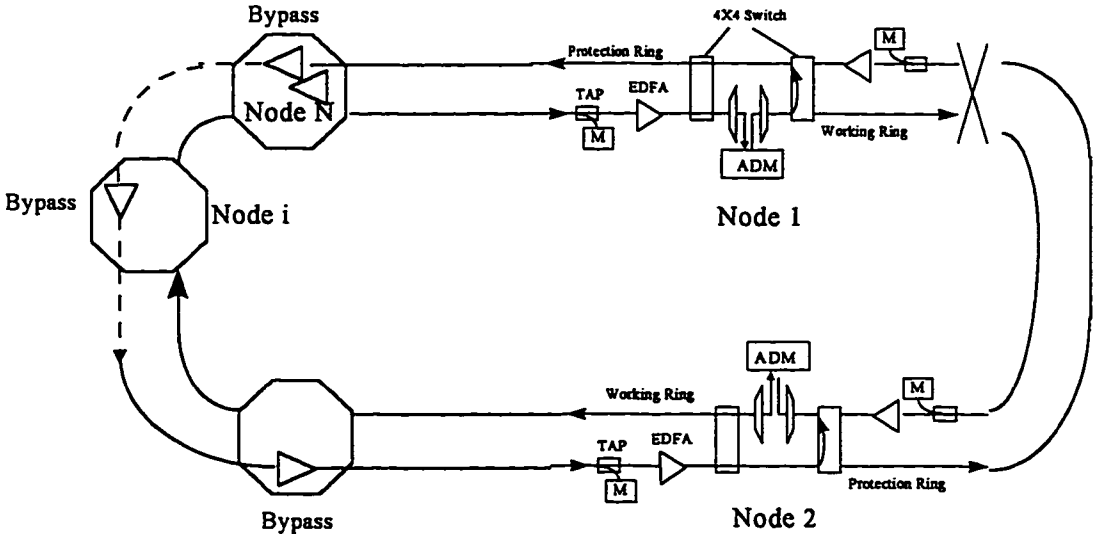

Figure 3.10: SHR Configuration of Fiber Cut Between N1 and N2

3.3 WDM 4-FIBER BI-DIRECTIONAL SELF-HEALING-RING

In the four-fiber bi-directional WDM ring, there are two working fibers that carry different transmission signals in the opposite direction, and the

corresponding two protection fibers to allow optical protection switching in the event of a failure on one of the working paths. The connectivity among offices depends on the wavelength dropping plan assigned to each office. As aforementioned in 2-fiber SHR, a physical 4-fiber ring can also be either logic star, logic ring and logic mesh-connection. As discussed in section 3.2, for mesh connectivity of 2-fiber uni-directional ring, the total wavelength number needed for N nodes are N(N-1)/2. The following sections will discuss the number of wavelengths needed for 4-fiber WDM BLSR, wavelength assignment for network growth and protection mechanism in the WDM BLSR. Figure 3.11 shows a 5-node WDM BLSR for illustration purposes.

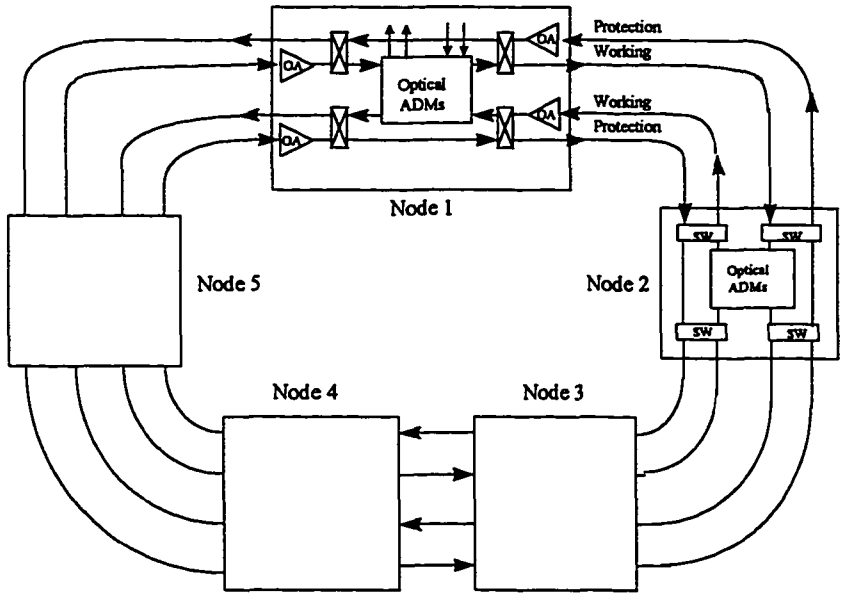

Figure 3.11: 4-Fiber WDM BLSR

3.4 WAVELENGTH ASSIGNMENT FOR MESH CONNECTION BLSR

3.4.1 NUMBER OF WAVELENGTH REQUIRED

For a bi-directional 4-fiber WDM ring with N nodes attached it, the mesh connectivity is each node N_i is connected to all other (N-1) nodes on the ring

via shortest path. For a bi-directional ring, the direction (either clockwise or counterclockwise) will give us the shortest path. Looking at the clockwise direction only (counterclockwise will give the same results due the network symmetry).

Since the shortest route always being chosen, the longest path for the interconnecting any two nodes will be equal to (N+1)/2 - 1 segments of the ring, a segment is defined as a link between two adjacent nodes on the ring. Here N is the odd number. Therefore at most (N+1)/2 nodes will share a common fiber. Thus, the number of wavelength required for full mesh connectivity is given by:

$$W = \begin{pmatrix} \frac{N+1}{2} \\ 2 \end{pmatrix} \tag{3.2}$$

$$\Rightarrow W = \frac{(\frac{N+1}{2})!}{(2!(\frac{N-3}{2})!)} = \frac{(N^2-1)}{8} \tag{3.3}$$

where, W = number of wavelengths

N = number of nodes in the ring for N = odd number.

When the number of the nodes on ring is an even number, the longest path for interconnecting any two nodes will be equal to N/2 segments of the ring. At most N/2 + 1 = (N+2)/2 nodes will share a common fiber. Thus, the number of wavelength required for full mesh connectivity is given by:

$$W = \begin{pmatrix} \frac{N+2}{2} \\ 2 \end{pmatrix} \tag{3.4}$$

$$\Rightarrow W = \frac{(\frac{N+2}{2})!}{(2!(\frac{N-2}{2})!)} = \frac{(N^2+2N)}{8} = \frac{(N+1)^2-1}{8} \qquad (3.5)$$

From equation (3.3) and (3.5) we can deduct that for N equal to even case we need as many wavelength as for the "next odd" case. Therefore, the formula remains as (3.3). The only two exemptions to this rule are the N = 4 and N = 6 cases. For these two cases we can achieve full mesh connectivity still with (3.2), which will be discussed in the wavelength assignments section. For an 8-node 4-fiber full mesh BLSR, to compare with the 2-fiber full mesh connectivity UPSR, the number of wavelength needed is $(9^2-1)/8 = 10$ instead of $8x(8-1)/2 = 28$ of 2-fiber UPSR.

There are two algorithms of wavelength assignment for different application. One is for the case where optical nodes are all fixed and with very slim chance to change. Another one is based on the network continuing evolution and growth. General requirements for wavelength assignment are fulfilling the mesh-connection and avoiding any wavelength clash. A wavelength clash is defined as the condition where optical signals sharing the same fiber are assigned the same wavelength. Two wavelength assignment approaches have been developed for these two different network requirements.

3.4.2 WAVELENGTH ASSIGMENT FOR FIXED NETWORKS

If no evolution growth is concerned for a given or the wavelength assigned to one node can be changed in the future time, this algorithm can used for any number of node (even or odd). A matrix approach was found to work best for this problem. By appropriately filling in the matrix, while following some simple rules, we can get all the wavelength assigned. A W x N has been determined as the wavelength assignment work sheet.

CASE 1: N = odd number, where N is number of nodes on the ring:

The general rules for the wavelength assignment algorithm for fixed optical network are:

1. K is the number of node for one wavelength cross over including the originating node. The maximum number is (N-1)/2.
2. In a row (wavelength), wherever put the number K in the matrix, one must leave K-1 spaces blocked not available for any number. If one does not block these spaces on that row, someone else uses the same wavelength on the same segments which cause two paths intersect.
3. In a column, one can not have two K values the same. Otherwise one would have duplicated path using different wavelength.
4. One must have all the possible K value exactly once in order to support the full mesh connectivity.
5. Summation of all the values in a row must equal to N. This is true because one wavelength has to go over the close the ring exactly once.

Table 3.1 to Table 3.3 show the examples of wavelength assignment for node equal to 5, 7, and 9 respectively. And Figure 3.12 illustrated the 5-node wavelength assignment routes.

CASE 2: N = even number

In the case where N is an even number, as mentioned before, one just need as many wavelengths as for the "next odd" case. Therefore, one can define as extra dummy node and follow the matrix approach to make the wavelength assignments. Then the dummy node can be removed along the "links" connected to it in order to get required wavelength assignment. There are only two exemptions to this rule. For the case of N = 4 and N = 6 one can use a perfect symmetric scheme which resulting a smaller number of wavelengths. Figure 3.12 illustrates the 4-node case.

The following are the examples of wavelength assignment for different the node which follow the above rules.

For a 5-node ring, the wavelength needed is $(5^2-1)/8 = 3$. The maximum number of K is (5-1)/2 =2. In the W1 row is the number of node W1

wavelength cross over (optical path). If number in the box is 1 (like in N1 column), there is no box blocked after that (K = 1 and K-1 = 0). If the number in that row is 2 (like in N2 column), there is one box blocked, because the wavelength W1 initiated from N2 will pass two span and cross over N3 to N4. Therefore, N3 can not initiate W1 any more. Same rules apply to W2 row. The total number in the row should be equal the total span number which is 5 in this example. In row W3 and column N1, a block must be fit in because no more K available. That means N1 can not use another wavelength to establish the same path as W1 or W2. These are illustrated in Table 3.1 Figure 3.13 shows the mesh link of this wavelength assignment for the 5-node ring.

	N1	N2	N3	N4	N5
W1	1	2	X	1	1
W2	2	X	1	2	X
W3	X	1	2	X	2

Table 3.1 Wavelength assignment for N = 5

	N1	N2	N3	N4	N5	N6	N7
W1	1	2	X	3	X	X	1
W2	2	X	3	X	X	2	X
W3	3	X	X	1	3	X	X
W4	X	1	2	X	2	X	2
W5	X	3	X	X	1	3	X
W6	X	X	1	2	X	1	3

Table 3.2. Wavelength assignment for N=7

For a 7-node ring, the wavelength needed is $(7^2-1)/8 = 6$, the maximum number of K is $(7-1)/2 = 3$, that is the maximum of span one wavelength can

cross over. When the number K is 3 (number of span) for a particular wavelength in one box, that this wavelength will cross over 2 nodes to the third node, 2 boxes after node have to be blocked in that row because the two nodes being crossed over by this wavelength can not use this same wavelength to initiate other channels. Table 3.2 shows the detail assignment following these rules. For a 9-node ring, the wavelength needed is $(9^2-1)/8 = 10$, the maximum K is equal to $(9-1)/2 = 4$, which means the maximum span one wavelength can cross over is 4. When one wavelength is cross over 4 span (3 nodes), the 3 nodes between these span can not initiate any channel using this wavelength. Table 3.3 illustrates the wavelength assignment matrix for the 9-node mesh connection.

	N1	N2	N3	N4	N5	N6	N7	N8	N9
W1	1	2	X	3	X	X	2	X	1
W2	2	X	3	X	X	1	3	X	X
W3	3	X	X	4	X	X	X	2	X
W4	4	X	X	X	1	4	X	X	X
W5	X	1	2	X	4	X	X	X	2
W6	X	3	X	X	2	X	4	X	X
W7	X	4	X	X	X	2	X	3	X
W8	X	x	1	2	X	3	X	X	3
W9	X	X	4	X	X	X	1	4	X
W10	X	X	X	1	3	X	X	1	4

Table 3.3. Wavelength assignment for N = 9

For the even number of nodes, the exceptional cases are for the node number of 4 and 6. Because of the symmetric, the wavelength required for the 4-node mesh bi-directional ring is 2. The assignment is showing in the Figure 3.12.

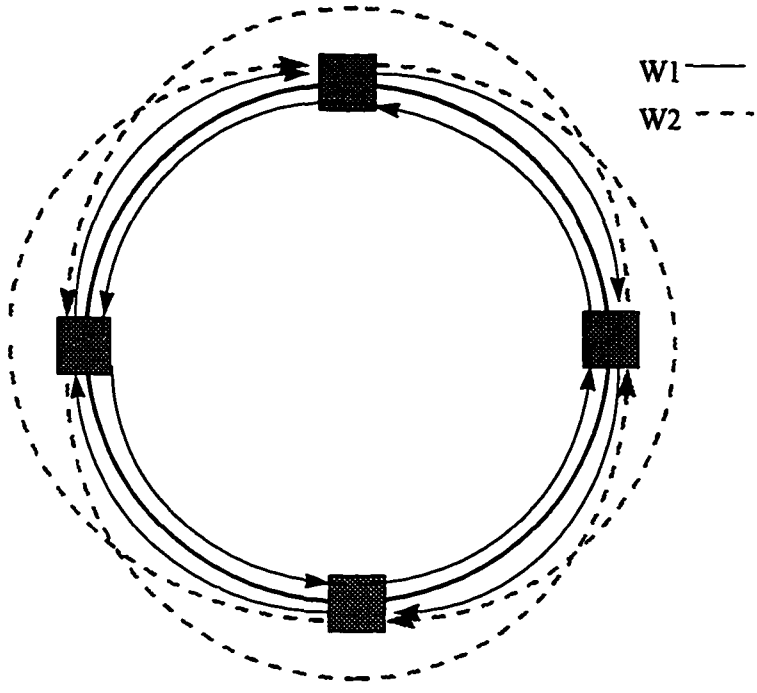

Figure 3.12: 4-Node 4-Fiber BLSR Ring

The wavelength required for the 6-node mesh bi-directional ring is 5 instead of 6. The connection is illustrated in Table 3.4.

	N1	N2	N3	N4	N5	N6
W1	1	1	1	1	1	1
W2	2	X	2	X	2	X
W3	X	2	X	2	X	2
W4	3	X	X	3	X	X
W5	X	X	3	X	X	3

Table 3.4 Wavelength Assignment for Node N = 6

3.4.3 WAVELENGTH ASSIGNMENT ALGORITHM FOR NETWORK EVOLUTION GROWTH

Another wavelength assignment algorithm not only considers the wavelength clash but also take into account the network evolution and growth. In which, the wavelength assigned must keep unchanged after when new nodes being added into the network. One possible scenario for network evolution is show in Figure 3.14 where the network starts with only 3 nodes (1, 2, 3) and one wavelength. It evolves to 11 nodes with the following criterion: the addition of every new node will not change the wavelength assignment for the nodes already in the network. In the example shown in Figure 3.14, the fourth nodes was added, without loss of generality, between 1 and 2. The fifth node was added between node 1 and 3, and in this case its location was one choice out of several possibilities. The entire sequence of adding nodes shown in Figure 3.14 was considered, and a connectivity and wavelength assignment matrix for the network evolution was determined according to the above criterion.

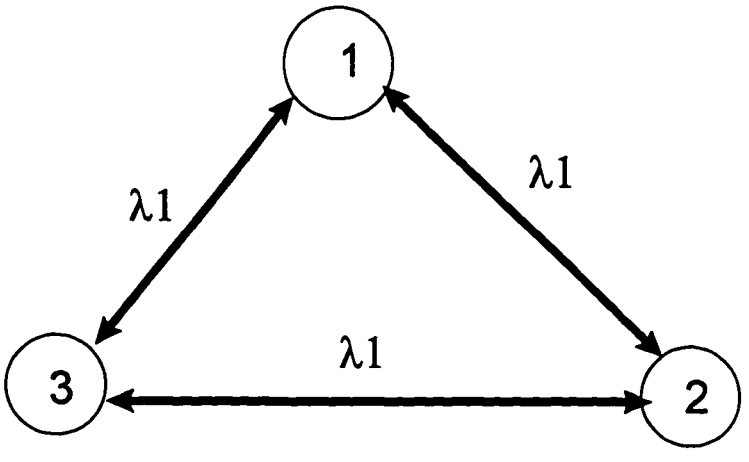

Figure 3.13: Network starrs with 3 nodes 1 wavelength

The disadvantage of this algorithm is that the node number can not be increased smoothly, which has to add two at a time (number of node must be odd) and the places of adding the node is not flexible. Because in the relationship of (3.3), the W (wavelength number) must be an integer. Table 3.5 shows the wavelength assignment based on the evolution and the thick black line in the table indicates the way of node number increment. The whole network capacity of the 4-fiber bi-directional ring is calculated by the channels connected in both directions times the bit rate per optical channel, which is: C=N(N-1)*d/2, where d is the bit rate. For a 11 nodes, if d=10 Gb/s, the total network capacity = 550 Gb/s.

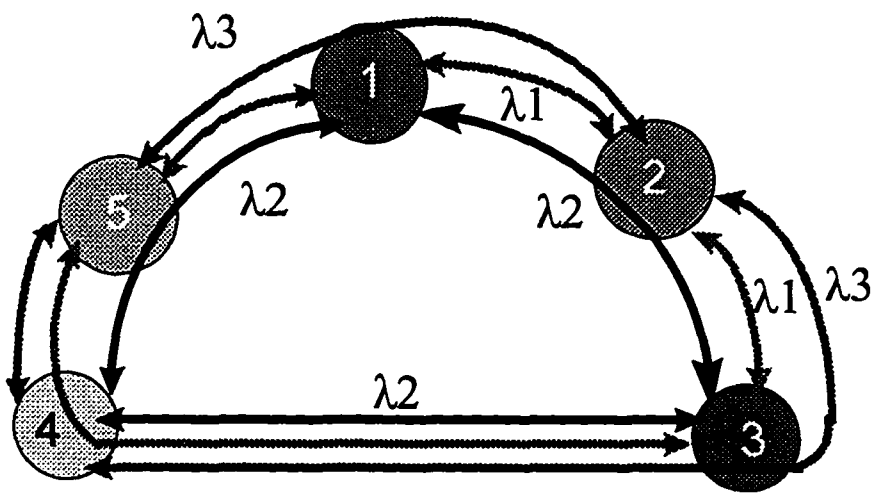

Figure 3.14. 5-node Bi-Directional Ring Mesh Connection Wavelength Assignment

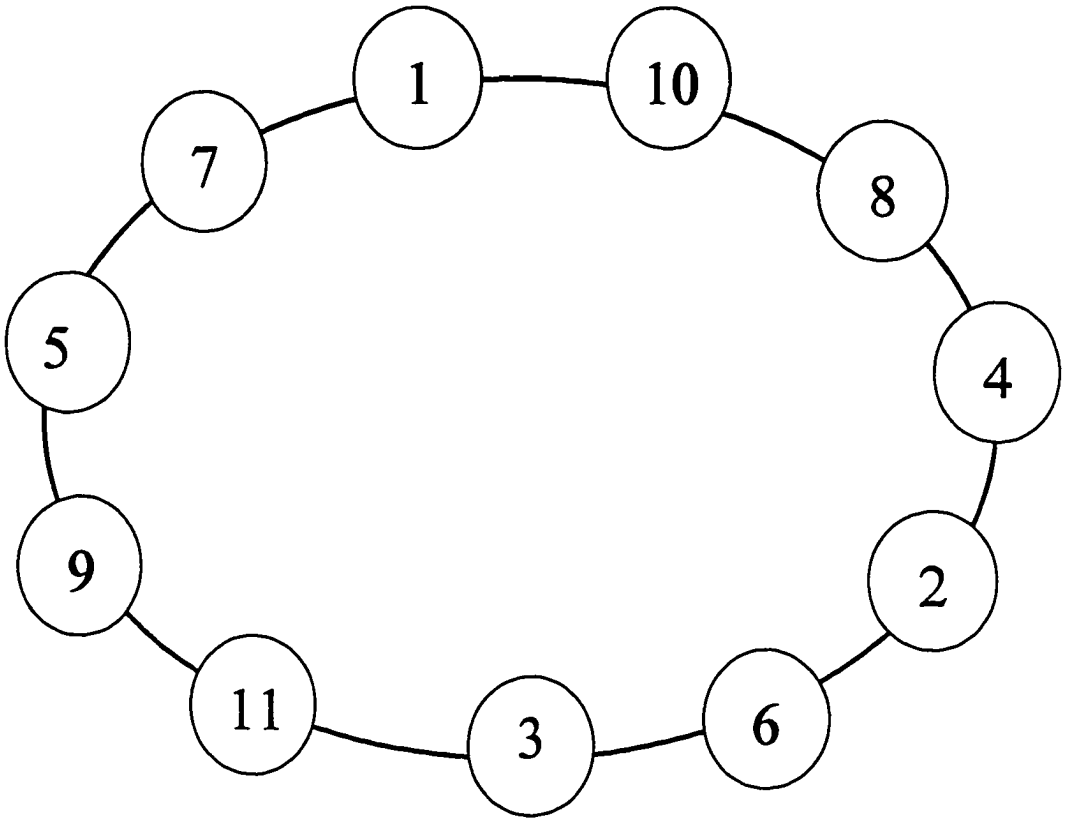

Figure 3.15: 11 nodes ring, the number indicating the adding sequence

Transmitting Office Number

Receiving Office Number

	1	2	3	4	5	6	7	8	9	10	11
1	–	$\vec{\lambda}_1$	$\overleftarrow{\lambda}_1$	$\vec{\lambda}_2$	$\overleftarrow{\lambda}_2$	$\vec{\lambda}_4$	$\overleftarrow{\lambda}_4$	$\vec{\lambda}_7$	$\overleftarrow{\lambda}_7$	$\vec{\lambda}_{11}$	$\overleftarrow{\lambda}_{11}$
2	$\overleftarrow{\lambda}_1$	–	$\vec{\lambda}_1$	$\overleftarrow{\lambda}_2$	$\vec{\lambda}_2$	$\vec{\lambda}_5$	$\overleftarrow{\lambda}_5$	$\overleftarrow{\lambda}_7$	$\vec{\lambda}_7$	$\overleftarrow{\lambda}_{11}$	$\vec{\lambda}_{11}$
3	$\vec{\lambda}_1$	$\overleftarrow{\lambda}_1$	–	$\overleftarrow{\lambda}_3$	$\vec{\lambda}_3$	$\overleftarrow{\lambda}_4$	$\vec{\lambda}_4$	$\overleftarrow{\lambda}_8$	$\vec{\lambda}_8$	$\overleftarrow{\lambda}_{12}$	$\vec{\lambda}_{12}$
4	$\overleftarrow{\lambda}_2$	$\vec{\lambda}_2$	$\vec{\lambda}_3$	–	$\overleftarrow{\lambda}_3$	$\vec{\lambda}_6$	$\overleftarrow{\lambda}_6$	$\overleftarrow{\lambda}_9$	$\vec{\lambda}_9$	$\overleftarrow{\lambda}_{13}$	$\vec{\lambda}_{13}$
5	$\vec{\lambda}_2$	$\overleftarrow{\lambda}_2$	$\overleftarrow{\lambda}_3$	$\vec{\lambda}_3$	–	$\overleftarrow{\lambda}_5$	$\vec{\lambda}_5$	$\vec{\lambda}_8$	$\overleftarrow{\lambda}_8$	$\vec{\lambda}_{12}$	$\overleftarrow{\lambda}_{12}$
6	$\overleftarrow{\lambda}_4$	$\overleftarrow{\lambda}_5$	$\vec{\lambda}_4$	$\overleftarrow{\lambda}_6$	$\vec{\lambda}_5$	–	$\vec{\lambda}_6$	$\overleftarrow{\lambda}_{10}$	$\vec{\lambda}_{10}$	$\overleftarrow{\lambda}_{14}$	$\vec{\lambda}_{14}$
7	$\vec{\lambda}_4$	$\vec{\lambda}_5$	$\overleftarrow{\lambda}_4$	$\vec{\lambda}_6$	$\overleftarrow{\lambda}_5$	$\overleftarrow{\lambda}_6$	–	$\vec{\lambda}_9$	$\overleftarrow{\lambda}_9$	$\vec{\lambda}_{13}$	$\overleftarrow{\lambda}_{13}$
8	$\overleftarrow{\lambda}_7$	$\vec{\lambda}_7$	$\vec{\lambda}_8$	$\vec{\lambda}_9$	$\overleftarrow{\lambda}_8$	$\vec{\lambda}_{10}$	$\overleftarrow{\lambda}_9$	–	$\overleftarrow{\lambda}_{10}$	$\overleftarrow{\lambda}_{15}$	$\vec{\lambda}_{15}$
9	$\vec{\lambda}_7$	$\overleftarrow{\lambda}_7$	$\overleftarrow{\lambda}_8$	$\overleftarrow{\lambda}_9$	$\vec{\lambda}_8$	$\overleftarrow{\lambda}_{10}$	$\vec{\lambda}_9$	$\vec{\lambda}_{10}$	–	$\vec{\lambda}_{14}$	$\overleftarrow{\lambda}_{14}$
10	$\overleftarrow{\lambda}_{11}$	$\vec{\lambda}_{11}$	$\vec{\lambda}_{12}$	$\vec{\lambda}_{13}$	$\overleftarrow{\lambda}_{12}$	$\vec{\lambda}_{14}$	$\overleftarrow{\lambda}_{13}$	$\vec{\lambda}_{15}$	$\overleftarrow{\lambda}_{14}$	–	$\overleftarrow{\lambda}_{15}$
11	$\vec{\lambda}_{11}$	$\overleftarrow{\lambda}_{11}$	$\overleftarrow{\lambda}_{12}$	$\overleftarrow{\lambda}_{13}$	$\vec{\lambda}_{12}$	$\overleftarrow{\lambda}_{14}$	$\vec{\lambda}_{13}$	$\overleftarrow{\lambda}_{15}$	$\vec{\lambda}_{14}$	$\vec{\lambda}_{15}$	–

Table 3.5: Wavelength Assignment for Network Growth

3.5 THE PROTECTION SCHEME OF 4-FIBER WDM BLSR

The 4-fiber bi-directional line-switched WDM self-healing ring has almost same protection scheme as 2-fiber's. In each direction, there are two optical switches at both sides of the optical ADM, which can protect either one working fiber cut, two working fibers cut or even 4 fibers (working and protection of both direction). Figure 3.16 shows functional block diagram of optical ADM. In each optical node, there are multi-SONET electronic ADMs with bi-directional line protection switches in that. Therefore, with the optical protection switches, the 4-fiber WDM bi-directional self-healing ring can provide both layer (optical and electronic) protections for the network redundancy. Figure 3.17 illustrates the optical level protection functional diagram.

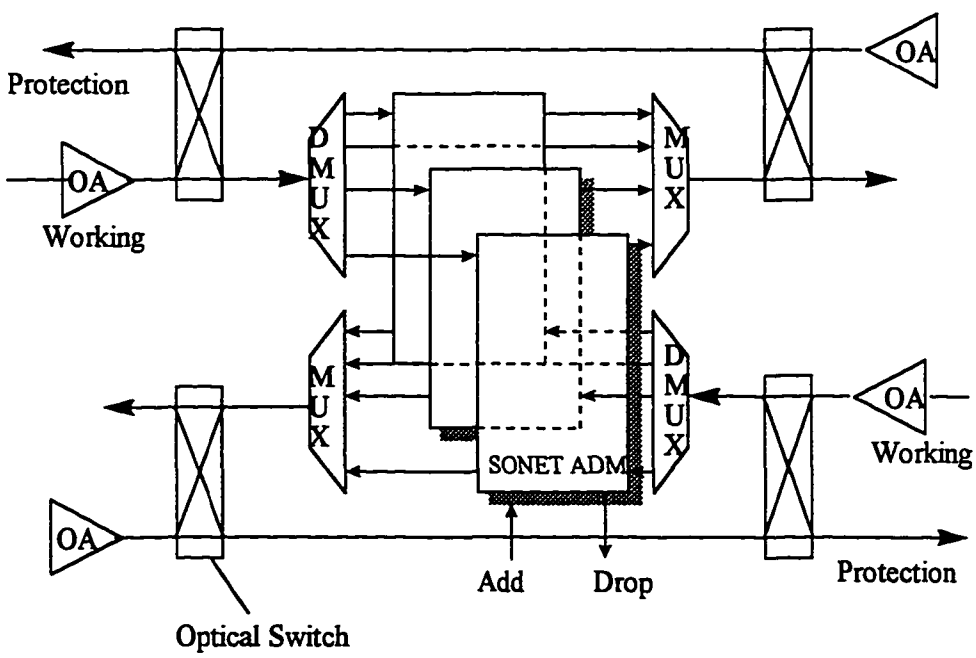

Figure 3.16: WDM Optical Node

When cable cut happens, the signal will be switched from working fiber to protection fiber by an optical switch. The signals on protection then go

through the cascaded EDFAs and bypass all the other nodes to the node at other side of the fiber cut. In the next chapter, the issues of signal pass through a cascade of EDFA and their impacts to the network performance will be discussed.

The WDM protection scheme is a very complicated issue which include monitoring, provisioning, and network control and management. The protection issue is still a research project and there is no standard yet. This thesis will not discuss this issue in details.

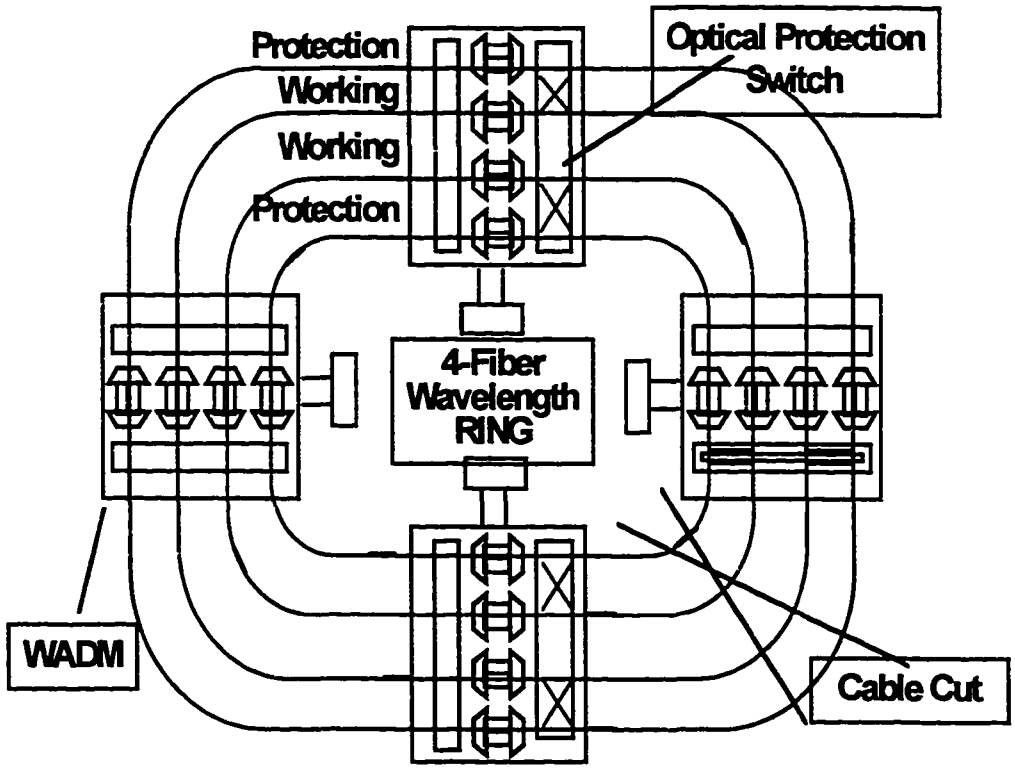

3.17 4-Fiber Bi-Directional Ring with Line Switch Protection

Chapter 4

PERFORMANCE ANALYSIS OF CRITICAL WDM COMPONENTS FOR THE RING NETWORK

4.1 INTRODUCTION

The WDM technology sees a tremendous potential for high-capacity and high-speed all-optic communications. The optical layer will support different levels of optical transparency which will be achieved by combining the network element (NE) in a variety of ways. The network elements include fiber-cross-connect (FXC), wavelength add-drop multiplexer (WADM), optical amplifier (OA) or wavelength amplifier (WAMP), wavelength terminal multiplexer (WTM), wavelength router (WR), wavelength interchanging cross-connect (WIXC), wavelength selective cross-connect (WSXC), etc. For the WDM self-healing ring, the WADM, OA and WTM are the most important NEs. WIXC and WSXC also will play a very important role in the network work monitoring and large reconfigurable network for traffic routing and network configuration. For the optical network, the real limitation is the need to regenerate WDM optical signals as they undergo attenuation and loss when propagating along a fiber link or network. The bandwidth available in the low-attenuation passband within a standard single-mode optical fiber is around 30 nm. How to fully utilize these range of bandwidth is the challenge for optical system and component designers.

Here we just briefly describe the functionality of the passive network element.

1) WADM: Each client on the WDM SHR that sends and receives his own information from the ring network is through the wavelength add-drop multiplexers (WADM). A wavelength add-drop multiplexer is a network

element that accepts multiwavelength signals from a transport facility and is capable of selectably dropping, adding, or passing through the single wavelength signals. The single wavelength signals that are passing through are multiplexed with added signals to form a multiwavelength signal. The insertion loss for different channels is dependent on the wavelength, which will add some constraints on the WDM signals of the working path of SHR. The structure and performance analysis of WADM in the ring network will be discussed in Chapter 4.

2) CROSS-CONNECT COMPONENTS

The fiber cross-connect (FXC) in the local exchange network functions as a component to rearrange the network connectivity, e.g. connecting between the SHR or other network, and is not strictly a network element. A Wavelength Selective Cross-Connect (WSXC) is a network element that accepts multiwavelength signals from a transport facility (any may accept single wavelength signals at the client network interfaces), and cross-connects individual wavelengths without wavelength interchange. A WSXC is a strictly non-blocking cross-connect, but only with respect to a particular wavelength. Wavelength Router (WR) is a network element with multiple transport interfaces that internally routes multiwavelength signals among specific, fixed transport interfaces. Wavelength Terminal Multiplexers (WTM) is a network element that accepts a multiwavelength signal from a transport facility and demultiplexes it into single wavelength signals. It also multiplexes single wavelength signals from the client network and creates a multiwavelength signal that interfaces with a transport facility.

Since the use of EDFA cascades represent the key technology which enables the realization of the WDM ring networks, this chapter will focus on the

challenges which face EDFA cascades with multiwavelength handling capabilities.

4.2 PRINCIPLE OF EDFA

Recent and forceful emergence of EDFA has bring the WDM technology for optical network all possible. Now the fundamentals of EDFA have been fully studied and understood[22][23]. New structure and material of EDFA to cope with the variety of applications are continuously being developed. In this thesis, a complete methodology of EDFA optimization for WDM multi-path access network has been developed. The optimization analysis for individual amplifier performance parameters and overall performance of an amplifier cascade for best overall system performance will presente in this chapter by using computer simulation.

The computer simulation of EDFA is based on the modeling of the light amplification in erbium-doped single-mode fibers. The erbium-doped fiber amplifier can be considered as the three-level laser system with energy level shown in Figure 4.1a [24]. By definition, level 1 is the ground level, level 2 is the metastable level characterized by a long time τ, and level 3 is the pump level.

Simplified energy-level of Er^{3+}:glass figure:

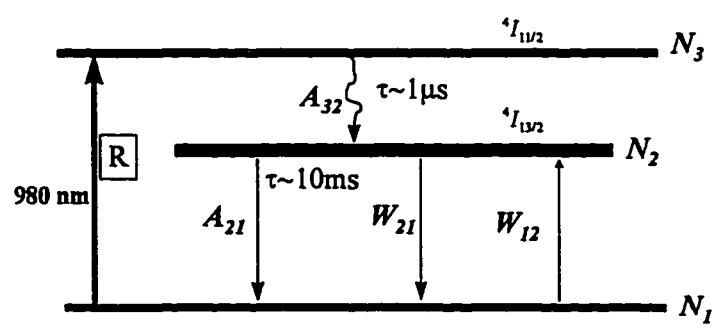

Figure 4.1a Simplified Energy Diagram of Er-doped Fiber

In the 980 nm pump region, we can use the two-level model to present the EDFA. This is because (1) no pump Excited State Absorption (ESA) occurs for 980 nm pumped amplifiers, (2) for pumping into the 980-nm absorption band, the population in the $^4I_{11/2}$ manifold is negligible, (3) the non-radiative decay on the third level is much faster than the intermediate level (1 μs and 10 ms respectively). Finally, direct pumping into the $^4I_{11/2}$-$^4I_{15/2}$ transition also behaves as a two-level system because of the rapid thermalization in the metastable manifold [24].

Based on the two-level system, the gain and noise properties of EDFA can be represented theoretically by a set of coupled partial differential equations [24-26]. We can think of light in the amplifier to be propagating as a number of optical beams of frequency bandwidth $\Delta\lambda_K$ centered at the optical wavelength $\lambda_K = c/\lambda_K$. This notation describes both narrow line beams such as pump and signal sources when $\Delta\nu \cong 0$, and broadband amplified spontaneous emission (ASE) where $\Delta\nu$ equals the frequency steps used in the simulation to resolve the ASE spectrum. Then integration over optical frequency is approximated by a summation over k.

For a given erbium-doped fiber, one can measure the loss spectrum $\alpha(\lambda)$ and gain spectrum $g^*(\lambda)$ by method provide in [24], which are:

$$\alpha(\lambda) = \sigma_a(\lambda)\Gamma(\lambda)n_t \tag{4.1}$$

$$g^*(\lambda) = \sigma_e(\lambda)\Gamma(\lambda)n_t \tag{4.2}$$

where $\Gamma(\lambda)$ is the overlap integral between the optical mode and erbium ions and n_t is the density of erbium ions. The absorption and emission cross sections are σ_a and σ_e respectively. The optical signals' behavior in the erbium-doped fiber can be characterized by set of rate and propagation equations. The

rate equations which describe the effects of absorption, stimulated emission, and spontaneous emission he populations of the ground and metastable states.

For this two-level system with the k optical beams:

$$\frac{dn_2}{dt} = \sum_k \frac{P_k i_k \sigma_{ak}}{h\nu_k} n_1(r,\phi,z) - \sum_k \frac{P_k i_k \sigma_{ek}}{h\nu_k} n_2(r,\phi,z) - \frac{n_2(r,\phi,z)}{\tau} \tag{4.3}$$

$$n_t(r,\phi,z) = n_1(r,\phi,z) + n_2(r,\phi,z) \tag{4.4}$$

Equation 4.4 is the particle conservation for the two level system, where $n_t(r,\phi,z)$ is the local erbium ion density.

The propagation equations describe the optical beams propagating in through the fiber, which are:

$$\begin{aligned}\frac{dP_k}{dz} = u_k \sigma_{ek} \int_0^{2\pi}\int_0^{\infty} i_k(r,\phi,) n_2(r,\phi,z) r dr d\phi (P_k(z) + mh\nu_k) - \\ .u_k \sigma_{ak} \int_0^{2\pi}\int_0^{\infty} i_k(r,\phi) \cdot n_1(r,\phi,z) dr d\phi (P_k(z))\end{aligned} \tag{4.5}$$

where each beam is traveling either in the forward (u_k = 1) or backward (u_k = -1) direction. Here $mh\nu_k$ is the contribution of spontaneous emission from the local n_2 population, and its growth through the amplifier. In models that have ASE, both forward and backward components should be included. The number of modes m is normally 2, as in the case of the optical fiber supporting only the two polarization states of the lowest order optical mode.

Once the boundary conditions for the k beams are specified at z = 0, L, (4.3) and (4.5) are integrated over space (z), optical frequency (k), and time (t). By setting the time derivative in (4.3) equal to zero, the problem is reduce to the steady-state case. This condition is applicable for CW beams, or those

modulated at frequencies greater than ~ 10 kHZ [27][28][29]. There are several steady-state models are presented base on different conditions and applications. The analytical model is used in this study [30].

The computer simulation is used in this thesis work for developing a numerical process of modeling a WDM self-healing ring network, and the relaxation approach bas been used. The relaxation method is the process that starts from a very general trial and reaches to the final result by several iterations.

One of the difficulties of using EDFAs in the multiwavelength lightwave system is that EDFA has a non-uniform gain profile in the 1550 nm region [31]. The effects of these gain differences tend to be cumulative, so adjacent channels traveling through a cascade of amplifiers may have significantly different power and signal to noise ratio (SNR) levels when delivered to a client receiver. A receiver designed to accept the lower power signal from one channel may be overloaded when presented with the higher power channel, the range of the signal power level which a receiver can receive is called the receiver's dynamic range. Thus, signals on different channels should remain within the receiver's dynamic range. More importantly, the degradation of the SNR of an optical channel through a cascade of EDFAs is a strong function of wavelength. Given an SNR specification that must be met at the end of a wavelength path, the line is limited by the SNR of the worst channel. The noise figure (ratio of input to output SNR) and gain flatness of an EDFA is a function of its design, its power levels, and wavelength channels. Therefore, the parameters of the EDFA should be optimized to achieve the optimum performance.

The general guideline for the EDFA optimization is to get largest gain and signal-to-noise ratio possible while keeping the spectral gain variation at the least. Maintaining the large gain insures that the fewest amplifiers are needed, and reducing gain variation either simplifies the practical implementation of gain equalizers required at each amplifier or totally obviates the need for

external gain equalization. In the general case, the EDFA optimization will include (1) the signal wavelength λs, (2) EDFA fiber length L, (3) pump direction, (4) the pump absorption band and the pump wavelength λp within this band, (5) peak erbium concentration ρ_o and concentration profile $\rho(r)$ and (6) fiber waveguide characteristics (λ_c, NA, a) and mode envelopes ψ. In this thesis, we are not going to discuss the EDF material and its waveguide characteristics. The optimization effort will focus on items (1) to (4).

4.3 WDM CHANNEL ALLOCATION OPTIMIZATION

As we know, the EDFA gain bandwidth in the 1550-nm low attenuation region is around 30-nm. But for a specific application, like given total wavelength number or given input optical signal level, how to select an optimized wavelength for a particular EDF is the first step in the network design.

Most of EDFAs used in the multipath WDM access network system usually have following common conditions: (1) total input power is high enough to saturate the EDFA (2) EDFA is pumped by 980-nm laser so that there is on relevant excited-state absorption, (3) the Stark-split energy levels of the erbium atoms are homogeneously broadened, and (4) the area of the erbium-doped active region is small compared to that of the optical mode at each wavelength of interest, so $\Gamma(\lambda)$ can be treated as a constant. Therefore, the EDFA can be well represented by the analytical model of Saleh *et at.* [30]. The basic equations of this model are the rate and propagation equations from which the ASE terms have been deleted.

The equations are [30]:

$$\frac{\partial n_2(z,t)}{dt} = -\frac{n_2(z,t)}{\tau} - \frac{1}{\rho A}\sum_j u_j \frac{\partial P_j(z,t)}{\partial z}$$

$$\frac{\partial n_1(z,t)}{\partial t} = -\frac{\partial n_2(z,t)}{\partial t} \tag{4.6}$$

$$\frac{\partial P_k(z,t)}{\partial z} = u_k((\alpha_k + g_k^*)n_2(z,t) - \alpha_k)P_k(z,t) \tag{4.7}$$

here, n_2 is the normalized number. For the steady-state case:

$$\frac{\partial n_2(z,t)}{\partial t} = 0$$

$$n_2 = -\frac{-\tau}{n_t A_{eff}}\sum_j \frac{u_j}{h\nu}\frac{dP_j}{dz} \tag{4.8}$$

insert (4.8) to (4.7), notice that: $\xi = A_{eff} n_t/\tau$ is the ratio of the linear density (m^{-1}) of ions to the metastable lifetime. If can be determined from measurement of the fiber saturation power P_k^{IS} as $\xi = P_k^{IS}(\alpha_k + g_k^*)/h\nu_k$.

$$\frac{dP_k}{P_k} = -u_k\left[\frac{(\alpha_k + g_k^*)}{\xi}\sum_j \frac{u_j}{h\nu_j}\frac{dP_j}{dz} + \alpha_k\right]dz \tag{4.9}$$

we use the photon flux to replace the power: $Q_k = P_k/h\nu_k$. The two sides of equation (4.9) are integrated over the EDFA length L:

$$Q_k = Q_k^{in}\exp\left\{(Q^{in} - Q^{out})\frac{\alpha_k + g_k^*}{\xi} - \alpha_k L\right\} \tag{4.10}$$

here, $Q^{in} = \sum_j Q_j^{in}$, $Q^{out} = \sum_j Q_j^{out}$. Summing (4.10) over all the k beams yields the final equation:

$$Q^{out} = \sum_k Q_k^{in} \exp\left\{(Q^{in} - Q^{out})\frac{\alpha_k + g_k^*}{\xi} - \alpha_k L\right\} \tag{4.11}$$

Equation (4.11) is an implicit equation for the total output photon flux from the amplifier, that depends only on the fiber parameters and input fluxes. The output power of the individual beams are obtained by solving (4.11) for Q^{out}, which can solved by Newton-Raphson technique, and substituting it into (4.10).

The signal profile is depended on both of the signal gain profile and ASE profile. The spontaneous emission noise at wavelength λ_k emitted in a single direction by a section of amplifier of length dz is given by:

$$dP_{sp} = g_k^* n_2 \Delta\nu dz \tag{4.12}$$

where, n_2 can get by combining (4.7) and (4.8):

$$n_2 = -\frac{1}{\xi}\sum_j (u_j u_j \frac{(\alpha_j + g_j^*)}{\xi} n_2 - \alpha_j)\frac{P_j}{h\nu_j}) \tag{4.13}$$

here, $u_j u_j = 1$, and $Q_j = P_j / h\nu_j$.

so that:

$$n_2 = \frac{\sum_j \alpha_j Q_j}{\xi(1 + \sum_j \frac{(\alpha_j + g_j^*)}{\xi} Q_j)} \tag{4.14}$$

The ASE emitted from the output or input end of the amplifier at wavelength λ_k can be obtained by multiplying the spontaneous emission from each section of the amplifier by the amplifier gain at λ_k from that section to the desired end of the amplifier and integrating over the length of the amplifier. Thus if G_k (z_1,

z_2) is the gain at λ_k between z_1 and z_2 the ASE power at the amplifier output is given by:

$$\begin{aligned} Q_k^{+ASE}(L) &= \int_0^L dQ_k G_k(z,L) \\ &= \Delta v g_k^* \int_0^L n_2(z) G_k(z,L) dz \end{aligned} \tag{4.15}$$

For the gain $G_k(z)$ at wavelength λ_k can be obtained by Q_k^{out} / Q_k^{in}, from (4.10), the gain of k beam at end of amplifier L for the forward direction is:

$$G_k = \exp\left\{(Q^{in} - Q^{out})\frac{\alpha_k + g_k^*}{\xi} - \alpha_k L\right\} \tag{4.16}$$

So the total output ASE is given by insert (4.16) into (4.15):

$$Q_k^{+ASE}(L) = \Delta v g_k^* \int_0^L \left[\frac{\sum_k \alpha_k Q^{out}(z)}{\xi(1 + \sum_k \frac{(\alpha_k + g_k^*)}{\xi} Q^{out}(z)} \exp\left\{ (Q^{in} - Q^{out}(z)) \frac{\alpha_k + g_k^*}{\xi} - \alpha_k L \right\} \right] dz \tag{4.17}$$

In (4.17), it expresses that the ASE spectrum is dependent on the total signal input and the EDF material. To decide the wavelength range, we can use one signal at 1550-nm region with its power equals to the sum of the all the signals, as the input signal into a given EDFA instead of the all the signals because we don't know what the wavelength of each signal could be. With one fixed input signal, the optimized wavelength bandwidth which is the most flat region of the EDFA's gain profile, optimized by varying the fiber length (assuming the pump power is fixed).

In this thesis work we choose the network of 16 wavelength and input power of -15 dBm (0.03662 mw) per channel as the study model which is practical for the regional access network [32]. The total input power of all the 16 wavelength is 16 x 0.03662 = 0.5059 mw (~ -2.9 dBm). To determine the optimal wavelength range and optimal fiber length [33], one signal of -2.9 dBm (probe signal) was launched into the EDFA with different fiber length, ranging from 4 m to 60 m at an interval of 4 m. The fiber is completely characterized knowing the four parameters; the Er^{3+} absorption coefficient $\alpha(\lambda)$, the gain coefficient $g(\lambda)$, the fiber excess loss l, and the fiber saturation parameter $\varsigma = An_t/\tau$. Here, A is the erbium core area, n_t is the ion density, and τ the metastable lifetime. Figure 4.1b shows the emission and absorption cross section of Lucent E002 EDF used in simulation where $\varsigma = 1.05 \times 10^{15}$, $\tau = 9.9$ ms.

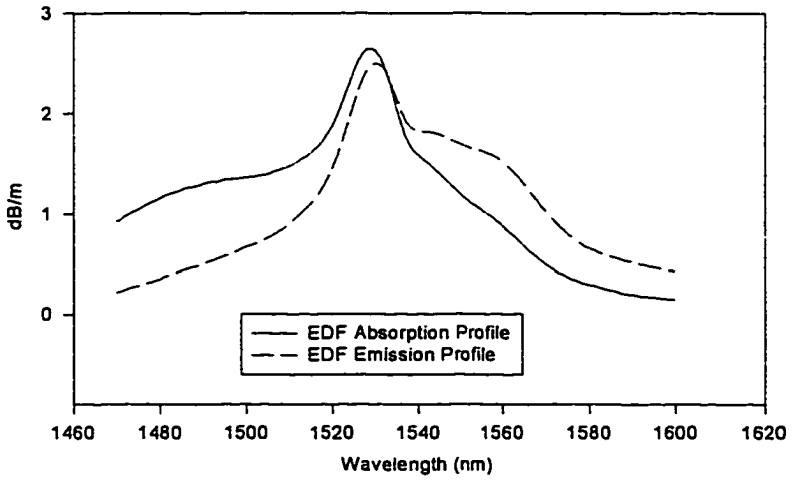

Figure 4.1b EDF E002 Absorption and Emission Profile

First the forward pumping by 980 nm pump at 90 mw is studied. The input signal wavelength is 1550 nm which is randomly chosen from the 1.5 μm

range. Computer simulation techniques are used to determine the signal level and noise spectra for the EDFA. Each amplifier is represented by (4.10) (4.11) and (4.17). The forward ASE spectra are resolved in 0.2 nm resolution. The results are shown in Figure 4.2. Complete theoretical studies have been made about the EDFA gain spectrum changes caused by the signal saturation, EDFA length, pumping power etc. in [34]. The Er:glass absorption and emission cross sections do not correspond to a single laser transition, but rather to a superposition of several individual transition, which initiated from , or terminated in the Stark levels of the ground and upper manifolds. Within each Stark manifold, a fast thermalizaiton process results in an equilibrium (or Boltzmann) population distribution.

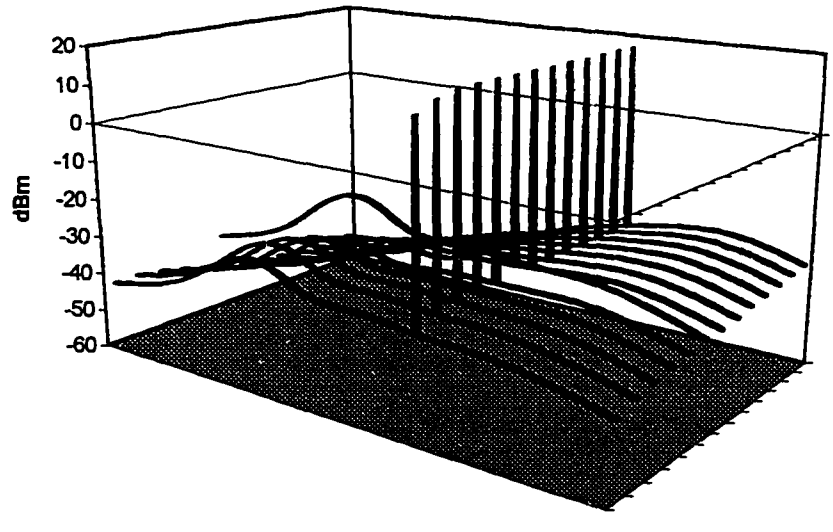

Figure 4.2 Spectra of signal and ASE for different EDF length with forward pumping and one signal input at 1550 nm.

An increase of stimulated emission from a monochromatic signal results in changes in the total manifold populatons (i.e. an increase of N_1 and a decrease

of N_2), while the equilibrium distributions remain unchanged. Since the cross section line shapes are only determined by this equilibrium distribution, and therefore remain also unchanged, the gain coefficient spectrum (i.e., $\sigma_e(\lambda)N_2-\sigma_aN_1$) homogeneous broadening EDF, the homogeneity of the forward pumped EDFA gain spectrum can be evidenced by the changes of the output ASE in presence of a strong, monochromatic saturating signal. The experimental and theoretical results [35] have shown that the changes observed in the forward ASE spectrum of a forward pumped EDFA $P_{ASE}^{forward}(\lambda, L)$ at z = L during saturation approximately follow the changes in the EDFA gain spectrum $G(\lambda, L)$ when the change in equivalent input noise factor are generally small. The ASE power spectrum closely emulates the gain spectrum, so it provides useful information on the EDFA operating characteristics in various signal power, fiber length and pump power regimes. Therefore, from the ASE spectrum, we can roughly tell the flat gain region. Figure 4.3 is a closer look at the ASE spectra of Figure 4.2. In the Figure 4.3, it shows that the flat gain range of Lucent E002 erbium-doped fiber is between 1542 nm to 1558 nm (16 nm) at the EDF length between 24 m to 28 m. With the existing technology of laser and optical filters such as MUX and DEMUX, the practical wavelength spacing can be chosen from 0.8 nm to 1.6 nm [36-39]. We use 1.6 nm spacing in this work, therefore 11 wavelength from 1543 nm to 1557.4 nm can be accommodated in this range. Following the first estimate of the 16 wavelengths -15 dBm signal input power, in order to keep the total input power unchanged, therefore to keep the gain profile unchanged, we can spread the total input power of -2.9 dBm to 11 signals which equals to 0.5059/11 = 0.0460 mW (~ -13.3 dBm) per channel. This is how we can decide the signal input power and wavelength based on the information of a single EDF and pump power.

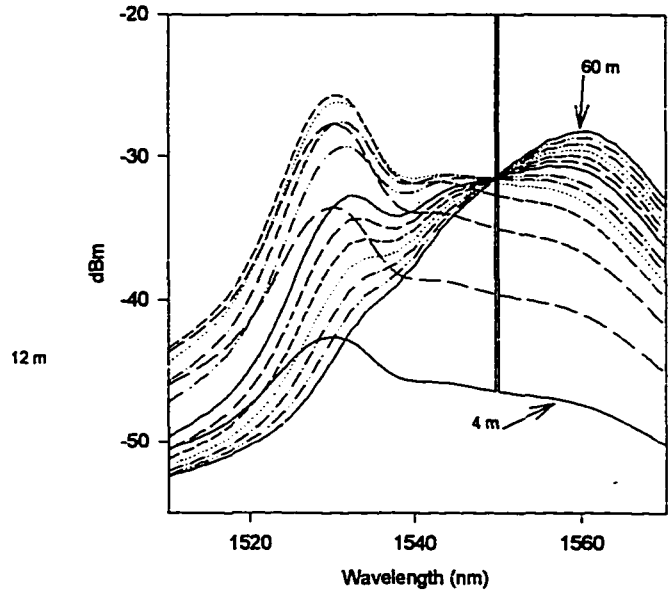

Figure 4.3: , Forward pumped EDFA ASE spectra for fiber length range from 4 m to 60 m with interval of 4m, the flat gain is at around fiber length of 24 m

4.4 EDFA FIBER LENGTH OPTIMIZATION

A general numeric procedure to determine the optimum erbium-doped fiber length for WDM operation based on the criteria that maximizes the difference between the least-favored signal gain and the spectral gain variation has been proposed [33] in this research. To determine the optimum fiber length, L_{opt}, the following procedure is carried out:

a) From individual spectral gain curves, determine the gain $G_L(L)$ and the spectral gain variation $\Delta G(L) = G_M - G_L(L)$ versus the amplifier length, where $G_L(L)$ is the least-favored signal gain from among all the signal wavelengths, and G_M is most-favored signal gain from among all of the signal wavelength.

b) Using the curve from a.) above, calculate the value of L which corresponds to the maximum of M, where M is a metric function defined as

$$M(L) = G_L(L) - \Delta G(L) \qquad (4.18)$$

Figure 4.4 shows the forward pumped EDFA's worst SNR among all the signals, G_L, ΔG and M by using the 11 signals we have got from the wavelength allocation optimization in section 4.3 with 90 mW of pumping power at 980-nm wavelength.

The resulting value, L_{opt}, is the optimum amplifier length. This is equivalent to determining the amplifier length that maximizes the difference between the curves of $G_L(L)$ and $\Delta G(L)$ in Figure 4.4, in which the optimum length L_{opt} = 24 m. In Figure 4.4, it also shows the worst SNR for the forward pumped EDFA among all the signals which can be used for the analysis of overall

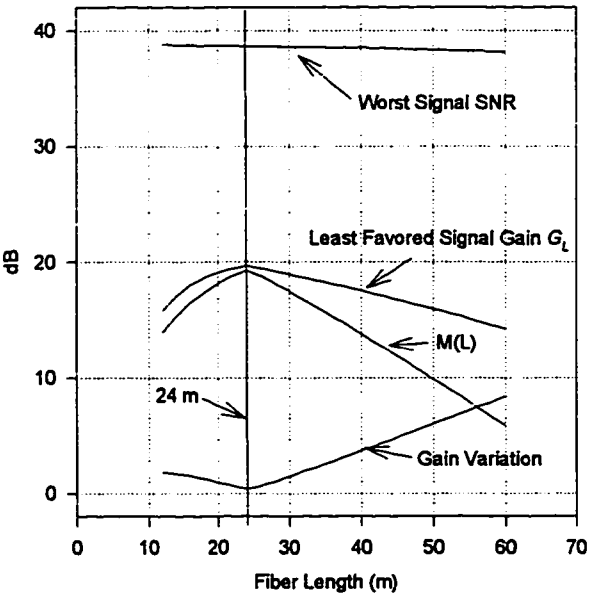

Figure 4.4: Forward pumped EDFA signal worst SNR, least gain, gain variation and M(L)

performance of an optimized EDFA. In this particular case, at optimum fiber length (24 m), the gain variation is about 0.39 dB and the worst SNR among all the signals is better than 38 dB. Figure 4.5 shows the signal gain spectrum of the EDFA operating at the optimum fiber length.

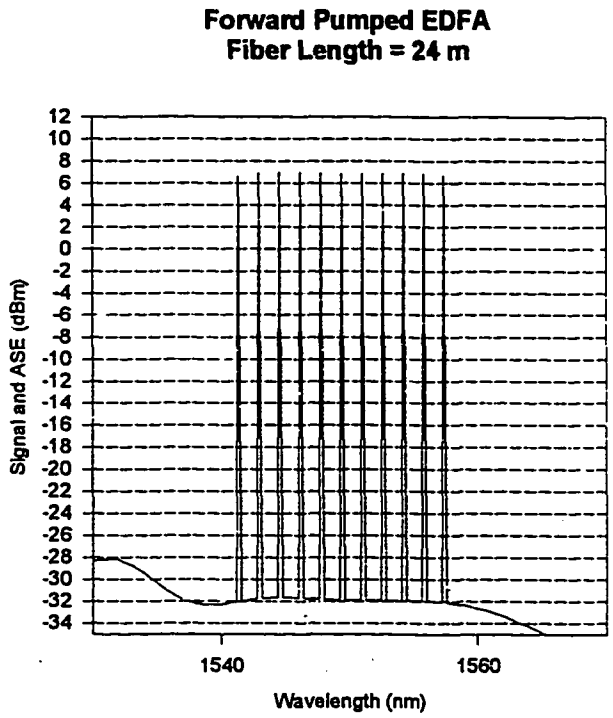

Figure 4.5: Signal and ASE spectrum of forward pumped EDFA at 24 m fiber length and 90 mW of 980-nm pump

4.5 ANALYSIS OF EDFA PUMPING DIRECTION

For EDFA operation, a very important parameter is the direction of the pumping which is either forward or backward or both. The pumping direction will effect the SNR, gain and gain variation of the EDFA [40]. The direction of the pumping is depended on the EDFA's application, operation condition, saturation level etc. [41].

The analysis of the pumping direction of the EDFA is basically to compare the gain, gain variation, SNR of the different pumping schemes at optimized condition. The optimized wavelength allocation of fiber length is obtained in the previous sectons. For the backward pumped EDFA we can use the same methodology to get the gain profiles at different fiber length to decide the wavelength allocation and, thereafter, optimum fiber length.

Figure 4.6 is the spectra of EDFA at different fiber length backward pumped by 980 nm laser of 90 mW with one input signal of -2.9 dBm. Figure 4.7 is a close look at the ASE of the Figure 4.6. Figure 4.7 shows the peak of the ASE (around 1530-nm) increasing quickly along with the increase of the fiber length, which will be discussed in the following.

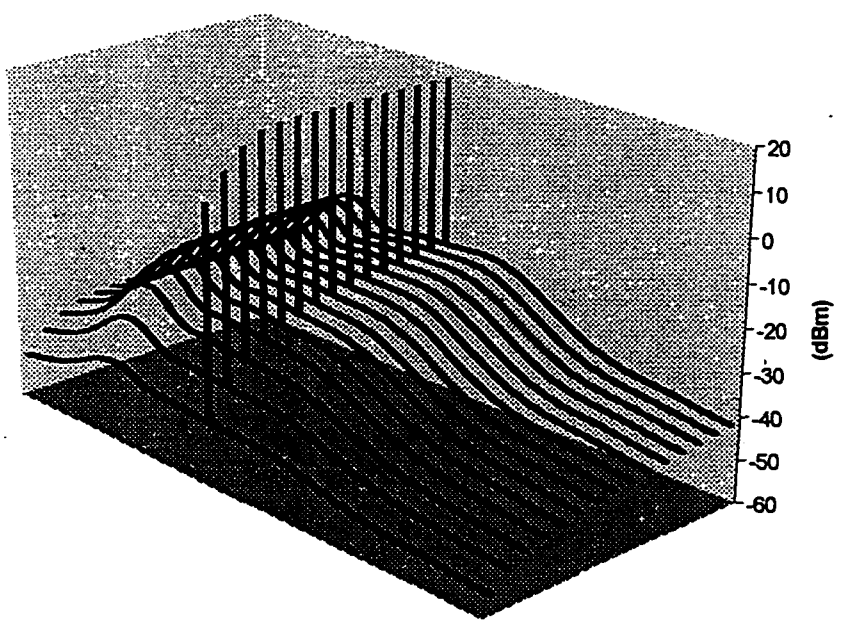

Figure 4.6: Backward pumped EDFA spectra

It is also shown in Figure 4.7 that the total backward pumped ASE power P_{ASE}^{out} (backward pumped) is much larger than forward pumped ASE. This is because the backward pumped ASE is amplified as it propagates in the direction of

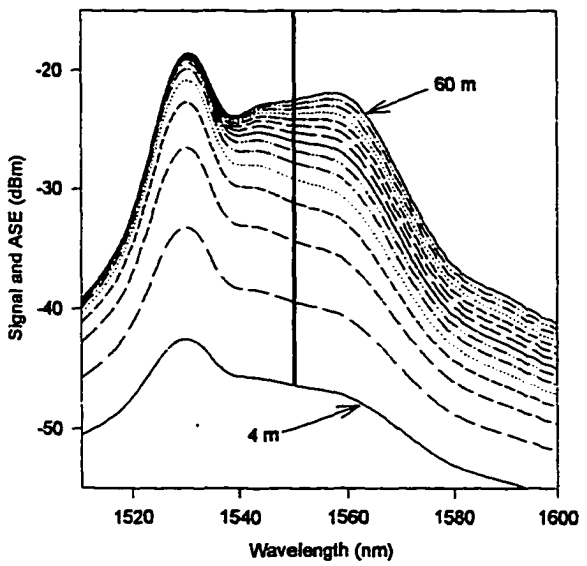

Figure 4.7: , Backward pumped EDFA ASE spectra for fiber length range from 4 m to 60 m with interval of 4m, the ASE increased quickly with the fiber length

transmission and forward pumped is absorbed instead. In the regime of low medium inversion, corresponding to low pump powers, ground level absorption dominates at short wavelength (λ = 1.52 - 1.54 μm), resulting in the vanishing of the main peak near λ = 1.53 μm. This absorption of the main peak is more important in the forward ASE (co-propagate with pump) than backward ASE (couter-propagate with pump). This phenomena is shown in the Figure 4.3 and Figure 4.7. In Figure 4.3, the main ASE peak (forward ASE) is vanishing along with the increasing fiber length. This is because the pump power is depleted along the fiber length which corresponding to low pump power and low medium inversion. But the main ASE peak in Figure 4.5 is still kept very high along with the fiber length increase. Due to the fact that ASE is much higher in a backward pumped EDFA, for single stage EDFA,

therefore, the total NF is larger than the forward pumped EDFA. The analysis of two different directional pumping results can be done by comparing the SNR and figure of merit M for forward and backward pumping over the fiber length.

By comparison, Figure 4.8 illustrated the curve of worst SNR, least gain G_L, gain variation ΔG and figure of merit M. The SNR drops quickly along with the fiber length increase, this is because the ASE propagate towards to the pump is amplified along the fiber. The SNR at fiber length of 24 meter is 5 dB lower than that of forward pumped EDFA. It becomes obvious that for the regional network, for which the total input signal is about -3 dBm, the forward pumped EDFA is superior when the EDFA is operating in the moderate or deep saturation. Figure 4.9 shows the signal and ASE profile at the optimum fiber length of 24 m of backward pumped EDFA, which shows the backward pumped EDFA has a higher and non-flat ASE and lower average gain compared to that of the forward pumped EDFA illustrated in Figure 4.5.

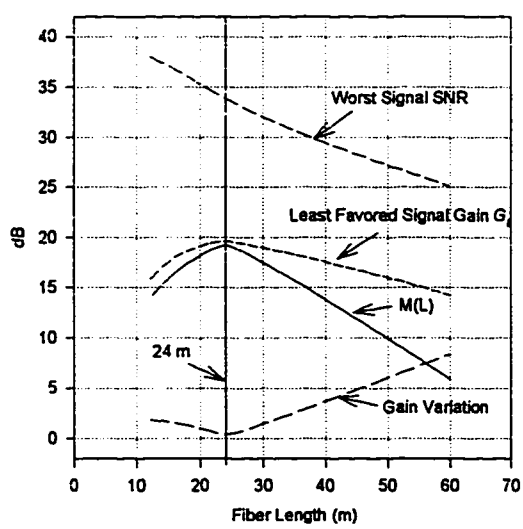

Figure 4.8: Backward pumped EDFA Signal Profile at Different Fiber Length

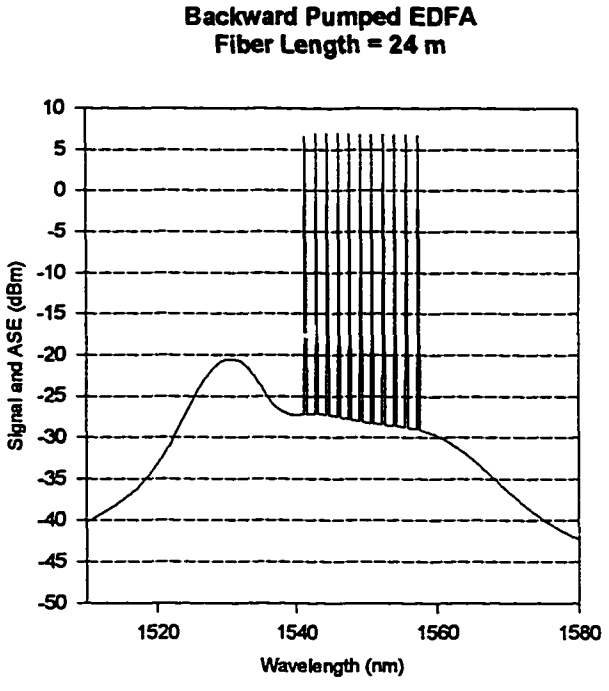

Figure 4.9: Signal and ASE spectrum for backward pumped EDFA at 24 m fiber length and and 90 mW of 980-nm pump

4.6 COMPARISON OF THE OVERALL OPTIMIZED PERFORMANCE OF 980 AND 1480 NM PUMPED CASCADE EDFA

Using computer simulation techniques, this section focuses on comparing the overall cascade performance of 980- and 1480-nm pumped EDFA cascade in WDM multiple access lightwave networks. The general question we address is which pump wavelength provides a more uniform gain spectrum and more equalized SNRs after a chain of amplifiers. To carry out these comparisons appropriately, we consider optimizing the individual amplifier performance parameters for multiple wavelength operation and relate these to the overall performance of an amplifier cascade for best overall system performance.

Issues considered are pump power, pump wavelength, Erbium-doped fiber length, and input signal levels and their spectral range.

Limitations to the capacity of such cascades, due to accumulated amplified spontaneous emission (ASE), are evaluated in terms of the amplifier and transmission system characteristics. The effect of inter-amplifier fiber loss and per-channel input signal level on the inter-channel power variations and SNR flatness is also analyzed. The relationship between a given population inversion and optimum gain flatness will be thoroughly examined. One of the main objectives of this work is to either simplify the practical implementation of gain equalizers required to achieve flat gain or to totally obviate the need for gain equalization, depending on the transmission system characteristics and the particular application under consideration.

First, a simple optimization analysis which has been briefly discussed in section 4.2 is suggested to relate the individual amplifier performance parameters to the overall performance of an amplifier cascade for best overall system performance. The general question we address is how to achieve an amplifier with the largest gain possible while keeping the spectral gain variation as small as possible. Maintaining a large gain insures that the fewest amplifiers are needed, and reducing gain variations either simplifies the practical implementation of gain equalizers required at each amplifier or totally obviates the need for external gain equalization. Specifically, we propose a general numerical procedure to determine the optimum amplifier length for best overall cascade performance based on a criteria that maximizes the individual amplifier gain subject to the constraint of minimizing the overall gain variation of the cascade, for a given total system gain. Then, the dependence of the optimum fiber length on pump power and input signal level will also be considered. We also optimize pump power, pump wavelength, and input signal levels and their spectral range for best overall cascade performance.

The optimization method is then used to compare the overall cascade performance of 980-nm pumping and 1480-nm pumping over four different spectral regions of the usable amplifier band. In the first spectral region, where we illustrate the optimization method, we consider the important case of a system using 15 signal wavelengths spanning the entire usable range of the amplifier from 1538 nm to 1566 nm. In the second spectral region, we have selected a relatively narrower band, the 1540-1560 nm amplifier band, over which it is practically easier to implement gain equalization. In the third spectral region, we have selected still narrower band, the 1542-1552 nm, where, as is shown below, it is possible to entirely obviate the need for gain equalization. This is in contrast to the fourth selected spectral region, the 1552-1562 nm band, also shown below, where there is still a need (although it is an equally narrow band, 10-nm) for gain equalization.

4.6.1 CASCADE PERFORMANCE OVER THE 1538-1566-nm AMPLIFIER BAND

In this section, a simple method to optimize the individual amplifier performance parameters and relate these to the overall performance of an amplifier cascade for best overall system performance is presented. The method determines the erbium fiber length required to maximize the individual amplifier gain subject to the constraint of minimizing the overall gain variation of the cascade, for a given total system gain. To illustrate the method, we use an example system with fifteen wavelengths in the range of 1538 to 1566 nm. The optimization method is then used to compare the overall cascade performance for 980-nm pumping and 1480-nm pumping, assuming there are fifteen signal wavelengths spanning the entire usable wavelength range of the amplifier from 1538 to 1566 nm.

Our main concern is on multi-access lightwave networks, where in addition to achieving adequate SNR for all channels, the inter-channel power variations must be kept as small as possible throughout the network in order to alleviate excessive dynamic range requirements on the optical receivers [42]. However, as will be shown below, we will encounter some cases where the overall cascade performance is not good enough for multi-access, but could be good enough for point-to-point applications, where achieving high SNRs for all channels is the primary concern without regard to signal level variations. The main objective is to keep the inter-channel power variations at the output of any amplifier in a cascade within a receiver dynamic range of less than about 10 dB while maintaining adequate noise performance at the less-favored signal wavelengths without resorting to external equalization.

Numerical Analysis

The EDFA model assumes an alumino-germano silicate fiber {core (mole %), GeO2/Al2O3 = 24/0.1}, with amplifier parameters the same as those of fiber 2a in [27], and thus all of the numerical conclusions reported here apply to this specific fiber. However, the optimization method can be applied more generally to any other EDFAs taking into account their specific characteristics. The fiber is completely characterized knowing only four parameters; the Er3+ absorption coefficient a(l), the gain coefficient g(l), the fiber excess loss l (0.06 dB/m), and fiber saturation parameter z = Ant/t = 1.37 x 1015 m-1 s-1 [27]. Here A is the erbium core area (the index-core radius a = 0.97 mm), nt is the ion density, t is the metastable lifetime (9.9 ms). Forward pumping schemes with 50 mW of pump power are assumed throughout the calculations at both the 1480-nm and 980-nm pump bands, unless otherwise specified. The signal and ASE noise spectra are calculated based on the spectrally resolved numerical model of Giles [24][27]. The forward and backward ASE spectra are well

resolved in 500 wavelength bands (Dl = 0.2 nm intervals) over the 1470 nm to 1570 nm range. As a starting point, to define the gain characteristics of the amplifier, the power gain versus amplifier length is calculated for each of the signal wavelengths. Typical results for an amplifier with 15 signal wavelengths and total input power of 0.5 mW (-15 dBm/channel), are shown in Figures 4.10 (a) and 4.10(b) for 980-nm and 1480-nm pumping, respectively.

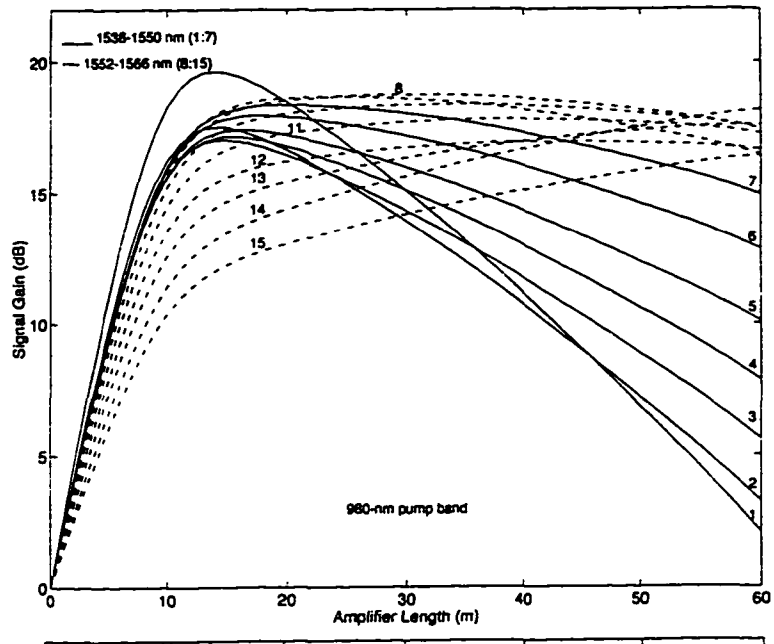

Figure 4.10 (a)

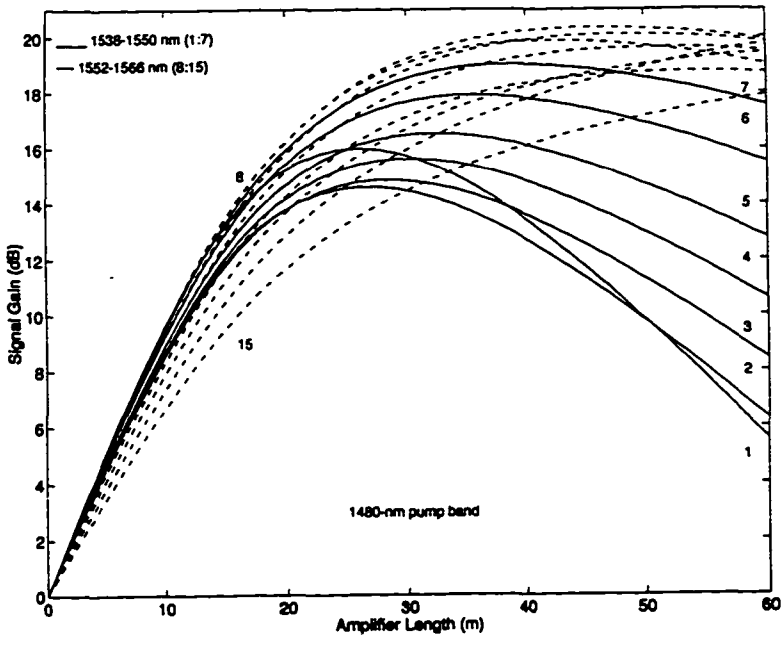

Figure 4.10 (b)

The system model consists of fifteen WDM channels spaced 2-nm apart in the 1538 to 1566 nm amplifier band. The input signal levels to the cascade of EDFAs are -15 dBm/channel at the input of the first amplifier. An optical filter with 1536-nm cutoff wavelength is inserted after each amplifier to remove the ASE in the spectral region below 1536-nm. An optical isolator is also assumed to be placed after each amplifier, which is codirectionally pumped with 50 mW of pump power at either 1480-nm or 980-nm. The span loss between amplifiers is set equal to the least-favored signal gain. As will be shown later, this is the optimal link-loss for optimizing the overall system performance. The accumulated optical SNR reported here is the ratio between the signal level and the accumulated ASE noise power in a 0.2-nm optical bandwidth. The overall system performance is estimated from the optical SNR, which must be more than 14.5 dB to achieve a bit-error ratio (BER) of 10-14 at 10 Gb/s [43].

Optimization Method

When considering the amplifier length for optimizing the cascade performance, we assume that the total system gain and spectral gain variations accumulate from stage to stage according to the simple approximate equations:

$$G_{tot} = N(L)\, G_L(L) \tag{4.19a}$$

$$\Delta G_{cascade}(L) = N(L)\, \Delta G(L) \tag{4.19b}$$

where N is the number of cascaded amplifiers. For the cascade, two optimization criteria should be simultaneously achieved: minimize the gain variation $\Delta G_{cascade}$ and minimize the number of cascaded amplifiers (maximize the individual amplifier gain) required to achieve a given total system gain G_{tot}. This can be achieved by selecting an optimum amplifier length, L_{opt} that maximizes the metric function, M (L), defined as:

$$M(L) = G_L(L) - \Delta G_{cascade}(L) \quad (4.20)$$

This optimization maximizes the individual amplifier gain subject to the constraint of minimizing the overall gain variation of the cascade, for a given G_{tot}. By substituting Eq. (4.19) into Eq. (4.21), the metric can be rewritten in terms of the individual amplifier parameters:

$$M(L) = G_L(L) - [G_{tot}/G_L(L)]\,\Delta G(L) \quad (4.21)$$

The procedure for optimizing the amplifier length for best overall cascade performance is as follows [44]:

i) The power gain versus amplifier length is calculated for each signal wavelength.

ii) Using these results, the least-favored signal gain $G_L(L)$ and the spectral gain variation $\Delta G(L)$ between signal wavelengths are determined versus the amplifier length.

iii) The metric $M(L)$ is calculated from Eq. (3) for a given value of Gtot, and the value of L which produces the largest M is the optimum amplifier length, L_{opt}.

Individual Amplifier Performance Parameters

Fig. 2 shows the least-favored signal gain G_L and the spectral gain variation ΔG between the fifteen signal wavelengths versus the amplifier length for both 980-nm and 1480-nm pumping. With the amplifier characteristics shown in Figure 4.11 and a total gain of 70 dB, the optimum amplifier length, L_{opt}, determined from Eq. (4.21) is 30 m and 29 m for 1480-nm and 980-nm pumping, respectively. Note that L_{opt} in this case can also be determined by merely using the individual amplifier performance parameters, independent of the total system gain. This is achieved by determining the amplifier length that

maximizes the difference between the upper and lower curves of Fig. 2, i., e., the amplifier length that maximizes the difference between the least-favored signal gain and the spectral gain variation of an individual amplifier. Thus, Eq. (4.21) is still applicable, however, with overall gain variation of the cascade $\Delta G_{cascade}$ being replaced with the gain variation of an individual amplifier ΔG. In this case, as can be seen from Fig. 2, the minimum individual gain variation (4.7 dB at either pump wavelength) and the maximum least-favored signal gain (14.0 dB for 980-nm pumping; 14.4 dB for 1480-nm pumping) both occur at a length that coincides with the optimum determined by the metric of (4.21) [33].

Pump Power (mw)	Input Signal per channel (dbm)	1480-nm Pump Band			980-nm Pump Band		
		L_{opt} (m)	ΔG_{min} (dB)	G_{max} (dB)	L_{opt} (m)	ΔG_{min} (dB)	G_{max} (dB)
20	-15	22	3.6	10.3	22	3.5	10.6
50	-20	37	6.0	18.2	35	5.5	17.0
	-15	30	4.7	14.4	29	4.7	14.0
	-10	23	3.9	10.0	22	3.6	10.4
100	-20	43	7.0	21.0	40	6.6	20.0
	-15	36	5.7	17.1	34	5.4	16.0
	-10	28	4.5	13.0	26	4.3	12.8

Table 4.1

Optimum Amplifier Performance For Different Pump Power, Wavelength, and Input Signal Level

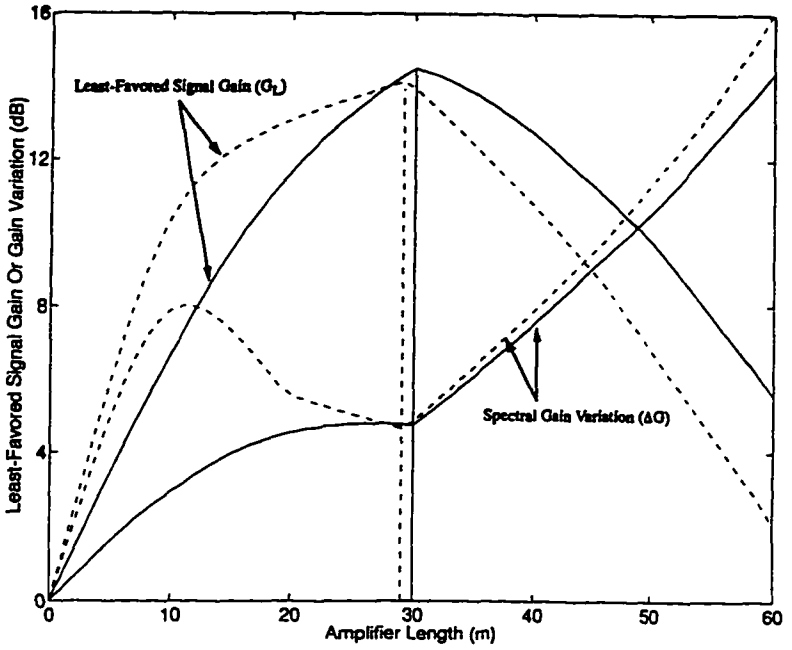

Figure 4.11. Least-favored signal gain G_L and spectral gain variation ΔG between 15-WDM signals versus the amplifier length. Pin = -15 dBm/ch. Ppump = 50 mW. The signal are spaced 2-nm apart in the 1538-1566 nm amplifier band.
- - - 980 nm pump band, ____ 1480 nm pump band

A series of calculations were carried out to determine how the optimum fiber length L_{opt} varies over a range of the input signal levels and pump powers [33]. This includes input signal levels of -10 dBm/channel, -15 dBm/channel, and -20 dBm/channel, together with pump power levels of 20 mW, 50 mW, and 100 mW. The results, tabulated in Table I, indicate that the optimum fiber length Lopt increases with pump power, decreases with input signal level, and is slightly longer for 1480-nm pumping. A general conclusion deduced from the tabulated results is that the input signal level and the pump power can be chosen to yield optimum multiwavelength performance for a given amplifier of fixed length. For example, at an amplifier length of 45 m, pump power higher than 100 mW and signal levels lower than -20 dBm/channel would be needed to achieve optimum performance.

Optimum Gain Flatness Versus Population Inversion of A Single Amplifier

The gain spectrum of the amplifier depends on the combination of the emission and absorption spectra of the doped fiber and may be roughly regarded as weighted averages of emission and absorption cross-sections, with weights supplied by the population densities of, respectively, the excited (n2) and ground states. Thus, a fully inverted amplifier has a gain spectrum whose shape essentially follows that of the emission cross section, since under these conditions, almost all of the Er3+ ions are in the excited state and the ground state is nearly empty. Consequently, a strong inversion should yield a flattened gain spectrum only if the amplifier band occupied by the WDM signals is relatively inherently flat. On the other hand, as will be shown below, an amplifier band which is not inherently flat, requires an optimal, though not critical, population inversion within the doped fiber for optimum gain flatness.

As an illustrative example, Fig. 3 shows the mean inversion parameter, n2/(n1 + n2), versus the amplifier length for both 1480-nm and 980-nm pumping and the fifteen signal wavelengths. For 980-nm pumping, as can be seen from Fig. 4.12, at L_{opt} (29 m), where the spectral gain variation is minimum, the corresponding value of the mean inversion parameter is 0.68 (about 0.65 for 1480-nm pumping). At fiber lengths less than optimum (i., e., L < 20 m), although the mean inversion increases monotonically and approaches unity, however, the spectral gain variations are maximum over this range. These results, which are in conformity with the experimental results reported in [45-46], indicate that strong inversion does not necessarily result in optimum gain flatness. Note also that at fiber lengths higher than optimum (i. e. L > 30 m), when the mean inversion was still decreased, the spectral gain variations increased sharply again. Thus, as indicated above, an optimal, though not critical (not too high, or too low), population inversion is required for

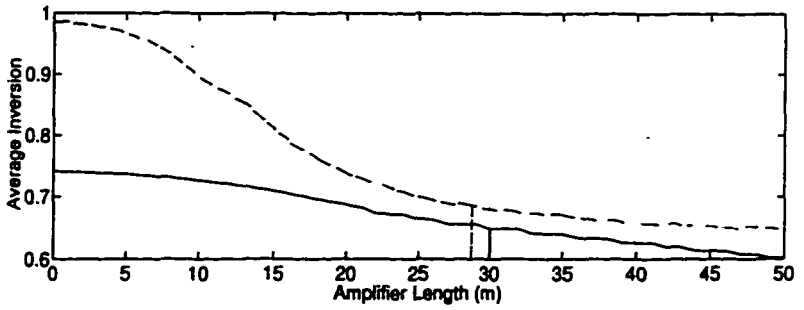

Figure 4.12. Average population inversion versus the amplifier length for both 980 and 1480 nm pumping and the 15 WDM signals. Operating conditions: same as Fig. 1.
___ 1480 pump band, - - - 980 pump band

optimum gain flatness. This is because the 1538-1566-nm amplifier band used in this example is not inherently flat.

Note that the inversion level which optimizes the gain flatness over the 1538-1566 nm amplifier band also maximizes the least-favored signal gain. As will be shown below, particularly for 980-nm pumping, this is almost the case over any spectral band which does not represent an inherently flat spectral gain region for the amplifier. While a gain flatness is linked to a given population inversion, however, the inversion level for optimum performance depends on the fiber composition, the wavelength range of operation, and the system criteria used for optimization, so the inversion parameter can not be used alone to establish optimum amplifier performance.

Comparison of 980-nm and 1480-nm Pumped Cascade Performance

Figure 4.13 shows the tradeoff between the number of amplifiers in the cascade and the overall gain variations for a total gain Gtot of 70 dB. Note that the overall gain variation is greater

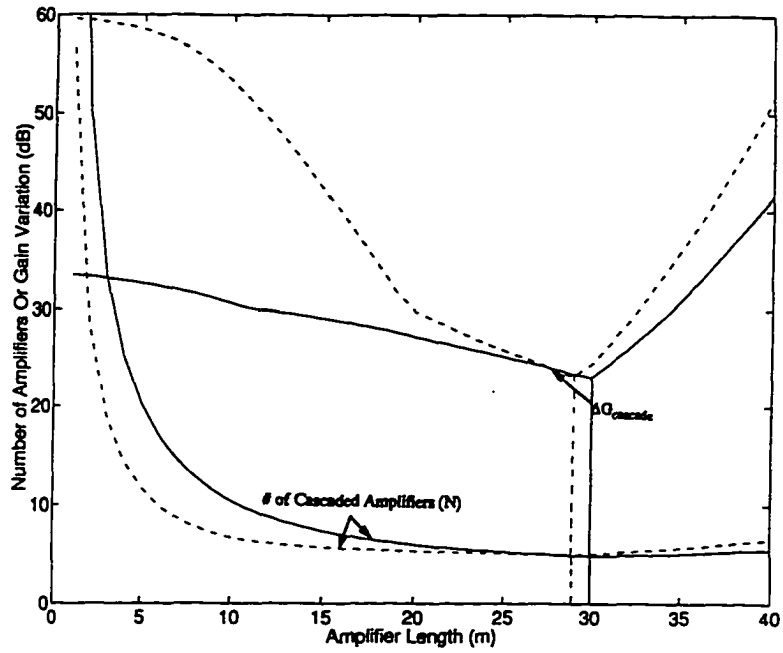

Figure 4.13 Total spectral gain variation $\Delta G_{cascade}(L)$ between the 15 WDM signals and number of cascaded amplifiers N(L) required to achieve a total system gain of 70 dB. Operating conditions: same as Fig. 1.
____ 1480 nm pump band, - - - 980 nm pump band

than 20 dB at either pump wavelength irrespective of the fiber length, too severe for multi-access applications without gain equalization. These results are calculated using the individual amplifier performance parameters shown in Fig. 2 along with the simple approximation of Eq. (4.19). To examine the accuracy of this approximation, we next compare these results with those obtained using the detailed cascade calculations.

For the 980-nm pumped cascade, the span loss between amplifiers is set equal to the amplifier gain of 14 dB. At the output of the 5th amplifier (about 70 dB total system gain), there is a 12.4 dB SNR variation, the inter-channel power variation is about 24.5 dB. These variations are too severe for proper multiple access system operation. Note, however, that the SNR (21 dB) is still adequate

at the 1540-nm channel (least-favored signal wavelength) for 10 Gb/s operation. These results suggests that it might be possible to exploit most of entire usable amplifier band for high capacity point-to-point WDM system applications over a modest transmission distance of about 200-250 km (about 50-75 dB total system gain), provided that each amplifier has the optimum length. The simple formula of Eq. (4.19) would indicate an inter-channel power variation of 23.5 dB (= 5 amplifiers x 4.7 dB), compared to a variation of 24.5 dB obtained using the detailed cascade calculations, confirming the accuracy of the approximation in Eq. (4.19).

For the 1480-nm pumped cascade, the span loss between amplifiers is equal to the gain of 14.4 dB, and in this case 5 cascaded amplifiers are needed to achieve a total system gain of 70 dB. The simulation results indicate that the overall cascade performance is almost the same as that of the 980-nm. Note, however, that the SNR at each channel at the output of the 1480-nm pumped cascade is about 1-2 dB less that that of the 980-nm.

The main conclusions deduced from these results are:

1) Both pump wavelengths perform almost equally over the entire usable amplifier band from 1538 nm to 1566 nm, provided that each amplifier has the optimum length.

2) Even with these optimal conditions, achieving adequate overall multi-access system performance over such a wide amplifier band would still necessitates resorting to external equalization methods even if the total system gain is as small as 40 dB. However, the obvious advantage that would be gained from the optimization method presented here is the simplification of the practical implementation of the external equalizers that would be needed.

4.6.2 CASCADE PERFORMANCE OVER THE 1540-1560 nm AMPLIFIER BAND

The system model consists of 11 WDM channels spaced 2-nm apart in the 1540 to 1560 nm amplifier band. The input signal levels to the cascade of EDFAs are -15 dBm/channel at the input of the first amplifier. Each amplifier is assumed to be codirectionally pumped with 50 mW of pump power at either 1480-nm or 980-nm. An optical filter with 1538-nm cutoff wavelength is inserted after each amplifier to remove the ASE in the spectral region below 1538-nm.

Figure 4.14 shows the least-favored signal gain G_L and the spectral gain variation ΔG between the eleven signal wavelengths versus the amplifier length for both 980-nm and 1480-nm pumping. With the amplifier characteristics shown in Fig. 5 and a total gain of 70 dB, the optimum amplifier length determined from Eq. (4.21) is 16 m and 22 m for 1480-nm and 980-nm pumping, respectively. For 980-nm pumping, the minimum individual gain variation
(2.5 dB) and the maximum least-favored signal gain (17 dB) both occur at a length that coincides with the optimum. With 1480-nm pumping, at Lopt, the gain variations are 1.8 dB, and the least-favored signal gain is 12.6 dB.

Fig. 4.15 shows the tradeoff between the number of amplifiers in the cascade and the overall gain variations for a total gain of 70 dB. As can be seen from Fig. 6, the minimum overall gain variation obtained using the simple formula of Eq. (4.19) are almost the same (about 10.2 dB) at either pump wavelength, compared to a variation of about 10.8 dB obtained using the detailed cascade calculations.

The following summarizes the main conclusions of this section:

1) Both pump wavelengths perform almost equally over the 1540-1560 nm amplifier band, provided that each amplifier has the optimum length.

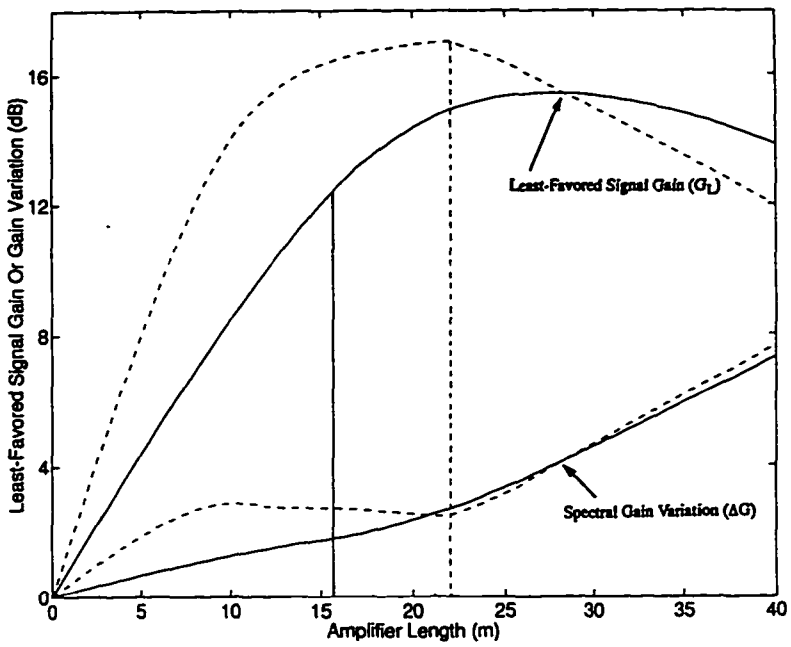

Figure 4.14 Same as Figure 4.11, except for only 11-WDM signals in 1540-1560 nm amplifier band.
____ 1480 nm pump band, - - - 980 nm pump band

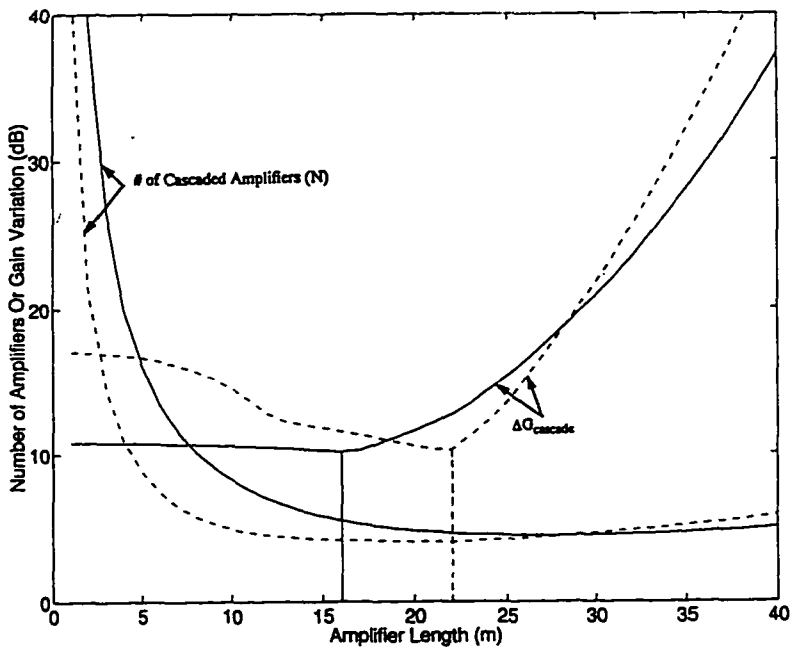

Figure 4.15 Same as Figure 4.13, except for only 11-WDM signals in 1540-1560 nm amplifier band.
____ 1480 nm pump band, - - - 980 nm pump band

2) With these optimal conditions adequate multi-access system performance for 11 WDM channels equally spaced in the 1540-1560 nm range, can be achieved at either pump wavelength, without requiring external equalization, provided that the total system gain do not exceed 70 dB.

4.6.3 CASCADE PERFORMANCE OVER THE 1542-1552 nm AMPLIFIER BAND

The system model consists of six 10 Gb/s WDM channels spaced 2-nm apart in the 1542 to 1552 nm amplifier band. The input signal levels to the cascade of EDFAs are -10 dBm/channel at the input of the first amplifier. Each amplifier is assumed to be codirectionally pumped with 50 mW of pump power at either 1480-nm or 980-nm. An optical filter with 1540-nm cutoff wavelength is inserted after each amplifier to remove the ASE in the spectral region below 1540-nm.

Figure 4.16 shows the least-favored signal gain G_L and the spectral gain variation ΔG between the six signal wavelengths versus the amplifier length for both 980-nm and 1480-nm pumping. With the amplifier characteristics shown in Fig. 7 and a total gain of 200 dB, the optimum amplifier length determined from Eq. (4.21) is 9 m, for both 980 and 1480-nm pumping. Note that the optimum length in this case is a function of the total system gain (decreases with the total system gain) and can not be determined solely from the individual amplifier performance parameters shown in Fig. 7. This is illustrated in Figure 4.16, which shows the metric M (L), for 980-nm pumping, versus the amplifier length for three values of the total system gain. As can be seen from the Fig., the maxima of M occur at fiber lengths of 8 m, 9 m, and 10 m. These correspond to the optimum lengths for a total system gain of 300 dB, 200 dB, and 100 dB, respectively.

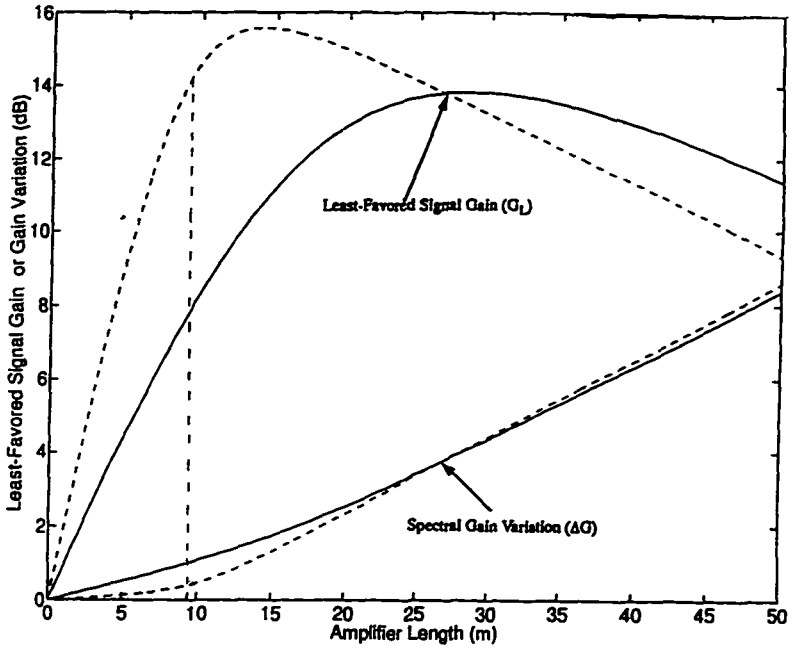

Figure 4.16 4.14 Same as Figure 4.11, except for only 6-WDM signals in 1540-1560 nm amplifier band.
____ 1480 nm pump band, - - - 980 nm pump band

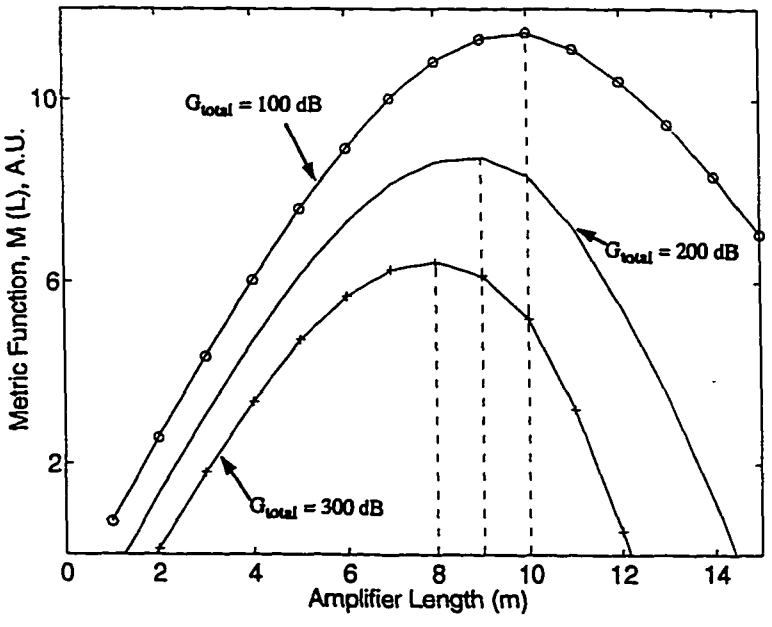

Figure 4.17 The metric M(L) versus the amplifier length for three different values of the total system gain. Operating conditions: same as Figure 4.16, except for 980 nm pumping only

For 980-nm pumping, at Lopt, the least-favored signal gain is 14.0 dB, the gain variations are 0.36 dB, and the corresponding value of the mean inversion parameter is 0.9, while for 1480-nm pumping the gain is 7.6 dB, the variations are 1.0 dB (about a factor of three larger), and the corresponding value of the mean inversion parameter is 0.62.

Figure 4.18 shows the tradeoff between the number of amplifiers in the cascade and the overall gain variations for a total gain Gtot of 200 dB. Note that for 1480-nm pumping the gain variation is greater than 20 dB irrespective of the fiber length, too severe for multi-access applications. With 980-nm pumping, a reasonable trade-off between the number of amplifiers and the gain variations occurs, with an optimum length of 9 m determined by the metric of Eq. 3 (see Fig. 8). These results indicate that 980-nm pumping is better than 1480-nm pumping for minimizing the inter-channel power variations at the output of a cascade, provided that each amplifier has the optimum length and that the range of wavelengths occupied by the WDM signals is a relatively flat spectral gain region of the amplifier band. This is explained as follows: As indicated above, a fully inverted amplifier has a gain spectrum whose shape essentially follows that of the emission cross section. Since the 1542-1552 nm amplifier band used here is almost inherently flat, a complete inversion is required to produce a gain spectrum whose shape essentially follows that of the inherently flat emission cross section. Consequently, the nearly flat gain spectrum reported here at 980-nm pumping results from its intrinsic superiority in producing a complete inversion because of the almost complete absence of pump-induced stimulated emission which limits the inversion for pumping at 1480-nm. Furthermore, the lower spontaneous emission factor of 980-nm pumped EDFAs also helps to reduce the build-up of ASE, which otherwise would degrade the inversion and increase the gain variations.

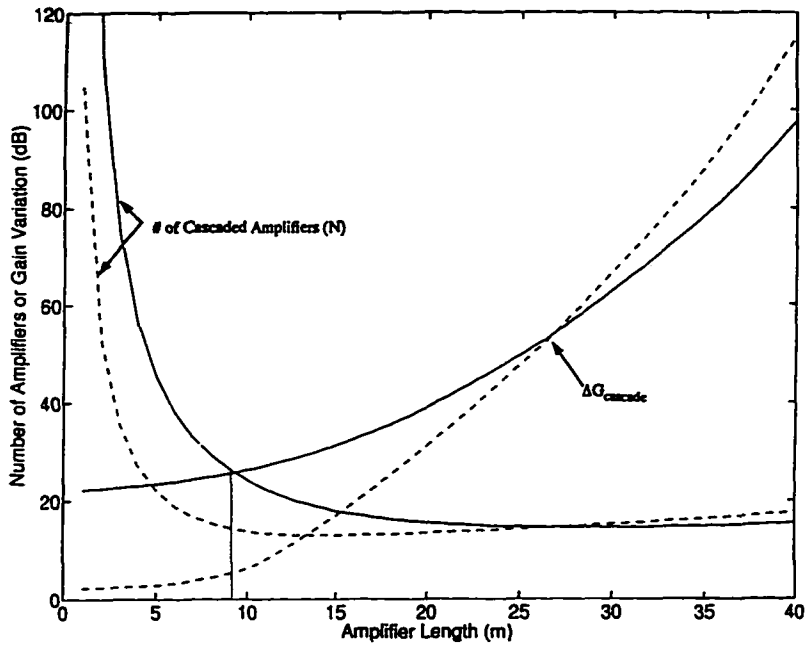

Figure 4.18. Same as Figure 4.13, except for only 6-WDM signals in 1540-1560 nm amplifier band.
____ 1480 nm pump band, - - - 980 nm pump band

Amplifier Cascade Calculations

For the 980-nm pumped cascade, the span loss between amplifiers is set equal to the amplifier gain of 14 dB. This corresponds to 50 km of fiber at 0.25 dB/km plus excess losses of 1.5 dB for each span. Figure 4.19 shows calculations of the signal levels and the accumulated ASE power in a 0.2-nm optical bandwidth at the output of the 15th amplifier (about 200 dB total system gain) along the cascade. Both the output signal levels and SNRs are nearly equal, with a 5.6 dB inter-channel power spread and a 2.8 dB SNR differential. The simple formula of Eq. (4.19) would indicate an inter-channel power variation of 5.4 dB (= 15 amplifiers x 0.36 dB), compared to a variation of 5.6 dB obtained using the detailed cascade calculations, confirming the accuracy of the approximation in Eq. (4.19).

For 1480-nm pumping, the span loss between amplifiers is equal to the gain of 7.6 dB, and in this case 27 cascaded amplifiers are needed to achieve a total

system gain of 200 dB. After the cascade, there is a 16 dB SNR variation, the inter-channel power variation is 28 dB (see Figure 4.20), and the 1542-nm channel is marginal for 10 Gb/s operation. These variations are too severe for proper

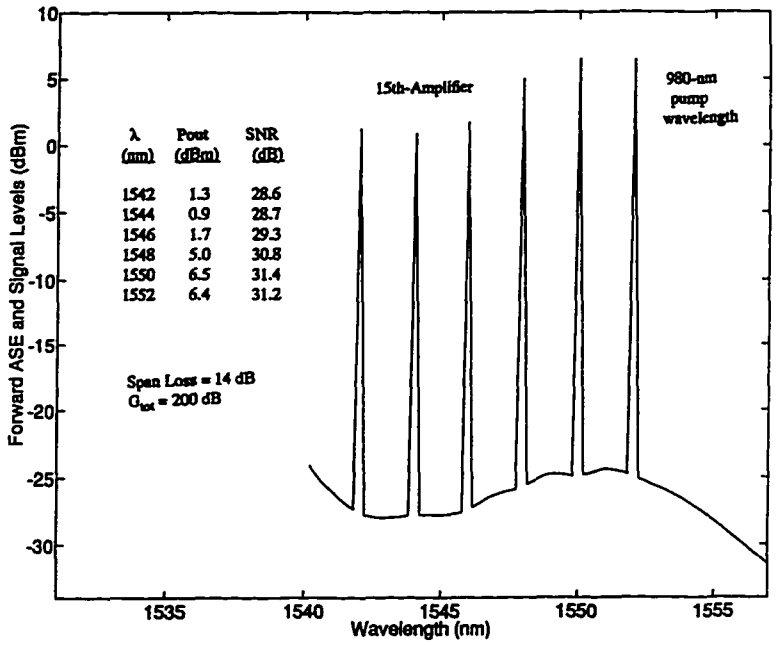

Figure 4.19

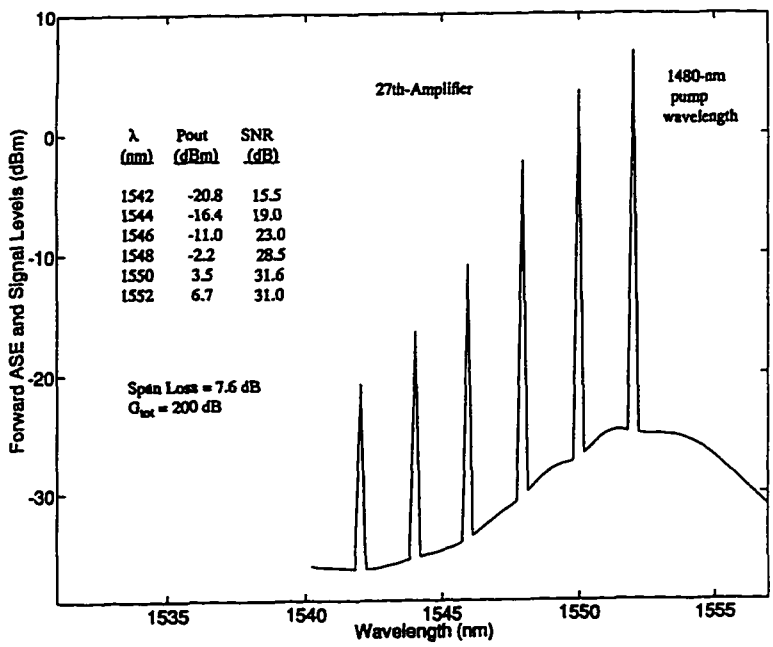

Figure 4.20

multiple access system operation. In contrast, after 27 amplifiers with 980-nm pumping, the total system gain is more than 350 dB, the SNR differentials are only 5.3 dB and the gain variations are only about 10 dB, suitable for multi-access network operation. These result are also in conformity with the experimental results reported in [47], where it has been shown that the total gain variation (about 2 dB), between 5 WDM channels spaced 2-nm apart in the 1546 to 1554 nm range, obtained with 980-nm pumped EDFA cascade (providing a total gain of about 105 dB) is much lower than that obtained with 1480-nm pumped EDFA cascade (about 15 dB) in the same range. The above results also indicate that the SNR flatness is directly related to the total system gain flatness. In general, a channel with a low system gain will have a low SNR. However, the variation of SNR is much smaller than that of the system optical gain. For example, with 980-nm pumped cascade and a total system gain of 350 dB, the gain variation is about twice the SNR differentials at the output of the cascade. This is understandable since the channel with a low gain will also have less noise power within its bandwidth, but the gain difference is accumulated exponentially with the number of the cascaded amplifiers while ASE power is accumulated linearly. In general, the equalization of SNR is less demanding than the equalization of output signals level.

4.6.4 CASCADE PERFORMANCE OVER THE 1552-1562 nm AMPLIFIER BAND

The system model consists of six 10 Gb/s WDM channels spaced 2-nm apart in the 1552 to 1562 nm amplifier band. The input signal levels to the cascade of EDFAs are -10 dBm/channel at the input of the first amplifier. Each amplifier is assumed to be codirectionally pumped with 50 mW of pump power at either 1480-nm or 980-nm.

Figure 4.21 shows the least-favored signal gain G_L and the spectral gain variation ΔG between the six signal wavelengths versus the amplifier length for both 980-nm and 1480-nm pumping. With the amplifier characteristics shown in Figure 4.21 and a total gain of 200 dB, the optimum amplifier length determined from Eq. (4.21) is 56 m and 50 m for 1480-nm and 980-nm pumping, respectively. In these two cases, the minimum individual gain variation (0.8 dB at either pump wavelength) and the maximum least-favored signal gain (14.4 dB for 980-nm pumping; 16.0 dB for 1480-nm pumping) both occur at a length that coincides with the optimum.

Figure 4.22 shows the tradeoff between the number of amplifiers in the cascade and the overall gain variations for a total gain G_{tot} of 200 dB. As can be seen from Figure 4.22, the minimum overall gain variations obtained using the simple formula of Eq. (4.21) are almost the same (11 dB) at either pump wavelength, compared to a variation of about 12.8 dB obtained using the detailed cascade calculations. The simulation results revealed that the 1530-nm gain peak of a typical EDFA completely disappears and, therefore, no optical filters were needed in these calculations to remove the ASE gain peak. The main conclusions of this section are:

1) Both pump wavelengths perform almost equally over the 1552-1562 nm amplifier band, with the advantage that the 1530-nm gain peak of a typical EDFA completely disappears and that optical filters are no longer needed to remove the ASE gain peak.

2) With these optimal conditions, adequate multi-access system performance for six 10 Gb/s WDM channels equally spaced in the 1552-1562 nm range, can be achieved at either pump wavelength, without requiring external equalization, provided that the total system gain do not exceed 150 dB.

The main reason that the performance of the 980-nm pumped cascade did not outperform that of the 1480-nm, is explained as follows: Since the 1552-

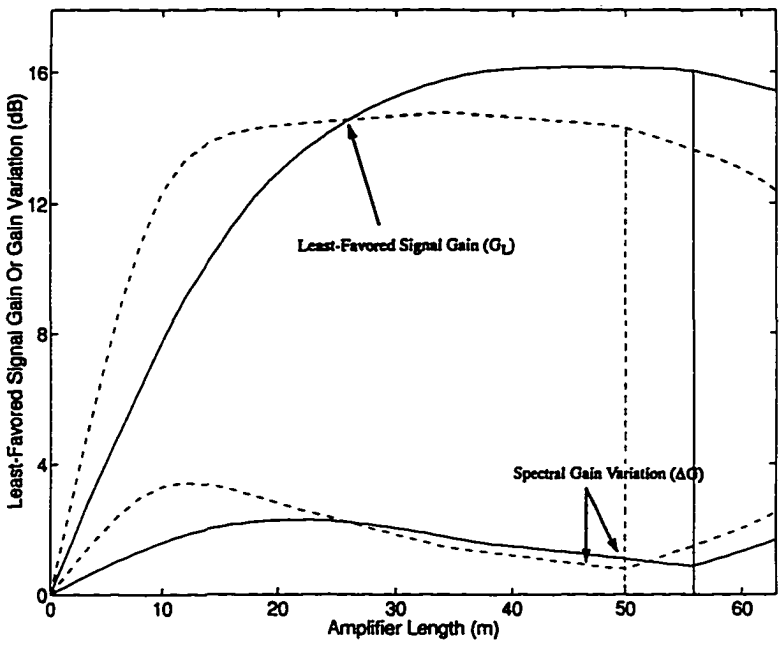

Figure 4.21 Same as Figure 4.16, except that 6-WDM signals now occupy the 1552-1562 amplifier band.
___1480 nm pump band, - - - 980 nm pump band

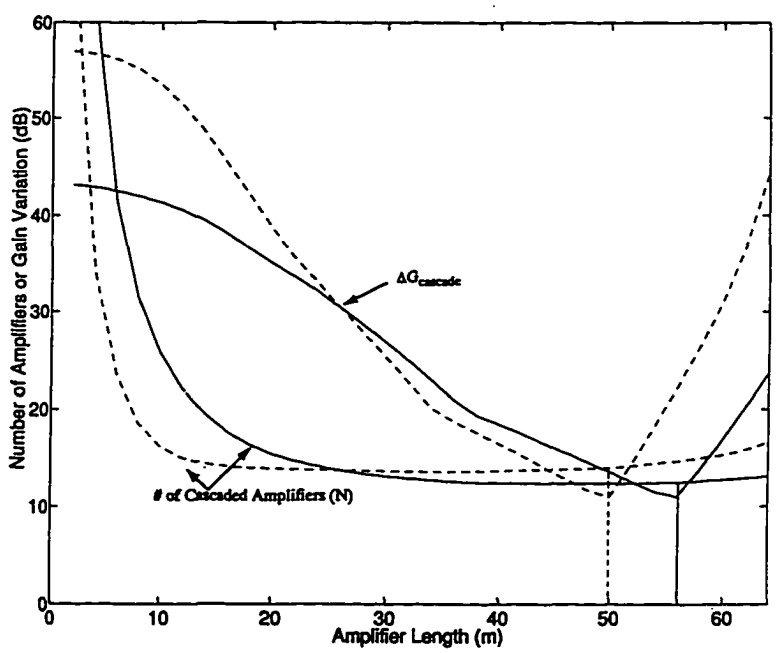

Figure 4.22 Same as Figure 4.18, except that the 6-WDM signals now occupy the 1552-1562 nm amplifier band. Operating conditions: same as Figure 4.21
___ 1480 nm pump band, 980 nm pump band

1562 nm spectral region used here does not represent an inherently flat spectral gain region for the amplifier, an optimal, though not critical, population inversion is required for optimum gain flatness. In this case, both pump wavelengths are capable of producing such an optimal modest value of inversion (0.62 at either pump wavelength), and, therefore, the intrinsic superiority of 980-nm pumping in producing a complete inversion is no longer needed.

4.6.5 ADDITIONAL CONSIDERATIONS

Optical Pump Power Levels

To investigate the effect of varying the pump power, we consider using 20 and 100 mW of pump power at each pump wavelength with the corresponding optimum amplifier lengths. These calculations are repeated for each of the four spectral regions examined above. The simulation results indicate that the effect of varying the pump power on the gain and SNR flatness is strongly dependent on the intrinsic flatness of the amplifier band allocated to the WDM signals. The following summarizes these results:

i) For three of the spectral regions examined above which do not represent flat spectral gain regions for the amplifier, namely, the 1538-1566 nm, 1552-1562 nm, and the 1540-1560 nm bands;

a) Increasing the pump power does not improve the system gain flatness at either pump wavelength. For 100 mW of pump power, the optimum amplifier is longer and the associated overall spectral gain variations for a given total system gain are almost the same as those achieved with 50 mW of pump power at either pump wavelength. The only advantage gained is a slight reduction in the number of cascaded amplifiers required to achieve a given total system gain.

b) Decreasing the pump power does not degrade the system gain flatness provided that the pump power is still sufficient enough to produce the critical inversion level required to achieve optimum gain flatness. For 20 mW of pump power, the optimum amplifier is shorter and the associated overall gain variations for a given total system gain are almost the same as those achieved with 50 mW of pump power at either pump wavelength. However, the price being paid is that the number of cascaded amplifiers required to achieve a given total system gain increase with the system gain.

ii) For the remaining spectral region which represents a relatively flat spectral gain region for the amplifier, namely, the 1542-1552 nm band;

a) For 980-nm pumping, increasing the pump power improves the overall system performance (flatter gain spectrum due to stronger inversion) provided that the total system gain is relatively large (> 400 dB). For 100 mW, the optimum amplifier is longer and the associated overall gain variations for a given total system gain are less than those achieved with 50 mW. This means that adequate overall system performance over longer transmission distance can now be achieved. This is illustrated in Figure 4.23, which shows the tradeoff between the number of amplifiers in the cascade and the overall gain variations for a total gain of 500 dB. These results are obtained assuming the same system parameters used in Figure 4.16, except with a 100 mW of pump power at either pump wavelength. Note that for 1480-nm pumping the gain variation is greater than 50 dB irrespective of the fiber length, too severe for any application. With 980-nm pumping, a reasonable trade-off between the number of amplifiers and the gain variations occurs, with an optimum amplifier length L_{opt} = 7 m.

b) Fig.4.16, at $L = L_{opt} = 7$ m, it is now possible to achieve a total system gain of 500 dB with as small overall gain variation as 6.9 dB. These are almost the same overall gain variations obtained with 50 mW of pump power, however, for a total system gain of only 200 dB. To further check the accuracy of these results (calculated using the simple approximate formula of Eq. (4.19), the detailed cascade calculations were carried out assuming the span loss between amplifiers = G_L = 12.8 dB, and in this case 39 amplifiers are needed to achieve a total system gain of 500 dB. After the cascade, the SNR differentials are only 3.5 dB, the gain variations are only about 7 dB, and the SNRs (24 dB at the least-favored signal wavelength) are adequate at all signal wavelengths for 10 Gb/s operation.

c) Decreasing the pump power degrades the overall system performance. For 20 mW of pump power, the optimum amplifier is shorter and the associated overall gain variations for a given total system gain are more than twice those achieved with 50 mW of pump power. This is because the pump power is not high enough to produce strong inversion which is needed, as explained above, to achieve optimum gain flatness over this flat amplifier band.

Input Signal Level

Another factor which may affect the system gain and SNR flatness is the total input signal power level. Since the amplifier length depends on the input signal levels, changing the input signal levels necessitates selecting the corresponding optimum amplifier length. For instance, reducing the signal levels to -17 dBm/ channel at the input of the first amplifier of the 980-nm pumped cascade (for the 6 WDM channels occupying the 1542-1552 nm amplifier band) requires a longer fiber but produces almost the same overall gain variations and SNR differential that were achieved at -10 dBm/channel. However, the SNR at each

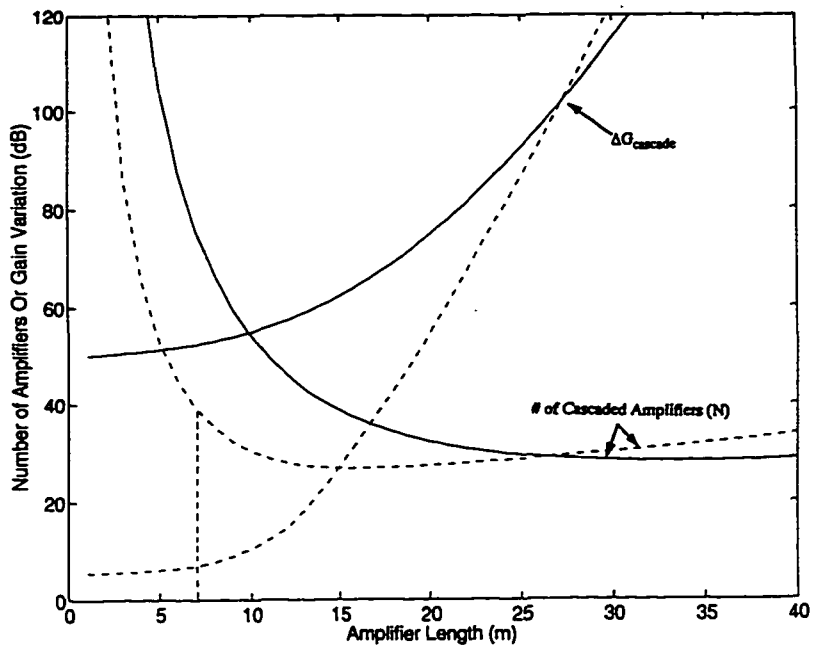

Figure 4.23 Same as Figure 4.18, except for a 100 mW of pump power and a total system gain of 500dB.
___ 1480 nm pump band, - - - 980 nm pump band

channel is about 3-4 dB poorer, indicating that lower input signal levels will not accommodate a cascade of as many amplifiers.

Inter-Amplifier Fiber Loss

Once the individual amplifier performance parameters have been optimized, the optimum inter-amplifier fiber loss for best overall cascade performance is simply equal to that of the least-favored signal gain of the individual amplifier. This is explained as follows: Since the first amplifier in the cascade is optimized so that it has an optimum gain flatness for a given total input power level, all amplifiers in cascade have to have roughly the same amount of input signal power so that their optical gain flatness is optimum. This is achieved by setting the inter-amplifier fiber loss approximately equal to the least-favored signal gain of the first amplifier. Thus, the matching between the gain and the

link loss ensures that all amplifiers in cascade have the correct input power levels for the optimum gain flatness.

The sensitivity of gain and SNR variations to inter-amplifier loss is investigated by considering a fiber transmission link using 10 identical EDFAs and 11 WDM signals spaced 2-nm apart in the 1540-1560 nm amplifier band. Figure 4.24 shows calculations of the signal levels at the output of the 10th amplifier (total system gain of about 126 dB) for three different values of inter-amplifier fiber losses, 12.6 dB (optimum link loss = G_L), 15.6 dB (optimum link loss + 3 dB), and 9.6 dB (optimum link loss - 3 dB). Each amplifier is assumed to be codirectionally pumped with 50 mW of pump power at 1480-nm; the input signal levels to the cascade are -15 dBm/channel at the input of the first amplifier. An optical filter with 1538-nm cutoff wavelength is inserted after each amplifier to remove the ASE in the spectral region below 1538-nm. As expected, best overall cascade performance (optimum gain and SNR flatness as well as adequate SNRs at all signal wavelengths) is obtained when the inter-amplifier fiber loss was equal to the least-favored signal gain (12.6 dB). To be more precise, best overall cascade performance is obtained when all amplifiers in cascade have almost the same correct input signal levels for the optimum gain flatness. If the fiber loss is below (higher input signal levels) or above (lower input signal levels) the optimum value, the amplifiers except for the first one will not have the correct input signal levels for optimum gain flatness, resulting in less uniform gain spectrum. As can be seen from Fig. 4.24, a 3-dB decrease in inter-amplifier loss results in a slight increase in gain variations (from 19 dB to 23 dB). On the other hand, a 3-dB increase in inter-amplifier loss does not cause significant gain variation degradation (from 19 dB to 20 dB). Note, however, that the SNR at each channel is about 6-11 dB poorer,

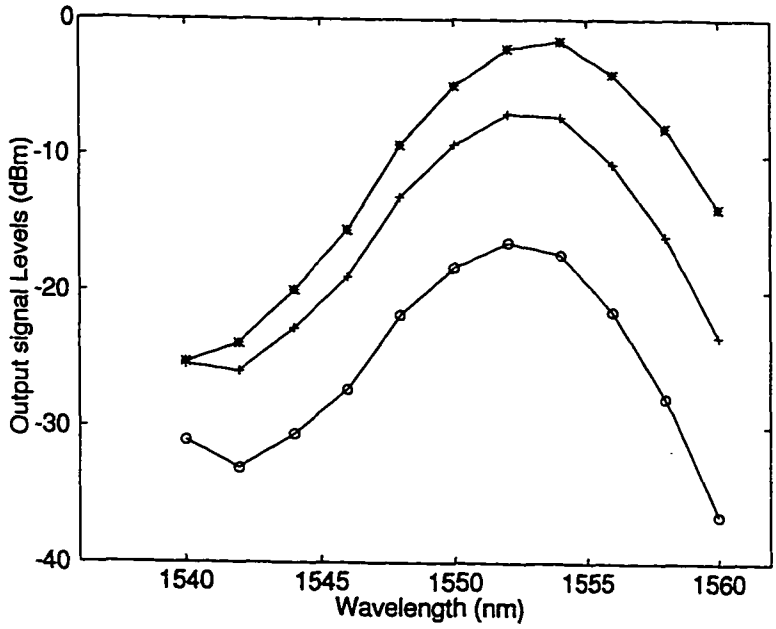

Figure 4.24. Output signal level for 11-WDM signals, spaced 2 nm apart in the 1540-1560 nm amplifier band, emerging after a cascade of 10 amplifiers with different interamplifier fiber loss. Each amplifier is codirectionally pumped with 50 mW of pump power at 1480 nm. Pin = -15 dBm/ch. At the inut of the first amplifier.
+++ Optimum link loss = G_L = 12.6 dB.
*** Optimum link loss -3 dB
o o o Optimum link loss + 3dB

indicating that higher inter-amplifier loss (lower input signal levels) will not accommodate a cascade of as many amplifiers.

These results indicate that the gain and SNR flatness is not strongly dependent on the inter-amplifier fiber loss (input signal level changes). The serious problem, however, is that, at lower input signal levels (higher inter-amplifier loss), the SNRs at the less-favored signal wavelengths might fall below a given acceptable value, rendering the overall system performance unacceptable. We conclude that the overall system performance is most sensitive to input signal level changes when considering slight changes in a given parameter.

4.6.6 RESULTS

A detailed comparison of the overall performance of 980-nm and 1480-nm pumped EDFA cascades over four different spectral regions of the usable amplifier band for multiple wavelength operation has been presented in this section. These comparisons are carried out by presenting a simple optimization method which relate individual amplifier performance parameters to the overall performance of an amplifier cascade for best overall system performance. Issues considered are pump power, Erbium-doped fiber length, accumulated ASE, inversion level, inter-amplifier fiber loss, and input signal levels and their spectral range. The following summarizes the main finding of these comparisons:

1) Both pump wavelengths perform almost equally provided that the spectral gain region of the amplifier is not inherently flat (for example, the 1538-1566 nm, 1540-1560 nm, and 1552-1562 nm bands) and provided that each amplifier has the optimum length; with the latter band having the advantage that the 1530-nm gain peak of a typical EDFA completely disappears and, consequently, optical filters are no longer needed to remove the ASE gain peak. In other words, if the optimum gain flatness for a given amplifier band does not correspond to a maximum population inversion, so that an optimal, though not critical (not too high, or too low, 0.62-0.68), inversion level is required. In this case, either pump wavelength is capable of producing such a modest value of inversion, and, therefore, both pump wavelengths would perform almost equally over that particular band.

2) Adequate overall system performance over the 1538-1566 nm amplifier band can be achieved for high capacity point-to-point WDM system applications over a modest transmission distance of about 200-250 km (about 50-70 dB total system gain) without requiring external equalization,

provided that each amplifier has the optimum length. Note, however, that adequate multi-access system performance is not achievable over such a wide amplifier band without gain equalization. For the 1540-1560 nm and the 1552-1562 nm amplifier bands, adequate overall multi-access WDM system performance can be achieved without requiring external equalization, provided that the total system gain do not exceed 70 dB for the former and 150 dB for the latter, and that each amplifier has the optimum length.

3) The overall system performance of 980-nm pumped cascade outperform that of 1480-nm provided that the emission spectrum for the amplifier is relatively flat, for instance, the 1542-1552 nm band. In this case, optimum gain flatness corresponds to a maximum population inversion, so that a strong inversion is required. This can only be achieved with 980-nm pumping due to its intrinsic superiority in producing a complete inversion.

4) 50 mW, 980-nm pumping with an amplifier length of 9 m provides adequate overall multi-access gain flatness and optical SNRs for six 10 Gb/s channels, spaced 2 nm apart in the 1542-1552 nm amplifier band, transmitted through a cascade of 27-EDFAs, providing a total system gain of more than 350 dB without requiring external equalization. With 1480-nm pumping, the inter-channel power variations are more severe, so that a cascade of only 9 amplifiers (< 70 dB total system gain) produces more than 10 dB inter-channel power variations.

5) The pump wavelength, input signal levels, and amplifier length are the most critical parameters for narrowing both the output signal level variations and the SNR differential between channels. It is found that the overall system performance is most sensitive to input signal level changes when considering slight changes in a given parameter

4.7 GAIN EQUALIZATION EMPLOYING MACH-ZEHNDER OPTICAL FILTER

In many cases, an external method has to be used for gain equalization. A variety of approaches have been used to address this problem. These include the use of "smoothing filters" such as Fabry-Perot or tunable Mach-Zehnder interferometers[48]. Previous work using Mach-Zehnder (MZ) filters [49] equalized up to 8-nm band and up to six cascade stages, using only the liner portion of the MZ filter sinusoidal transmittance characteristics for equalization.

In this section, we use most of the period of the MZ filter sinusoidal transmittance characteristics to equalize both 980-nm and 1480-nm pumped EDFA cascades. This approach can support the signals in the 20-nm up to a cascade of 10 amplifiers with inter-channel power differences of less than 5 dB. The transmittance characteristics of the MZ filter is given by:

$$T(\lambda) = 1 - 4\alpha(1-\alpha)\sin^2((\pi c\tau)/\lambda + \phi/2) \qquad (4.22)$$

where α is the coupling ratio of the branches, τ is the time difference between the two waveguide paths with different lengths, and ϕ is the additional phase difference of the two paths which we use to tune the filter. The period of the sinusoidal transmittance characteristics of the filter is determined by τ.

4.7.1 EQUALIZATION APPROACH

The initial objective of our approach is to simplify the practical implementation of the transmittance characteristics of the MZ filter required to make the EDFA-filter combination have an output as flat as possible. This is achieved by optimizing the individual amplifier performance parameters as follows:

a) Individual EDFA parameters should be designed so that they have a maximum average gain over the WDM signal bandwidth and optimum gain flatness for the designed total input level. This is achieved by determining

the optimum amplifier length, L_{opt} , required to achieve a maximum gain subject to the constraint of minimum spectral gain variation $\Delta G = G_M - G_L$.

b) The optimized WDM signal gain spectrum at L_{opt} must have a sinusoidal or quasi-sinusoidal shape. This is because an MZ filter has a sinusoidal transmittance characteristics, which imposes an additional constraint on L_{opt}. It is possible to change the fiber length to alter the signal gain spectrum close to a sinusoidal or quasi-sinusoidal form as illustrated in next section.

c) From the optimized WDM signal gain spectrum, $G_{opt}(\lambda)$ determine the normalized equalization function $F_{eql}(\lambda)$ defined as:

$$F_{eql}(\lambda) = G_L / G_{opt}(\lambda) \qquad (4.23)$$

Using Fourier series curve fitting techniques, the parameters of the MZ transmittance characteristics, α, τ, and ϕ are adjusted to make $T(\lambda) \cong F_{eql}(\lambda)$ in the signal band, so that the output of the combination of the amplifier and the MZ filter is as flat as possible.

4.8 EDFA CASCADE PERFORMANCE WITH AND WITHOUT GAIN EQUALIZATION

As discussed in previous sections, the usable wavelength bandwidth is limited by the flat gain region of EDFA. Due to the intrinsic physical characteristic of EDF, the usable wavelength become a very precious source in the WDM networks. There are two ways to expand the network size. One is to use the reconfigurable network which allows the use of wavelength cross connection, wavelength conversion, and optical switch technologies,[2][5]. Another, relatively easy way, is to increase the number of wavelength. Many efforts have been made to expand the EDFA flat gain range [50] [51]. As calculated in Chapter 3, for the mesh-connected WDM ring, the number of wavelength

required is proportional to the square of the number of node when the node is large. Figure 4.24 shows the relationship of the number of mesh connected node and its required number of wavelength as listed in Table 3.4.

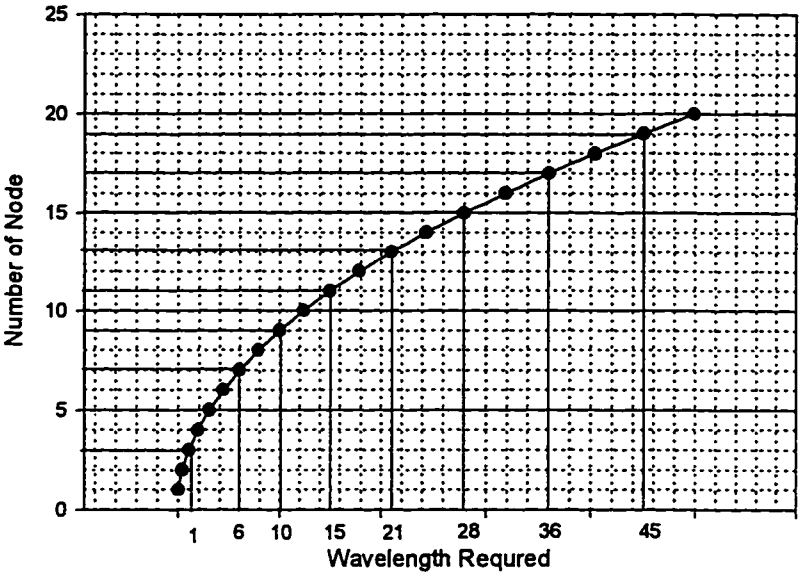

Figure 4.25: Relationship of Wavelength and node number

As indicated in the Figure 2.24, for a mesh connection ring, if the node number is 9, the required number of wavelength is 10; if the node number is 11, the required wavelength is 15; when the node number is 13, the number of wavelength required will be 21, etc. The number of wavelength used in the flat band of EDFA can be increased either by narrowing the space between the adjacent wavelengths or use the wider band of the gain profile of the EDFA while keep the wavelength spacing unchanged. The interval space between the wavelength is determined by the cross-talk of the optical multiplexer and demultiplexer, by the wavelength stability of the transmitters and by the optical filers misalignment, etc. In this section, we focus on the system using wider-band of EDFA's gain profile by optimized the individual and cascade EDFA as

discussed in section 4.6. The objective of EDFA optimization is either to totally obviate the need for external gain equalization or to simplify the practical implementation of external gain equalization, depending on the transmission system characteristics and the particular application under consideration.

4.8.1 1543 - 1557 nm BAND CASCADE PERFORMANCE

As shown in section 4.4, for a 90-mW forward pumped EDFA at the fiber length of 24 m, 11 signals with 1.6 nm apart can be accommodated in 1543 - 1557 nm band with very small gain variation (0.39 dB) and average gain of (19.65 dB)(Figure 4.5). 11 wavelength can be used for a 11-node of 2-fiber uni-directional ring. If the working fiber is cut in this 11-node uni-directional ring, the WDM signals will be routed to the protection fiber and pass all the EDFAs on the protection path. The maximum possible number of cascaded EDFA in the protection path could be equal to the number of nodes, which is 11 in this case. Therefore, the signal quality after passing 11 cascaded EDFA is the real limitation for this uni-directional ring network. Figure 4.26 shows the gain profile of 11 cascade EDFAs under optimized conditions. The optimized conditions are: 1). each individual EDFA is optimized (L_{opt} = 24 m, co-directional pumped by 980-nm pump at 90 mW); 2) signals input to the first EDFA are equal (-13 dBm/ch.); 3) the transmission loss between the EDFAs are equal to the least signal gain which can ensure that EDFAs on the line are all operated in almost the same condition as required by the optimization. Figure 4.26 shows that the worst SNR among all the signals is better than 27 dB which is adequate for 10 Gb/s bit rate, and gain variation is about 5 dB which is within the receiver's dynamic range (usually around 15 dB). This indicates that for the 2-fiber uni-directional ring, the ring network can survive

under the fiber cut or equipment failure: the signals not only are being switched

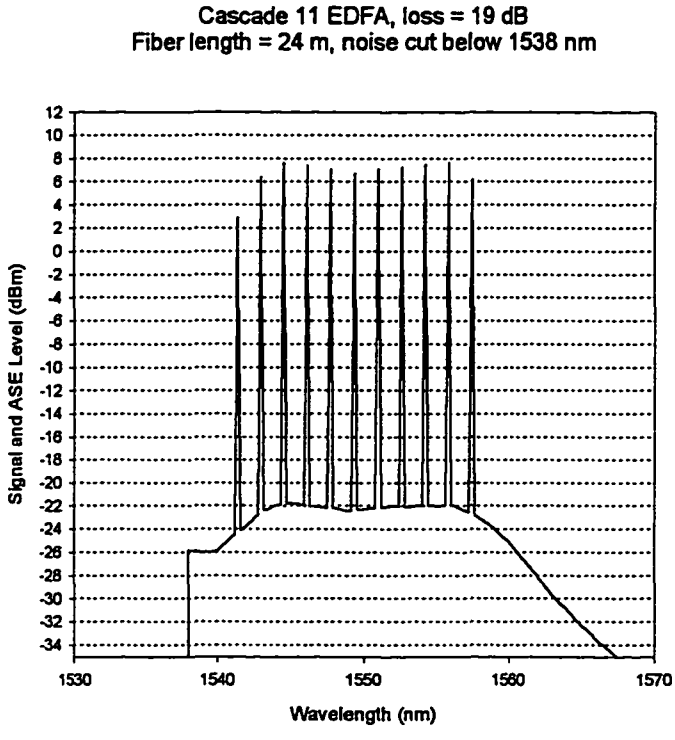

Figure 4.26 Gain Profile of Cascade of 11 Optimized EDFA
With Optimized Transmission Loss Between EDFAs

to the protection path, but also have to follow the optimization requirements on the protection path to guarantee signal quality. The number of wavelength required for the mesh-connection of 9-node ring is: $M = (9^2-1)/8 = 10$ for a self-healing ring. In this band, 9-node WDM SHR can be supported. When there is a cable cut or equipment failure, following the discussion of 2-fiber uni-directional ring, the WDM signals have to be routed to the protection path and pass all the cascaded EDFAs on the protection path. The maximum number possible for the 9-node SHR could be 9. If one follows the same roles of optimization for the cascade EDFAs as in the 11-node unidirectional ring, the

signal quality after a cascade of 9 EDFAs will be guaranteed due to the smaller band (only 10 wavelength needed here) and less number of cascaded EDFA comparing to the 11-node uni-directional ring case.

4.8.2 1538 - 1560 nm BAND CASCADE PERFORMANCE

In the 1538.2 - 1560.6 nm band, 15 signals may be accommodated which can be used for either a 15-node unidirectional ring or an 11-node bi-directional mesh-connected ring. The real limitation of the application to a 15-node uni-directional ring and an 11-node mesh-connection ring is that imposed by the cascade of EDFAs (which will be discussed in the next chapter.)

In order to keep the total input signal power (-2.9 dBm) unchanged as calculated in section 4.1, the individual signal input power is, therefore, (-2.9 dBm/15) = -14.6 dBm per channel. Figure 4.27 shows the

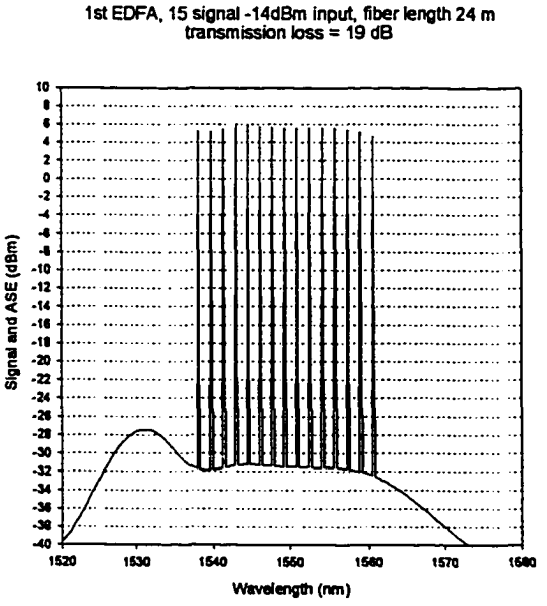

Figure 4.27, Gain spectrum output of one EDFA of 15 signal in 1538-1560-nm band, EDFA has same operation parameter as in Fig. 4.25.

output of 15 signals after one EDFA which is operated under optimized condition. The gain variation between these 15 signals is about 1 dB, average gain is about 20 dB and SNR is over 35 dB. As demonstrated in Eq. 4.20, the gain variation of the cascade EDFA is proportional to the number of EDFA cascaded (N) and gain variation of each individual EDFA: $\Delta G_{cascade} = N\Delta G_{individual}$ For the uni-directional ring, there could be a cascade of 15 EDFAs in the protection path, the total gain variation will be around 15 dB in this case which might exceeds the receiver's dynamic range and also will degrade the SNR. Figure 4.28 illustrates the output of a cascade of 15 EDFAs where the gain variation is around 14 dB and the worst SNR is only about 18 dB.

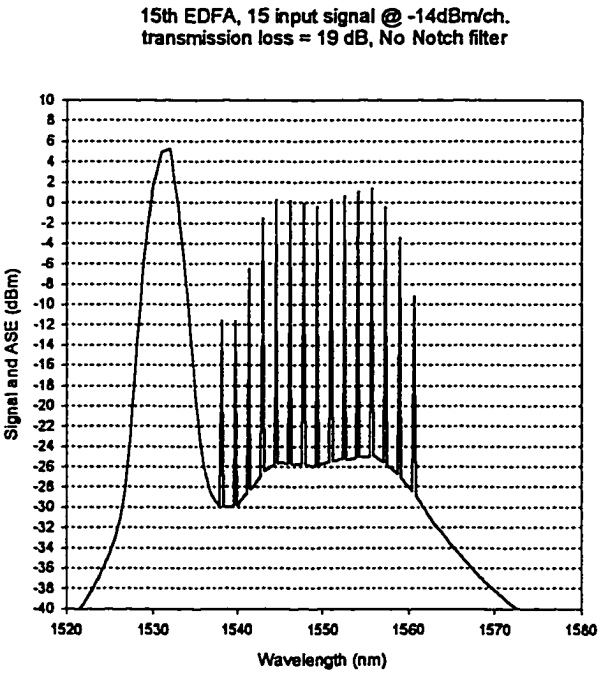

Figure 4.28, Gain profile of output of a cascade of 15 EDFAs.

Figure 4.28 also shows an ASE peak at 1530 nm which competes forthe pump power with signals and causes the degradation of average gain and gain variation. To improve the performance of cascaded EDFA, the first trivial method is to filter out the ASE peak. Figure 4.29 shows the output after filtering out the ASE noise of each EDFA in the cascade. The improvement is tremendous that average gain improved about 8 dB and gain variation was reduced by about 2 dB.

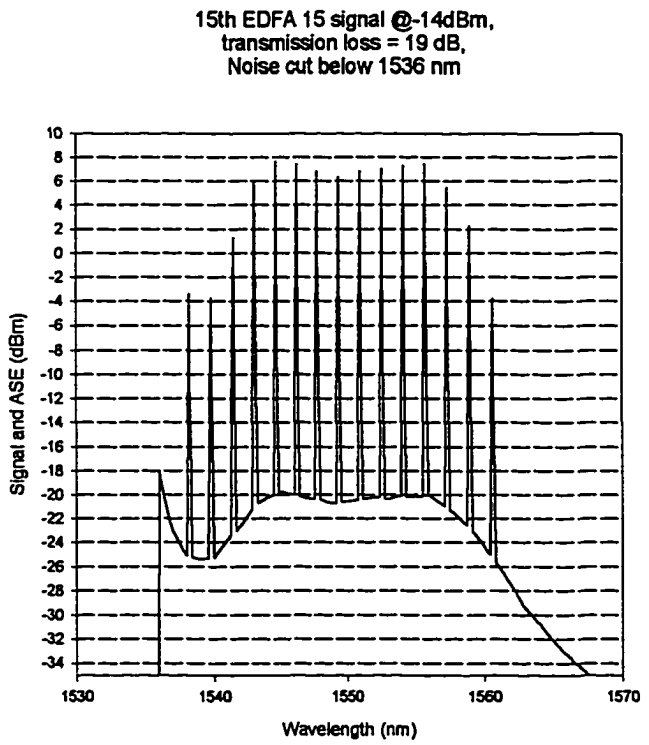

Figure 4.29, Gain profile of output of cascade of 15 EDFA with ASE cut below 1536-nm

The results can be further improved if some external gain equalization device can be used which will be discussed in next section. If these 15 signals are used in mesh-connected ring, a total of 11 nodes can be linked. There could be a cascade of 11 EDFAs in the protection path. The total gain variation accumulated along the cascade could be up to 11 dB according to Eq. 4.19b. Figure 4.30 shows the gain profile of cascade of 11 EDFAs without the ASE filtering. The gain variation is about 9 dB and the least signal level is about -3.45

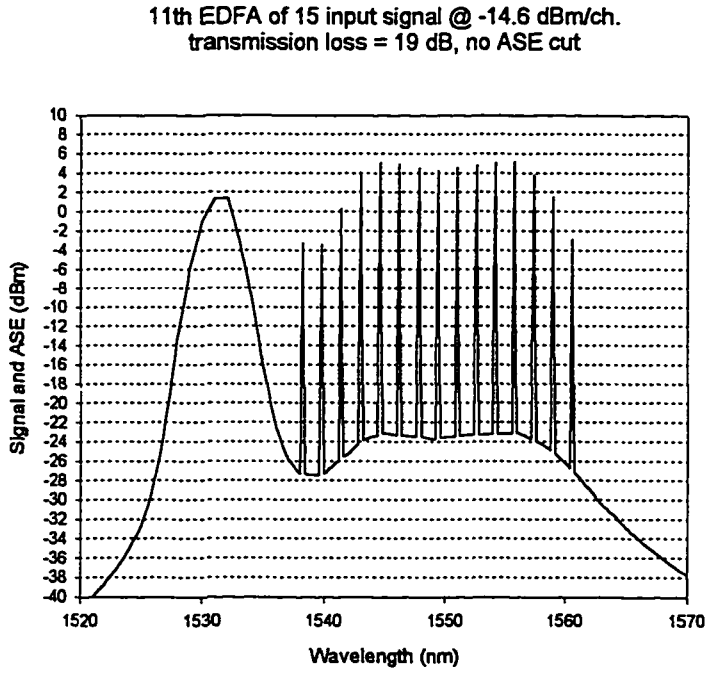

Figure 4.30, Gain profile of 11 cascaded
EDFA without ASE cut

dBm. Also there is an ASE peak competing for the pump power with the signals. By cutting the ASE noise, we can improve the signal level by 3 dB and gain variation by 1 dB. Figure 4.31 shows the results from the same cascaded EDFA as in Figure 4.30 but with the ASE filtered out below 1536 nm.

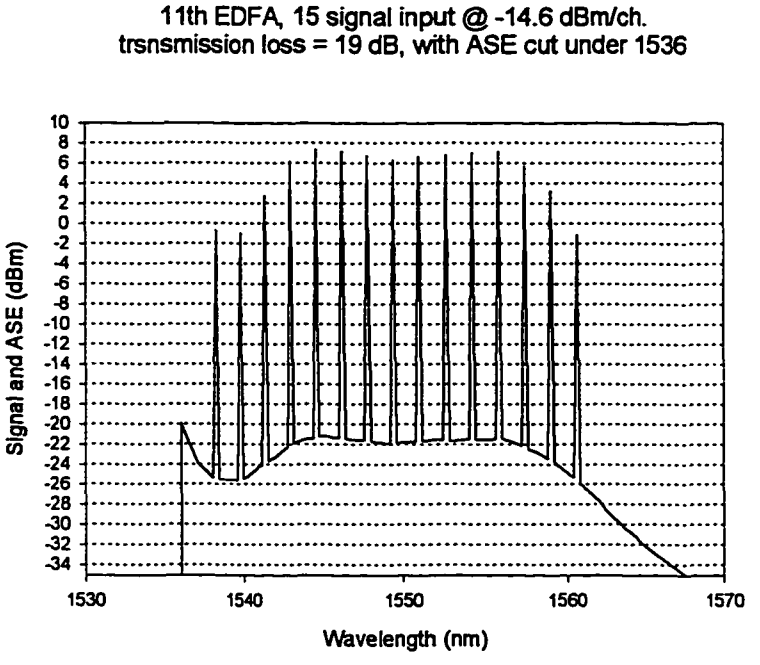

Figure 4.31, Gain profile of 11 cascaded
EDFA with ASE cut below 1536 nm

With an 8 dB gain variation and SNRs all over 24 dB as shown in Figure 4.31, the signal is adequate for 10 Gb/s transmission even after a cascade of EDFAs on the protection path. Note that the result of Figure 4.31 came from an ideal input yet there still have 8 dB gain variation which has very limited room for additional tolerance. Therefore, for a real ring network system with 11 node and 15 signals, gain equalization in the working path and the optical link and EDFA in protection path need to be optimized in order to keep the signal's gain variation and SNR within the limits for 10 Gb/s transmission.

4.4.3 1538 - 1572 nm BAND CASCADE PERFORMANCE

For a larger size of ring network, it will require more wavelengths. For example, a 13-node mesh-connected ring will require 21 wavelength. If we keep all the operation parameters of the EDFA unchanged, the ASE spectrum as well as the signal gain profile will keep the same as Figure 4.5 at the specific fiber length. Figure 4.32 shows such a gain profile at a fiber length of 26 m and total input power of -2.9 dBm (-16 dBm/ch.).

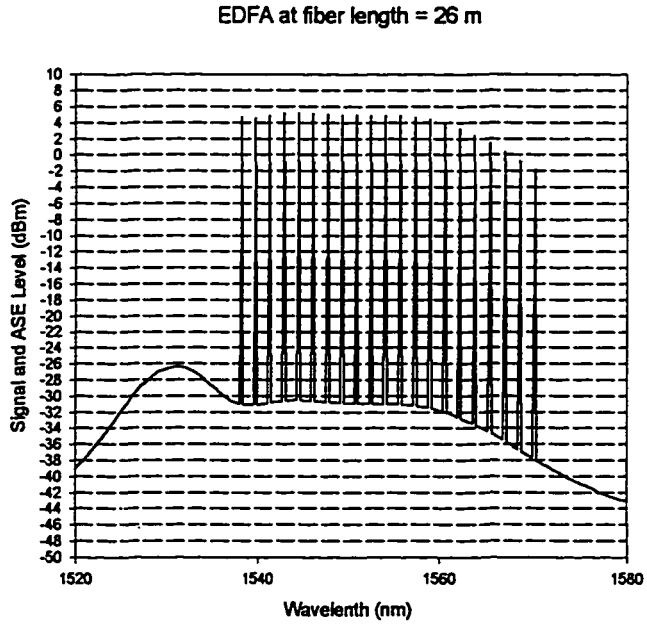

Figure 4.32, Output of one EDFA at length of 26 m,
21 signal input at -16 dBm/ch.

If these EDFAs are used in the protection path of the 13-node SHR, the number of cascaded EDFA could be up to 13. Figure 4.33 shows the output of cascade of 13 such EDFAs. 3 channels in the band over 1565 nm are totally lost in the ASE, which demonstrates that this kind of EDFA design is not suited for such wide wavelength band for cascade applications.

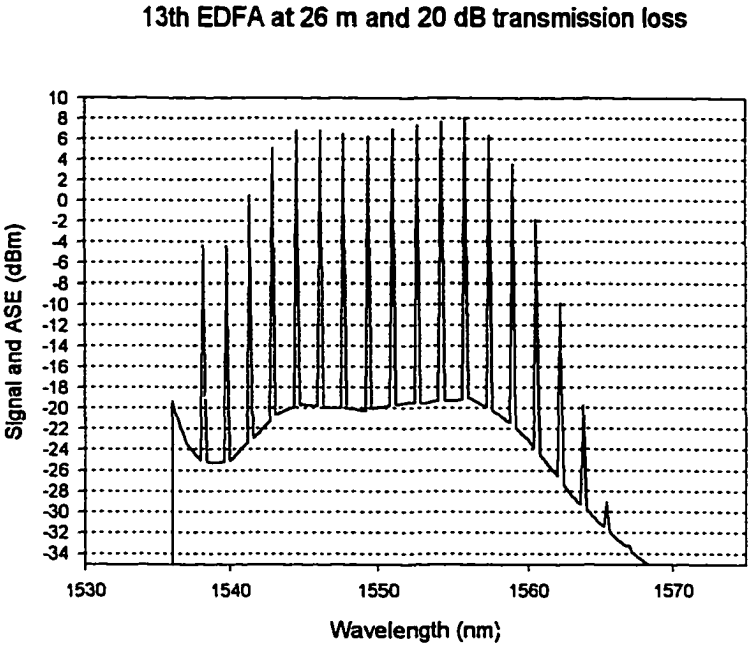

Figure 4.33, Output of 13 cascaded EDFA with fiber length of 26 m and transmission loss of 20 dB.

This is because of the intrinsic EDFA characteristics over the band of 1538-1572 nm, therefore, it is impossible to have a flat gain over such a wide range by just optimization of the EDFA. With the method we introduced in section 4.7, a Mach-Zehnder (MZ) device can be used for EDFA gain equalization[52], which requires the output of EDFA to have an sinusoid or quasi-sinusoid shape. By only changing the EDFA fiber length and keep other parameter unchanged, we can alter the shape of the EDFA close to the sinusoidal shape as suggested in 4.7.1. Figure 4.34 shows that at a fiber length of 42 m, the same fiber material and with the same 90 mw pump one can generate an output gain profile close to the sinusoidal shape. Therefore, it is possible to use the Mach-Zehnder device to do the equalization.

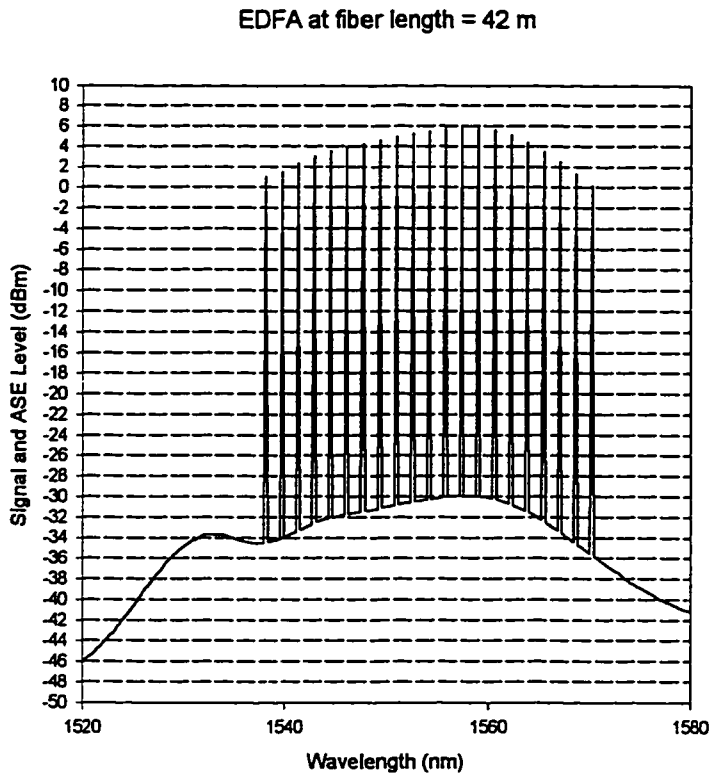

Figure 4.34, Gain profile of one EDFA at fiber length of 42 m.

With the sinusoidal shape of gain output from the EDFA, if without equalization, the signals after cascade of EDFAs are obvious unacceptable. Figure 4.35 and 4.36 show the output of cascade of 13 and 6 EDFA respectively. In Figure 4.35, there are signal at both edge of the signal are lost in to the ASE. To make the system work, some equalization method have to be used.

The MZ filter's transmittance should be the same as the inverted shape of the gain profile which is equal to $F_{eqi}(\lambda) = G_L / G_{opt}(\lambda)$ (4.23). By using curve fitting techniques, one can find the corresponding parameters of MZ which

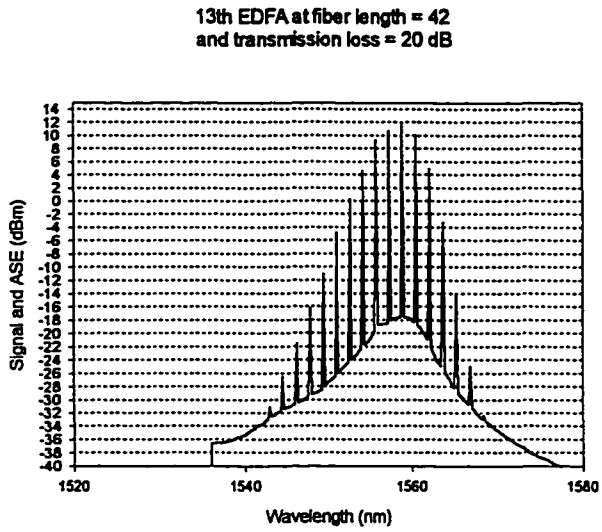

Figure 4.35, Output of 13th EDFA at fiber length = 42 m
and transmission loss = 20 dB

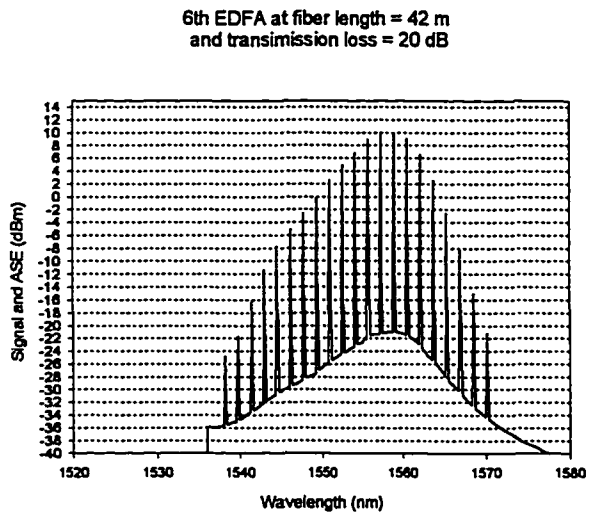

Figure 4.36, Output of 6th EDFA at fiber length 42 m
and transmission loss = 20 dB

have the transmittance of MZ $T(\lambda) = F_{eq}(\lambda)$. The parameters of the MZ filter which are mach the $F_{eq}(\lambda)$ of the spectrum illustrated in Figure 4.34 is :

$$\alpha = 0.22, \tau = 2.0\ \text{E}{-13}, \phi = -0.1$$

Where α,τ and ϕ defined in Eq. 4.22 are illustrated in the Figure 4.37.

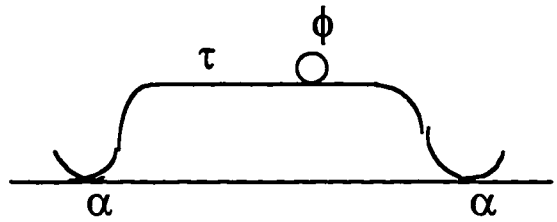

Figure 4.37, Block diagram of MZ filter

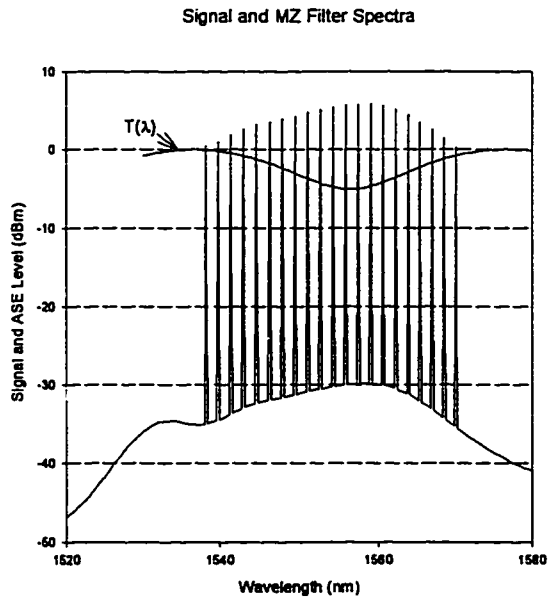

Figure 4.38 The Transmittance of MZ Filter T(λ)

The transmittance of the MZ filter and its corresponding gain profile are shown in the Figure 4.38. The physical implementation of the MZ filter is shown in Figure 4.39.

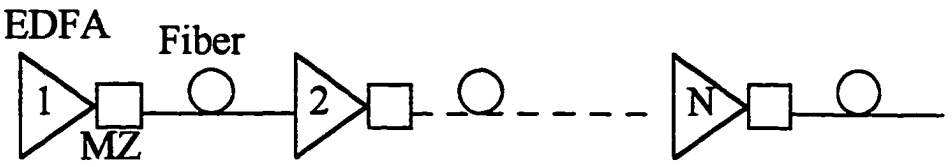

Figure 4.39 Block diagram of MZ filter implementation

The output of the combination of one EDFA and one MZ filter is shown in Figure 4.40 Figure, where the gain variation is reduced from 5 dB without equalization to 2 dB with the equalization.

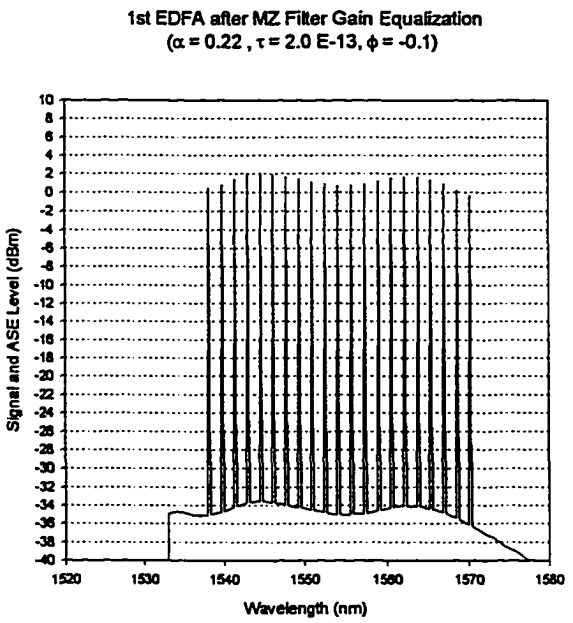

Figure 4.40 Output of the combination of the EDFA and MA filter

More important results are the output of cascade EDFA and MZ combination. Figure 4.41 and 4.42 shows the results of cascade of 13 and 6 EDFA respectively.

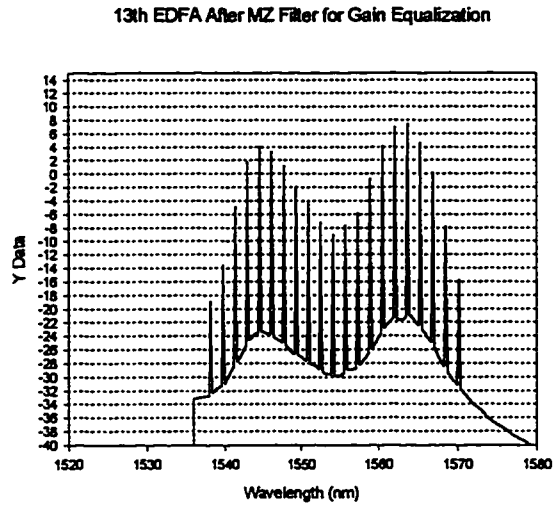

Figure 4.41, Output of 13th EDFA in cascade using MZ filters for equalizations

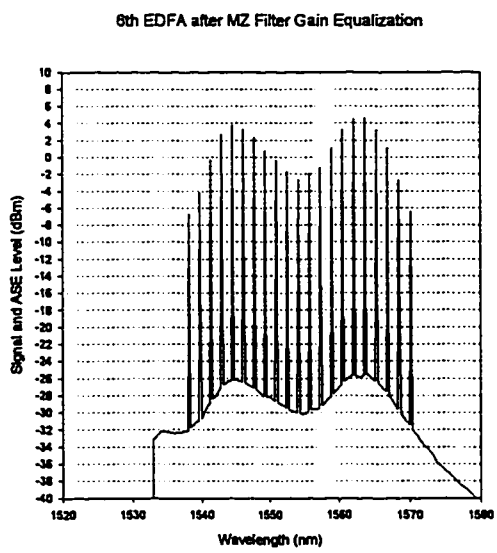

Figure 4.42, Output of 6th EDFA in cascade with MZ filter for equalizations

Comparing Figure 4.35 and 4.41, we can see a big improvement by this equalization scheme. In Figure 4.41, the signal at both edges of the bandwidth are shown and have about 10 dB SNR. But there was still about 25 dB gain variation in the Figure 4.41, which means this method of gain variation is not suited up to cascade of 13 EDFAs. Comparing Figures 4.36 and 4.42, the gain variation in Figure 4.36 which doesn't have a MZ filter for equalization is more than 36 dB and the gain variation shown in Figure 4.42 is only 10 dB. The worst SNR improved from 10 dB in Figure 4.36 to 24 dB in Figure 4.42 where equalization has been used.

In a further study of difference between the optical node in the working path and the protection path, we find that the power loss in the protection path is much smaller than that in the working path. In the node on the working path, there are multiplexer and demultiplexer, optical attenuators and switch fabrics all of which will bring a huge power loss. But in the protection path, the only thing inside the node is the optical switches. Therefore, the power loss in the optical node will be equivalent to the fiber transmission loss. Half of the gain of the EDFA in the optical node will to be used to cover the node equipment loss and half will be used for transmission. The gain of the EDFA in the protection path will be all used for transmission which means each EDFA in the protection path can cover the transmission for two nodes. For a 13-node mesh-connection ring, there are 13 EDFAs in the working path and might only have 6 or 7 EDFAs in the protection path. When 6 EDFAs are used for the protection path, the gain variation and SNR which were shown in Figure 4.42 are sufficient enough for 10 Gb/s transmission.

Chapter 5

END-TO-END SYSTEM PERFORMANCE

5.1 INTRODUCTION

The computer simulation technique is being used for end-to-end evaluation of the ring network performance. To study the performance of the WDM ring networks, we represent each amplifier by using the spectrally resolved analytical model [30], whose results agree within ~ 0.5 dB with the numerical model [24] in our operating regime. There are two kinds of ring configurations: one is an open configuration in which the ring itself is not closed and the information exchange is through a Central Office (or Hub), another one is a closed ring and the information exchange is by the direct communicating between the nodes. For a closed ring, due to the initial signal status in any node is unknown, therefore, the relaxation method has been used to reach the convergence from two adjacent iterations.

5.2 END-TO-END PERFORMANCE OF 2-FIBER RING

Uni-directional two-fiber WDM ring is an open ring configuration and is built on widely deployed uni-directional two fiber SONET ring for upgrading. The uni-directional SONET ring means that the electronic SONET ADMs (add and drop multiplexers) and DXCs (digital cross-connectors) are uni-directional. The SONET ring has a nice feature in being robust to failures, at the same time consuming a low volume of fibers, compared to a star network, since a number of sub-nodes are connected to the Central Office (CO) via one common ring. Figure 3.2 shows such a ring in which one of the node is used as CO to process all the traffic and do the switching for the network. However, a SONET ring is expensive to upgrade as mentioned in 5.1. If any change is

made in one sub-node, e. g. for an increase the capacity, changes have to be done in all the other sub-nodes around the ring as well. By using the WDM technology, the physical ring can be divided into either a logic star or a logic mesh. To upgrade the conventional two-fiber uni-directional ring, the logic star is one of the best choice. By keeping all the uni-directional electronic devices, such as electronic ADMs and DXCs, unchanged, each node will connected by different wavelength as a circuit switched network to the CO (or HUB) directly. Therefore, the capacity of the entire ring of conventional network can be used for each single node, and the total capacity of the same physical ring will become N times the whole capacity of the conventional ring. N is the number of nodes. For a logic star 2-fiber uni-directional ring, one fiber is used as the working path and another is served as the protection path. The wavelength in the working fiber is always equal to the number of the nodes on the ring in each link segment. One link segment is the fiber between two adjacent nodes.

5.2.1 TWO-FIBER WDM PATH SWITCHED RING

There are two protection schemes can be used in 2-fiber uni-directional ring. One is called path switched ring (UPSR) and another is called line switched ring (ULSR). As mentioned in 3.1.2 and illustrated in Figure 3.2, the path switched ring is that the signals are sent to both path (working and protection) simultaneously and the are select a better one by receiving end. This protection scheme is assuming the working and protection are on the different route and only protect for either one of the path failure but not both. In the optical transport layer, there is no difference in optical node working and protection. The advantage of the UPSR is network structure simplicity and management simplicity. All the signals in the either protection path and working path are being demultplexed in each node, therefore, the optical signal quality such as gain flatness is very easy to control. The protection decision is made at

electronic level so that there is no traffic reroute, which make the network management much easier. Figure 5.2 shows a block diagram of a UPSR node. In the WDM optical ring network, the mutliwavelength signals traverse a cascade of erbium-doped fiber amplifiers, each followed by optical add-and-drop filters. The amplifiers' nonflat gain spectra and accumulation of ASE, in generally, impose size and capacity limits of the network. For a 2-fiber uni-directional ring, due to the logic star configuration, some of the wavelength pass more EDFAs on the path than other wavelength when dropping in a node as shown in Figure 3.8. For example, an N node 2-fiber ring, all N wavelength are originated from and terminated in the CO. Each wavelength dropped in a node, the same wavelength will be added from that node carrying

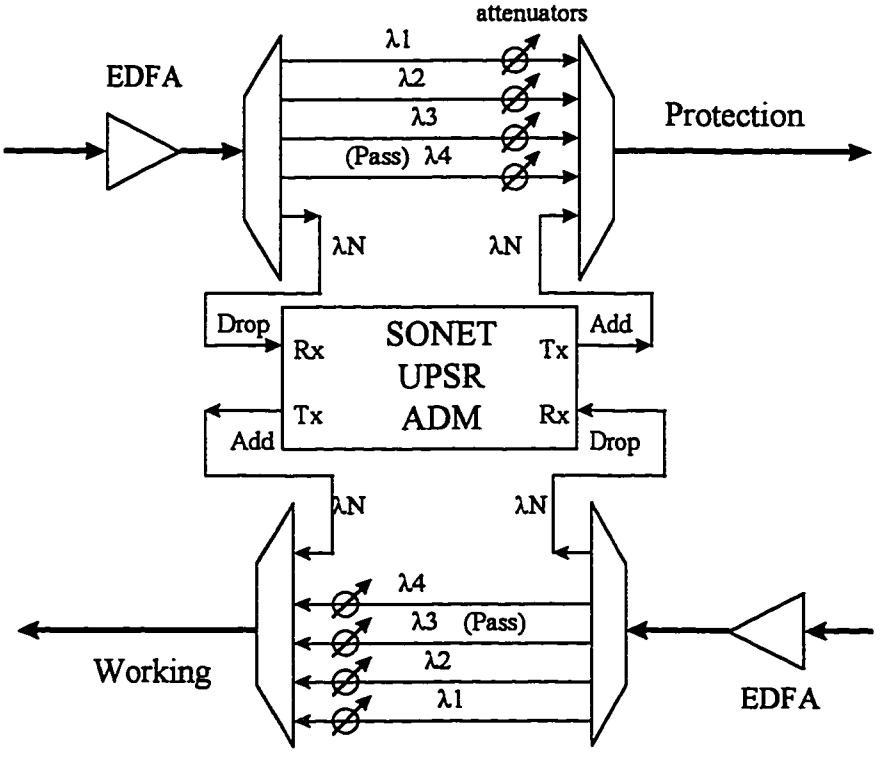

Figure 5.2 Block Diagram of Local Office of 2-Fiber WDM UPSR

the information to the CO. If wavelength λ1 drops at node one, the same wavelength will be added at that node and bypasses rest of the nodes with

EDFAs to the CO. At the CO, the signal from node 1 and signal from node N which may passes only one EDFA will have totally different level and SNR. The thesis work has shown that for different size of WDM UPSR, there are different techniques can be used to alleviate the signal degradation imposed from these signal imbalance. For a smaller size ring, a well optimized EDFA can obviate any external device [52][53]] as well as wavelength reordering [53]. For a medium size ring, we can reorder the wavelength add and drop assignment [53] to improve the over all performance. For a larger size ring, there more wavelength occupying wider EDFA's bandwidth and more cascade EDFAs are involved, the external equalization (such as atteunators or MZ filters) has to be implemented to ensure the network performance.

The physical ring models we going to study have the following characteristics:

1) The EDFA is aluminosilicate Lucent E006 erbium-doped fiber with gain and absorption spectra shown as Fig. 4.1.
2) Each amplifier is forward pumped by a 980 nm of 90 mW light and has an average gain of 19.5 dB.
3) All optical multiplexers and demultiplexers have flat 1-nm passband and 6 dB combined insertion loss.
4) All EDFAs are operating under the optimized conditions discussed in previous sections.

Follow the same sequence in 4.4, we will discuss 1543-1557-nm band (11signals), 1538-1560-nm band (15 signals) and 1538-1572-nm band (21 signals) separately.

(1) 11-Node WDM UPSR in 1543-1557-nm band

As shown in Figure 3.2, all the signals are originated in the CO office followed by an EDFA. Figure 5.3 shows simulation results of the signal gain profile after this EDFA. When the signals travel along the ring, 1st wavelength will be dropped in the node 1 and be added on in node 1 again, 2nd wavelength will be

dropped in node 2 and be added on in node 2, and so on. Figure 5.4 shows simulation results of the signal gain profile just after node 10, in which, as we can see, each signal has a different ASE level. This is because the each signal is added at different node and passes different number of cascade EDFA. The signal which has the worst signal-to-noise ratio is the one that is dropped and added first which will pass most of the EDFAs; in this case, it is the wavelength number 1. Figure 5.4 also shows the worst possible SNR in the local node which is the last node in the ring and last signal going to be dropped which is wavelength located on 1557.4-nm. The SNR of signal of 1557.4 shown in Figure 5.4 is larger than 28 dB. The simulation results of gain and ASE profile of signals coming to the central office is shown in the Figure 5.5, where the gain variation is less than 5 dB and the worst SNR is better than 27 dB. This result shows that for a well designed EDFA, it can totally obviate any need for external equalization or wavelength reordering for an 11-node, 11 wavelength signals UPSR.

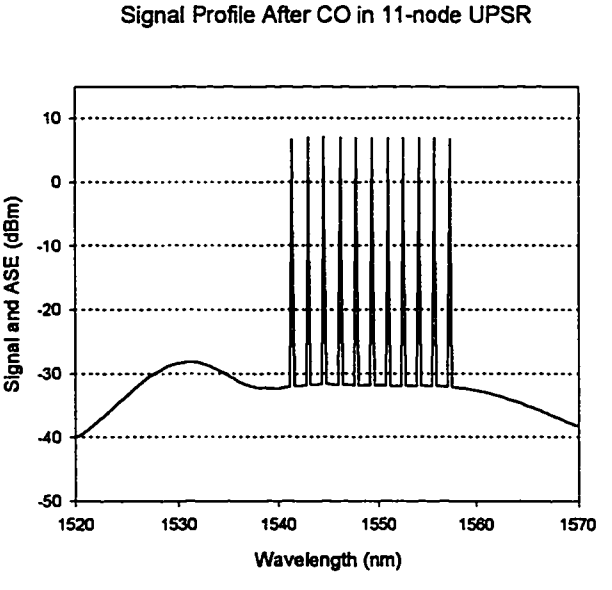

Figure 5.3

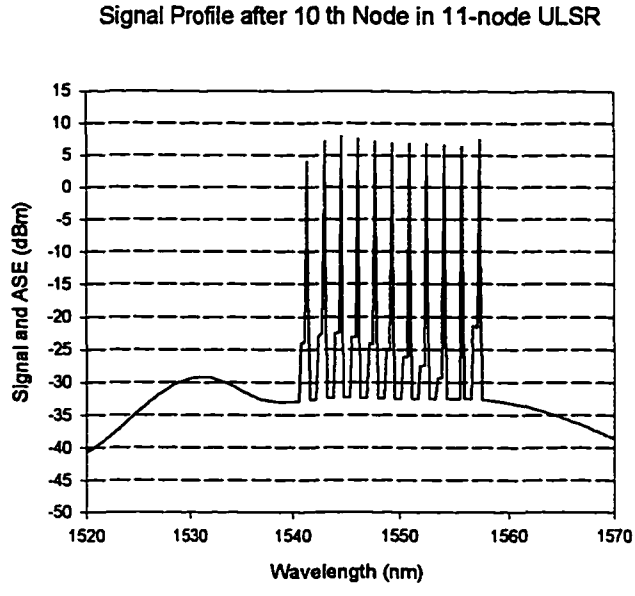

Figure 5.4

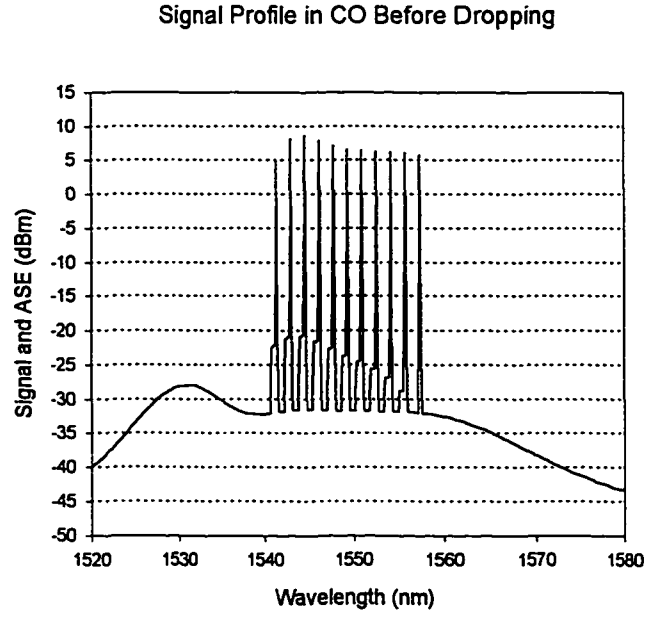

Figure 5.5 Gain Profile in Central Office

(2) 15-Node WDM UPSR in the 1538-1560-nm band

The wavelength assignment for the two-fiber uni-directional ring is that one wavelength is designated for each node. When the node size increases, the number of wavelength increases which means wider band of EDFA gain profile will be used. As we already known, the wider the bandwidth and the more EDFAs in the cascade, the larger the gain variation and the worse the SNR. In this case, both the signal degradation in the local node and in in CO have to be considered. The worst possible SNR happened to the last signal to be dropped and the first signal being added in the last local node and the CO respectively. Figure 5.6 and Figure 5.7 show the gain profile in the local node and in the CO respectively.

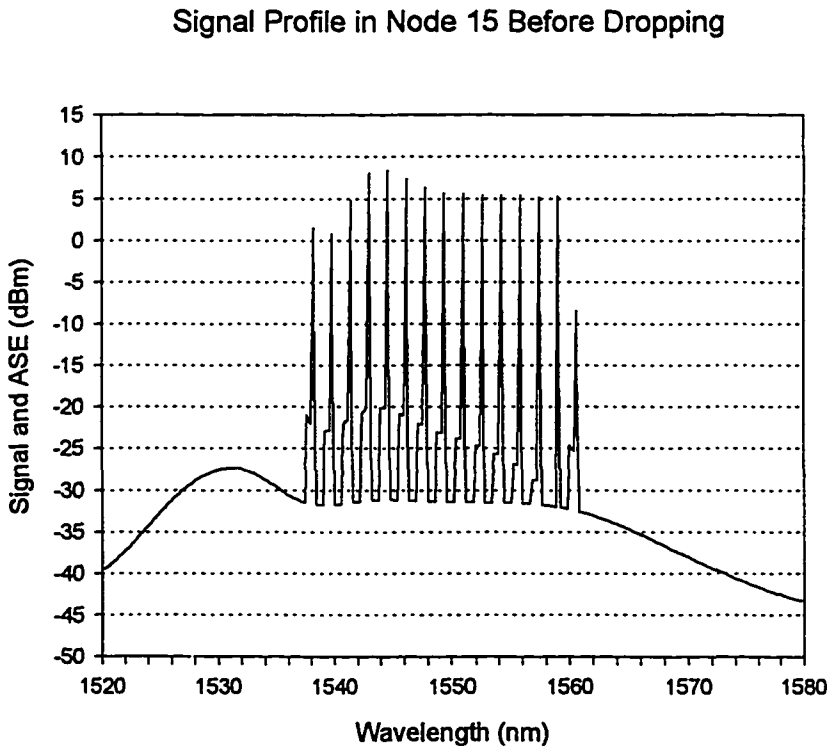

Figure 5.6 Signal Profile in Node 15 Before Dropping

Figure 5.6 shows that the signal going to be dropped (at wavelength 1560.6-nm) has the worst SNR (about 18 dB) among all the signals. This SNR is enough for 10 Gbit/s transmission. The gain variation in this node is not an issue because only this signal will be dropped.

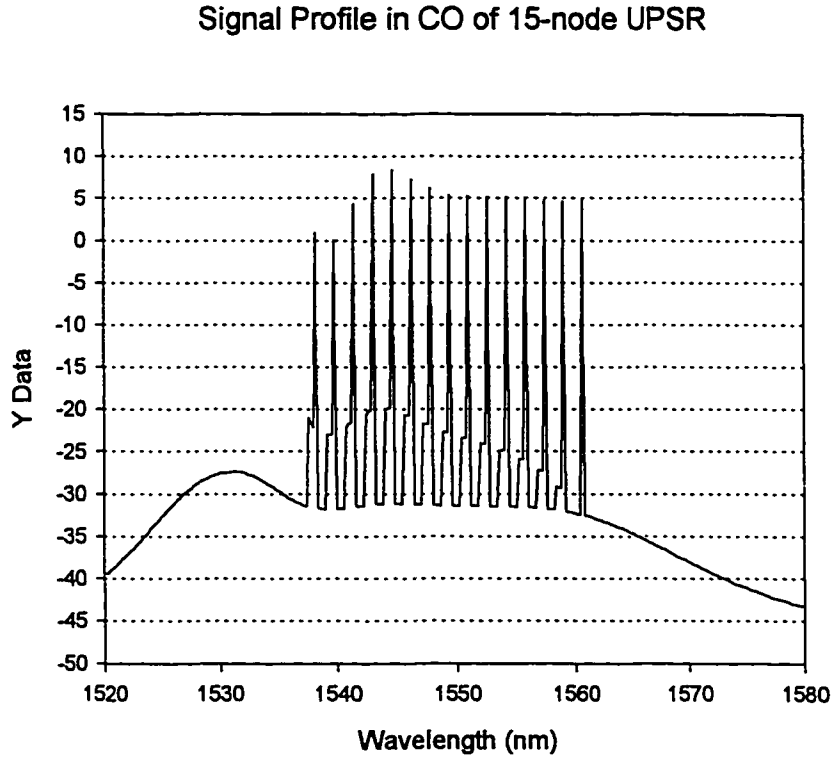

Figure 5.7 Signal Profile in Central Office

In the CO, both gain variation and SNR are important. Fig. 5.7 shows that the worst SNR is better than 25 dB and gain variation is less than 10 dB which is within the receiver's dynamic range.

The results in Figure 5.6 can be further improved by reordering the add and drop wavelength assignment. As we can see the last signal (at wavelength

1560.60-nm) get less and less gain along the cascade of EDFA. In stead of having it pass most of EDFA, we can drop this wavelength in the middle of the ring which break the chain of cascaded EDFAs in half for this wavelength. The accumulation of the saturation and ASE of this wavelength will be cut in half. Figure 5.7 is the gain profile at Node 8 before dropping. All the Figures (5.6, 5.7, 5.8) are shown that the fourth wavelength (1544.6-nm) has the strongest gain and the best SNR among all the signals. Therefore, we are going to drop the fourth signal last.

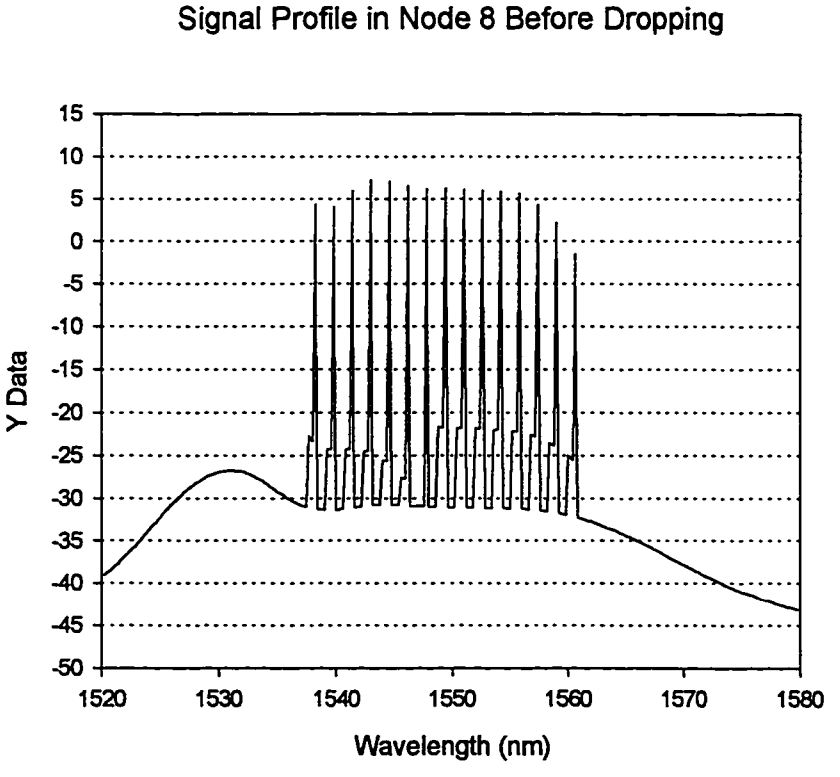

Figure 5.8 Signal Profile in Node 8 Before Dropping

To have a better results for all signals, we can drop the 7th signal at Node 4, 15th signal at Node 7, and 4th signal at last (Node 15). Figure 5.9 and Figure 5.10 are

the results of reordering the add and drop plan in Node 15 and CO before dropping.

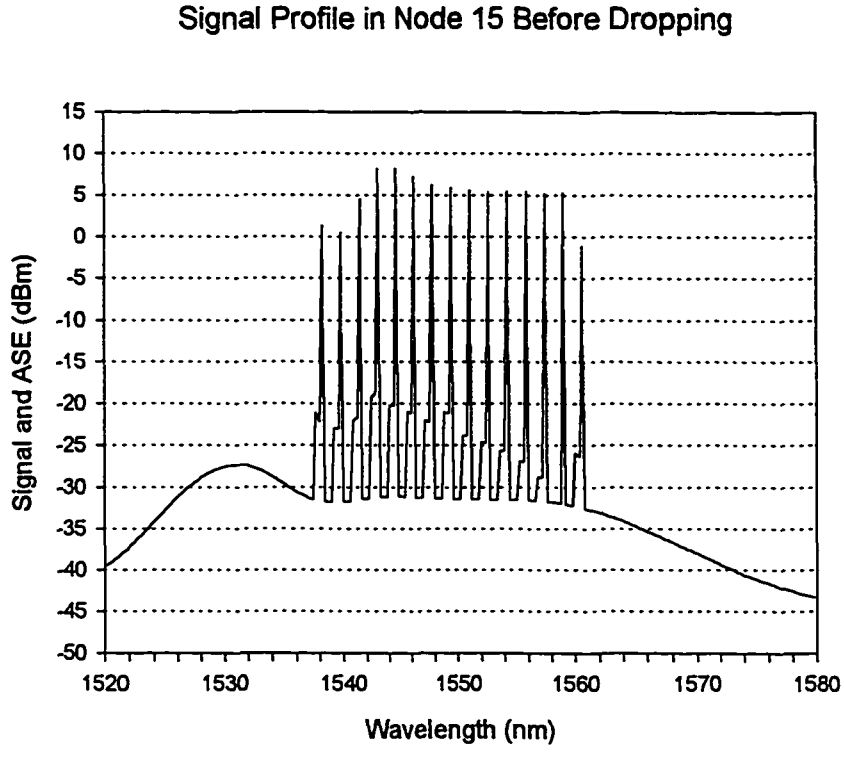

Figure 5.9 Signal Profile in Node 15 Before Dropping

Notice that, in Figure 5.9, the wavelength number 4 which experiences the most EDFA in cascade still have a decent SNR of 28 dB and wavelength number 15 which is being added in the Node 8 now has more than 24 dB SNR, a 6 dB immediate improvement from Fig. 5.6.

Figure 5.10 shows the signal profile which finally reached the CO after the add and drop plan reordering. The total gain variation is less than 10 dB and the worst SNR is better than 25 dB.

In conclusion, because of the characteristics of the EDFA gain profile, it is possible to reach the optimized results by combining the EDFA optimization and wavelength add-and-drop assignment optimization.

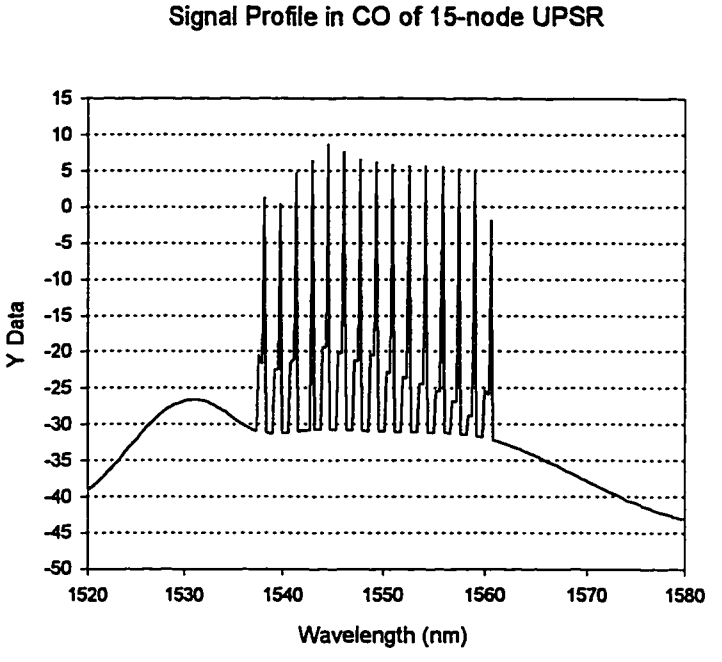

Figure 5.10 Signal Profile in CO of 15-node UPSR

(3) 21-Node WDM UPSR in the 1538-1572-nm band

For a 21-node WDM UPSR, the wavelength needed is 21, which will occupy 32-nm of EDFA gain bandwidth. As demonstrated in section 4.3, the intrinsic gain profile of the EDFA in this bandwidth is far from being flat. The gain variation method has to be used in the 21-node ring, which can be demonstrated in Figure 5.11 where no equalization scheme has been used. In Figure 5.11, it shows that the signals are actually lost when they are reaching the local nodes after several cascade of EDFA. In Figure 5.11a, the signals which are added in the first few nodes and the signals which haven't been

dropped are either total disappeared or degraded to unacceptable level. With these dramatic change of signal level, even add and drop plan reordering will

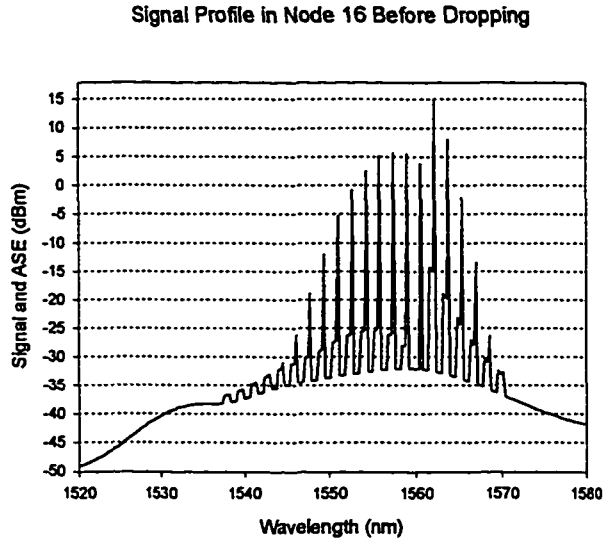

Figure 5.11a Signal Profile in Node 16 Before Dropping

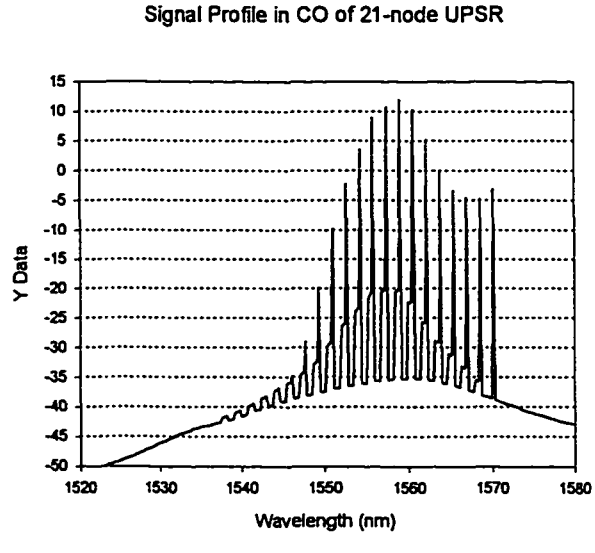

Figure 5.11b Signal Profile in CO Before Dropping

not help the ring system work. The only solution is doing equalization at each node [53]. As illustrated in Figure 5.2, the tunable attenuator is attached to the individual fiber for equalization. Figure 5.12 show the some of gain profiles of the 21-node ring networks with equalization in each node. Figure 5.12a is the signal profile in node 16 before demultiplexing, where the signal number 16 (wavelength 1560.60) which is going to be dropped at node 16 has more than 28 dB SNR, and the signals at both edge of the band have also the decent power level and SNR, a contrast to that in the Figure 5.11a.

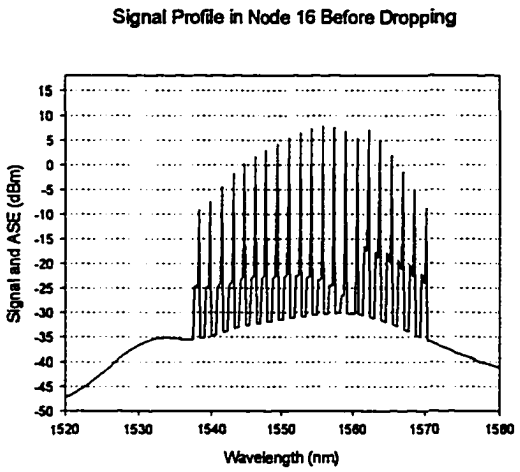

Figure 5.12a Signal Profile in Node 16 with Equalization
in Each Node of a 21-Node UPSR

The worst possible signal in this ring with equalization are the 1st signal and the last signal at CO and node 21 respectively. In Figure 5.12b shows the signal profile at node 21, where the last signal has about 10 dB of SNR before dropping. In Figure 5.12c illustrates the signal profile in the CO, where the signal added at first has passed most of the EDFAs and has the worst SNR which is about 15 dB. This research shows that for a very wide band of

wavelength and a long chain of cascade EDFAs, using the equalization can reduce the gain competition between the strong and the weak signals, and improve the SNR for the whole wavelength band. Due to the wide bandwidth, the gain difference is extremely large (approximately 18 dB), and gain equalization will cut the power of the strongest signal about 18 dB which reduce a lot of power budget for the system.

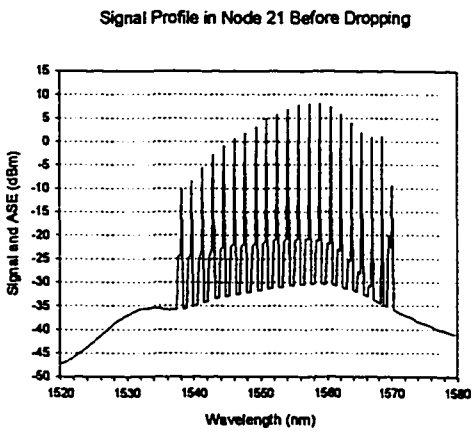

Figure 5.12b Signal Profile in Node 21 Before Dropping

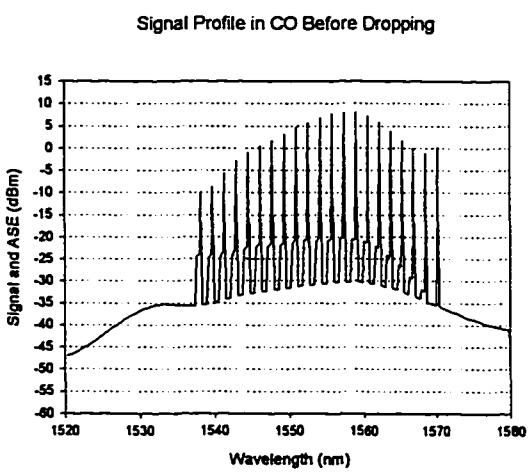

Figure 5.12c Signal Profile in CO Before Dropping

These results indicate that for a large ring network to use so many wavelengths, the better solution might be a smaller wavelength spacing. If 100 GHz wavelength spacing is used in the 21-Node ring case, the bandwidth is only about 16-nm, which can be fitted into the most flat range as discussed in section 4.2. Therefore, the results can be dramatically improved. Figure 5.13 show the incredible results by using the 0.8-nm spacing for the 21-node UPSR. In this research simulation, the cross-talk due to the narrower signal spacing is not included.

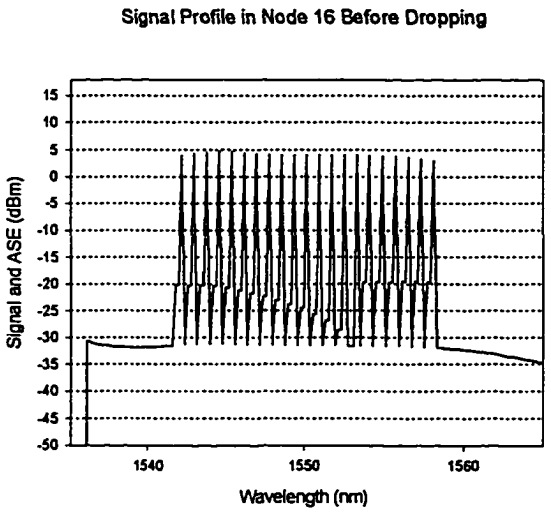

Figure 5.13a The Local Node 16 of the 21-Node UPSR
Using Attenuators for Equalization

Figure 5.13a shows a typical local node in the ring, where all the signal to noise ratio for either after or before dropping are better than 23 dB, and the signals are excellently flat. Figure 5.13b and 5.13c are two worst cases in the ring for the last and the first signal respectively. The worst case seems that is the last signal to be dropped in node-21, which has over 20 dB SNR and the gain variation after 21 nodes (21 EDFAs) is within 3 dB. These improvement shows

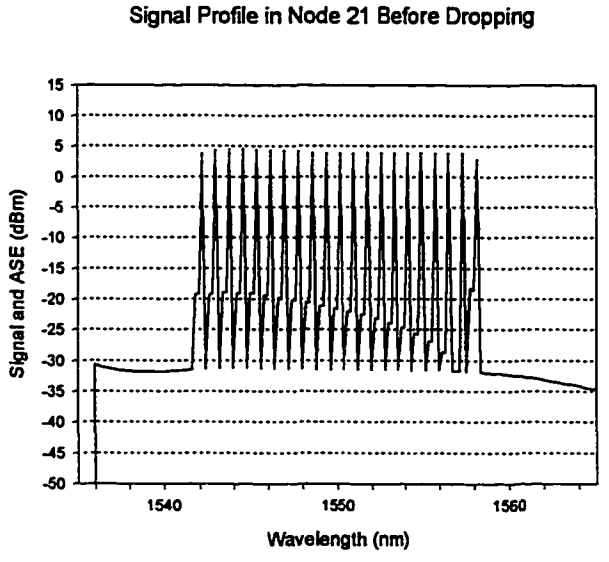

Figure 5.13b Signal Profile in Node-21 Before Dropping, It Shows the Excellent Gain Flatness and SNR

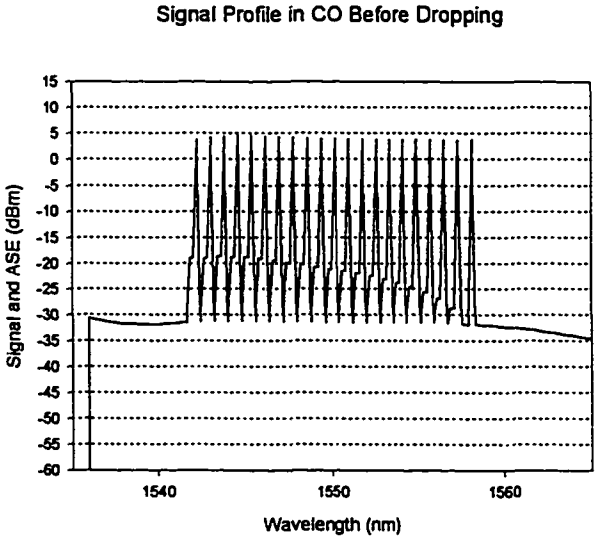

Figure 5.13c Signal Profile in CO which have passed 21 nodes and 22 EDFAs in the ring, the worst SNR is better than 25 dB, Signals are flat.

a large ring can be practically deployed in real network systems.

5.2.2 UNI-DIRECTIONAL TWO-FIBER WDM LINE SWITCHING (ULSR) RING WITH FIBER CUT

For a Uni-Directional Line-Switched WDM Ring (WDM ULSR), its normal working status is exactly as same as the UPSRs which has been discussed in 5.1. The difference between ULSR and UPSR is on the protection scheme. Only the performance of ULSR at the status of protection is discussed in this section. An ULSR block diagram is shown in Figure 3.10. In the ULSR, the protection path is not carrying any information until the network failures happened. There are two kinds of failure for the UPSR ring network: link failure and equipment failure. A link failure is the transmission line being cut or sever damaged for signal transmission. A equipment failure is the signal can not be drop or add and processed in a node. In the ULSR, as shown in the Fig. 3.10, there is a 2x2 optical switch in both sides of the node. When either link failure or equipment failure was happened, the optical switch at the both sides of the failure will switch the signal to the protection path to isolate the failure, as shown in the Fig. 5.14.

ULSR s' Protection Status for Failures

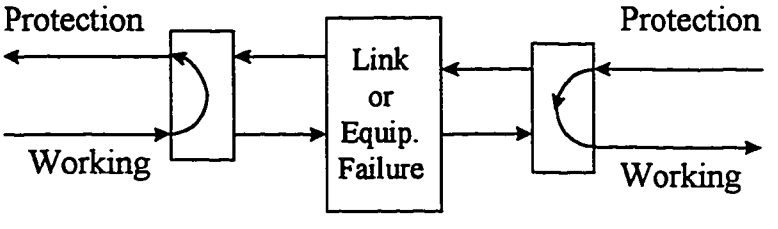

Figure 5.14

When the ring in the protection status, all the signals in the working fiber will be switched to the protection path, where the signals pass all the nodes (with EDFAs) to the other side of failure. Then the signal will be switched back to the working path as normal traffic. The challenge in the ULSR system design and performance analysis is that the signals should be maintain in a good quality after going through the protection path. Figure 5.15 is the ring traffic flow when it is in the protection status.

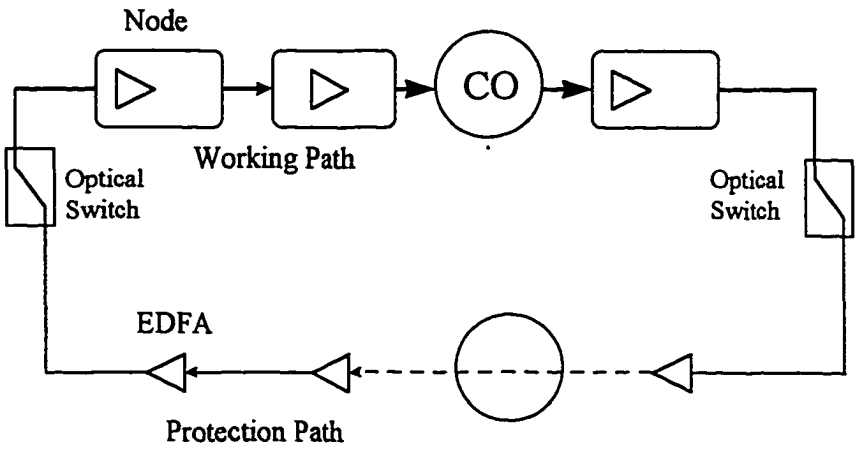

Figure 5.15 Traffic Flow in the Protection Status of ULSR

The difficulties to have a adequate SNR and minimum gain variation is increased when the ring size is increased (with more wavelength and EDFAs). To simplify the implementation of the self-healing WDM, the most critical part is the EDFA optimization. For a limited bandwidth, a well design the EDFA can eliminate any external device for the signal go through the working path and protection path. Figure 5.16 shows such a case. It is assumed that the fiber cut is happened between node 9 and 10 for a 11-node 2-fiber ULSR. Figure 5.16a is the signal profile in node 10 just before the fiber cut. It shows that last 3 signals which have not been dropped have a decent SNR value and all signal variations are within 3 dB. Due to the fiber cut, the signal after node 9 will be switched to the protection path and bypass all the nodes on the protection to

the node 10. Figure 5.16b shows the signal profile after the last EDFA in the

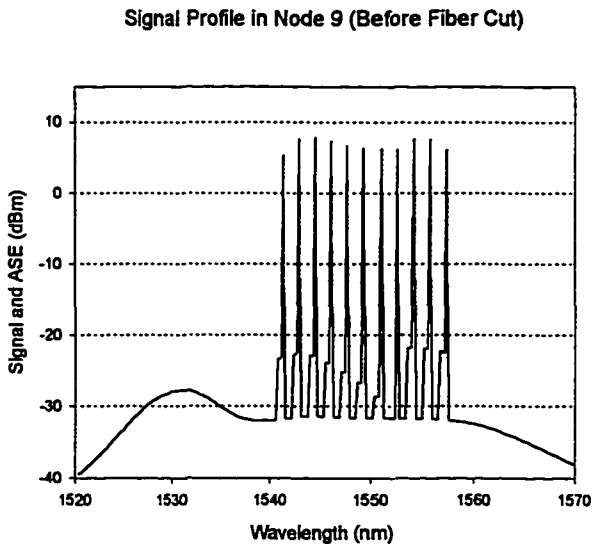

Figure 5.16a Signal Profile Before Fiber Cut

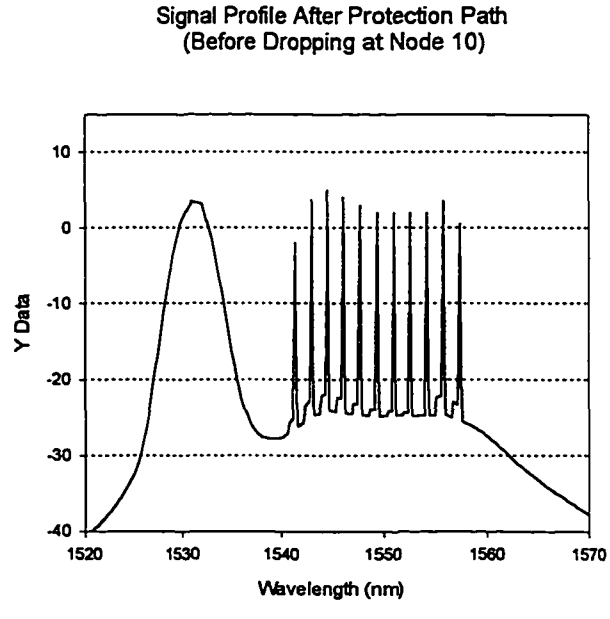

Figure 5.16b Signal Profile After Protection Path

protection path, where the worst SNR among all the signals is degraded from 20 dB to 12 dB. The ASE peak also accumulates from the cascade of EDFAs. Figure 5.16c shows the signal profile reaching at the CO. The SNR at the CO

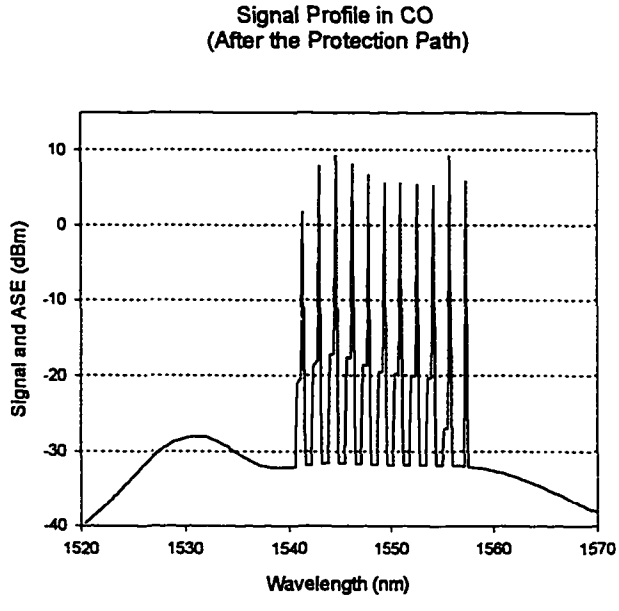

Figure 5.16c Signal Profile in CO in Protection Status

is very low SNR. The worst SNR is about 11 dB when no external equalization method is used.

To improve the SNR performance, one can filter out the ASE accumulation in the protection path by just inserting a Notch filter in the EDFA. Figure 5.17a shows the signal profile after last EDFA in the protection path where the ASE peak is filter out in every EDFA. 5.17b shows the signal profile in the CO followed 5.17a, which the signals have more gain than that the case of without ASE filtering out (about 2 dB). At the same time, the SNR also improved about 2 dB for all the channels.

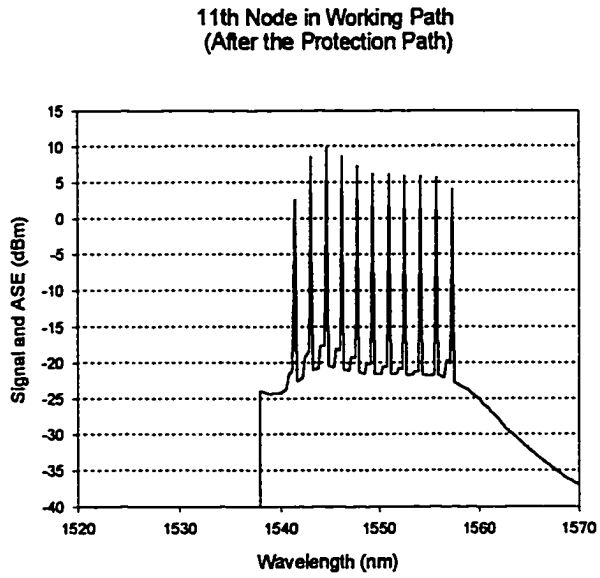

Figure 5.17a Signal Profile after Protection Path

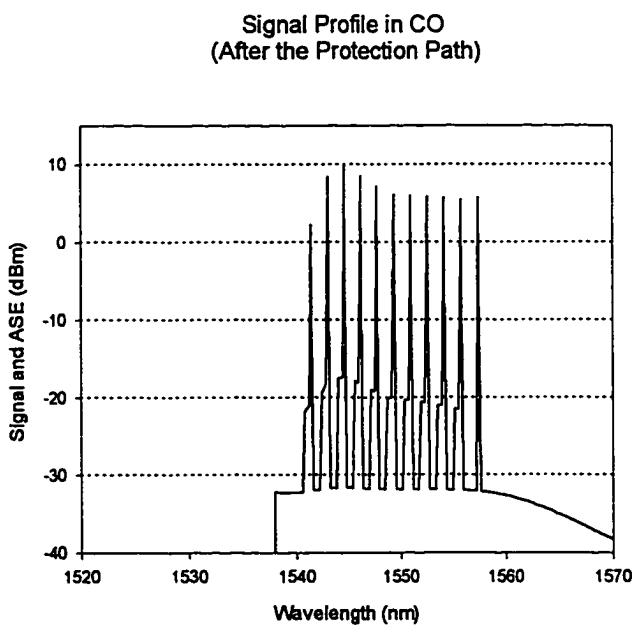

Figure 5.17b Signal Profile in CO

5.3 END-TO-END PERFORMANCE OF 4-FIBER RING

The bi-directional 4-fiber mesh connection line-switched ring network is totally different with the 2-fiber UPSR and ULSR. First, there is no central switch for the mesh-connection ring, therefor the ring is a closed self-healing ring. Secondly, the add and drop plan is more complicated than the 2-fiber ring. The add and drop plan is based on the mesh connection's wavelength assignment. The computer simulation program for the this ring network is also a challenge for the research. For a closed ring system, the results are not accurate until the signals traveling in the ring are stabilized. The status of the signal profile is unknown prior to the beginning of the simulation, therefore, several iterations to reach the convergence results are necessary. The wavelength assignment plan should make sure all the wavelengths (signal and ASE) are dropped at least once along the ring to avoid the oscillating of the signal or ASE to saturate the EDFAs. Following the same sequence as in 5.1, different number of node size with different signal bandwidth are discussed.

Performance of 9-node WDM BLSR in 1543-1556-nm band at failure free status

As discussed in 3.3, the number of wavelength needed for 9 nodes mesh connection is equal to $(9^2-1)/8 = 10$. The optimized wavelength range as we have discussed in 4.2 for 10 wavelength is around 1543 - 1556-nm. Table 5.1 is the wavelength allocation which follow the ITU standard wavelength allocation grid of 200 GHz.

Wavelength No.	W1	W2	W3	W4	W5
Wavelength (nm)	1541.4	1543.0	1544.6	1546.2	1547.8
Wavelength No.	W6	W7	W8	W9	W10
Wavelength (nm)	1549.4	1551.0	1552.6	1554.2	1555.8

Table 5.1 Wavelength Allocation

The wavelength assignment algorithm has been fully discussed in 3.3. Following the rules in Table 3.4 which is evolved from the network growth, Figure 5.15 shows the distribution of the wavelength add and drop assignment. Table 5.2 shows the wavelength add and drop plain for the 9-node mesh ring. The order of the number of the node has been rearrange to keep in a continuous sequence fashion.

The network performance analysis simulation has been done according to the Add & Drop plan indicated in Table 5.2. The cable failure is assumed happened in between node 1 and node 9. Therefore, the traffic flows from node 1 to node 9 on the working path, then switches to the protection path after node 9. On the protection path, the signal and ASE pass a cascade of 9 EDFAs before switched back to node 1. The iterations are not stopped until the signal level in the node 1 are within 10^{-6} margin between two iterations.

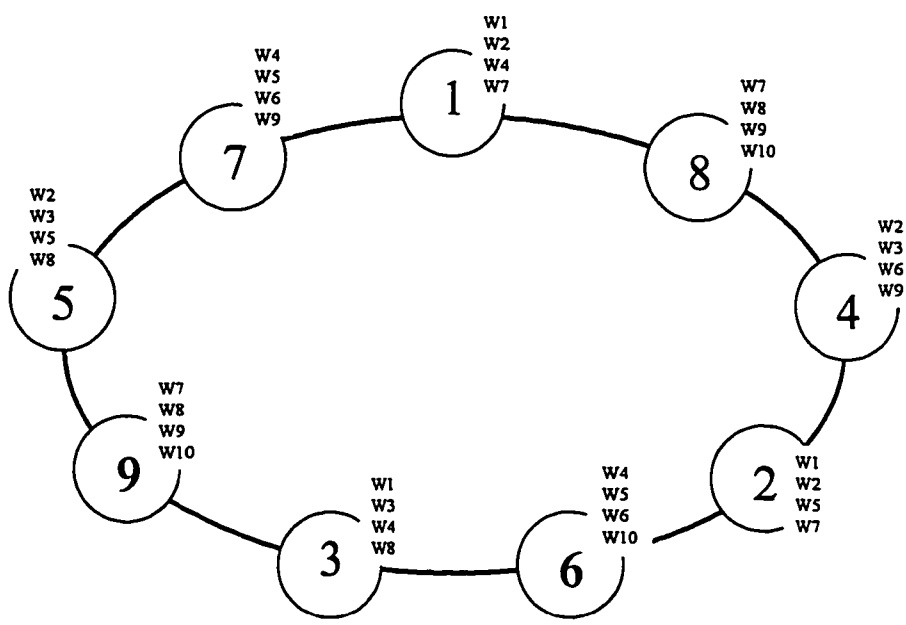

Figure 5.18 9-node ring, the numbering of the node indicates the new node adding sequence

Node	1	2 (8)*	3 (4)	4 (2)	5 (6)
A&D	W1,W2, W4,W7	W7,W8, W9,W10	W2,W3, W6,W9	W1,W2, W5,W7	W4,W5, W6,W10
Node	6 (3)	7 (9)	8 (5)	9 (7)	
A&D	W1,W3, W4,W8	W7,W8, W9,W10	W2,W3, W5,W8	W4,W5, W6,W9	

Table 5.2 Wavelength Add and Drop Plan for A 9-Node Mesh Ring

*The number in parentheses indicates the sequence of ring growth as shown in the Figure 5.15.

The results of the previous iteration of calculation are used as initial value for the next iteration. Some of the results are shown in the Figure 5.19 and Figure 5.20. EDFA has an optimized performance in band of 1543-1556-nm as discussed in the section 4.2. The results shows in Figures 5.19 and 5.20 indicate that no external equalization method is necessary for the mesh ring.

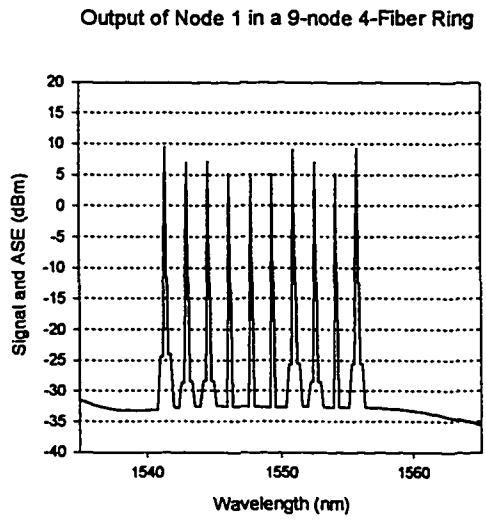

Figure 5.19 Signal Profile in Node 1

In Figure 5.19, it shows the wavelengths W4, W5, W6 and W9 which are just being added in the previous node (node 9) have the best SNR. The worst SNRs are the signal of W1 and W10 which were added in node 6 and node 7 respectively and experienced most of the EDFAs.

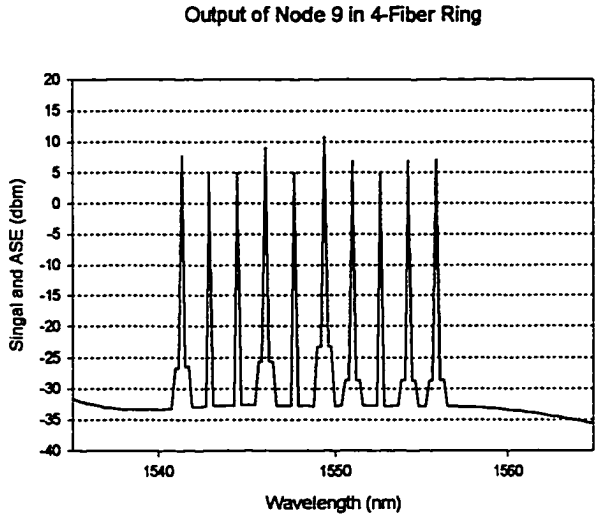

Figure 5.20 Signal Profile in Node 5

Similar to Figure 5.19, the Figure 5.20 is showing the simulation results of node 9. Both Figure show that signal gain variations are within 5 dB and worst SNR is better than 35 dB.

5.3.1 BI-DIRECTIONAL FOUR-FIBER MESH CONNETTION WDM RING WITH FIBER CUT

A ring network performance analysis without concerning the performance at the failure status is meaningless. The self-healing ring network has to be functional when the fiber is cut or equipment is failure. The signals have to be routed via protection path to recover the failures. The difficulty will become doubled when the ring size increases. The large ring not only means the

number of nodes are bigger, but also means more wavelength which will occupy wider wavelength band, and more EDFAs in the cascade of the protection path, both of them will exaggerate the gain unflatness and degraded the SNR severely.

The 9-node and 11-node mesh WDM ring are used to study performances and find the way to improve the network system.

(1) 9-Node WDM BLSR in 1543-1556-nm Band with fiber cut

Following the simulation results in 5.3, we assume that the fiber cut is happened in between node 1 and node 9. Therefore, the traffic after node 9 will be routed to the protection path. On the protection path, the traffic goes through node 8, 7, ... all the way to node 1. The signal on the protection path is not dropped in any node until it reach to the node 1 which is the destination the traffic. The signal profile before it is switched to the protection path is showing in Figure 5.20. After passing 9 EDFAs (including the one in node 1), the signal profile is shown in Figure 5.21. The ASE is accumulated from -33 dB to -23 dB, and the gain variation is still kept within 5 dB which is attributed to the optimized EDFA design for this bandwidth. This results demonstrate that for a well design EDFA it is possible to have 4-fiber WDM BLSR functioning without any external gain equalization for a certain limit of ring size. Previous work only showed 6-node using 7 wavelength [54]. Figure 5.22 shows the signal quality in node 2, where the signal were not dropped in node 1 have a worse SNRs. The worst SNR is channel 5 (about 15 dB) in Node 4, which is not dropped until Node 4. The ASE of the channel 5 is accumulated from cascaded EDFAs in the protection path and the EDFAs in the Node 1, 2 and 3 of the working path. It is shown in Figure 5.23

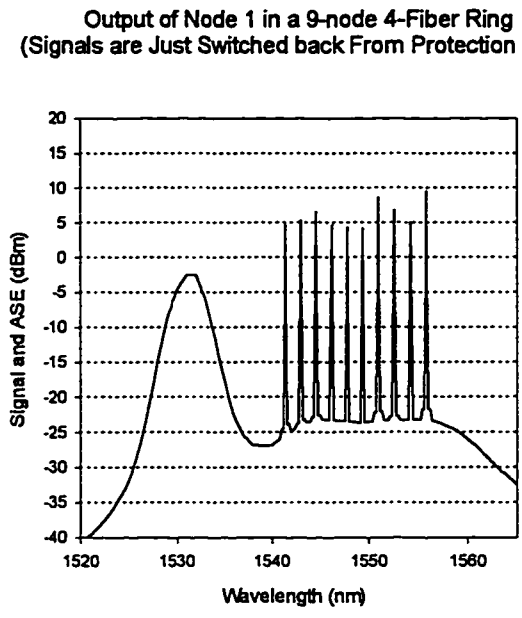

Figure 5.21 Signal Profile in Node 1 After the Protection Path

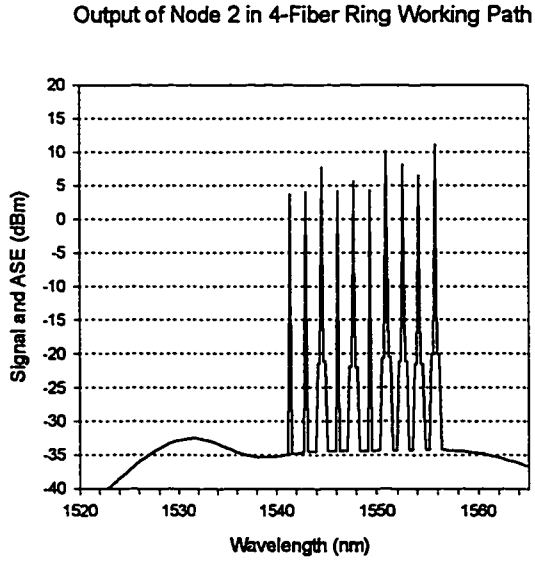

Figure 5.22, Signal Profile in Node 2

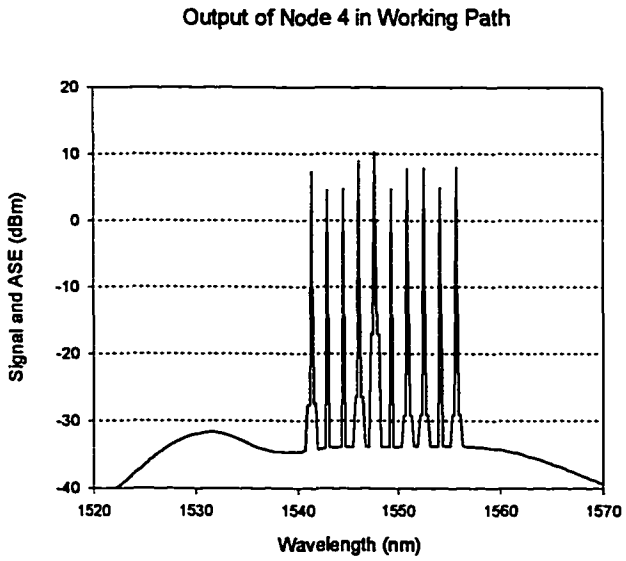

Figure 5.23, Signal Profile in Node 4, where channel 5 has the worst SNR among all the signals in all the nodes.

(2) 11-Node WDM BLSR in 1538-1560-nm band

For a 11-node mesh connection ring, the number of wavelength required is 15. If the 1.6-nm spacing is used, these signal will occupy the bandwidth from 1538-nm to 1560-nm. For the signals occupy the wider bandwidth, the signal at both edges have less gain as the signal in the center wavelengths, which cause a large gain variations. These gain differences increase exponentially along the cascaded EDFAs as the strong signal competing for more pump power and experienced more gain.

The wavelength assignment for a full mesh connection of 11-node ring is shown in the Figure 5.24. The number of the node indicate the sequence of network growth as discussed in Chapter 3. The add and drop plan according to the traffic flow is shown in the Table 5.3. The wavelength numbers in the box of the Table 5.3 are the wavelength being dropped in the node, and the same

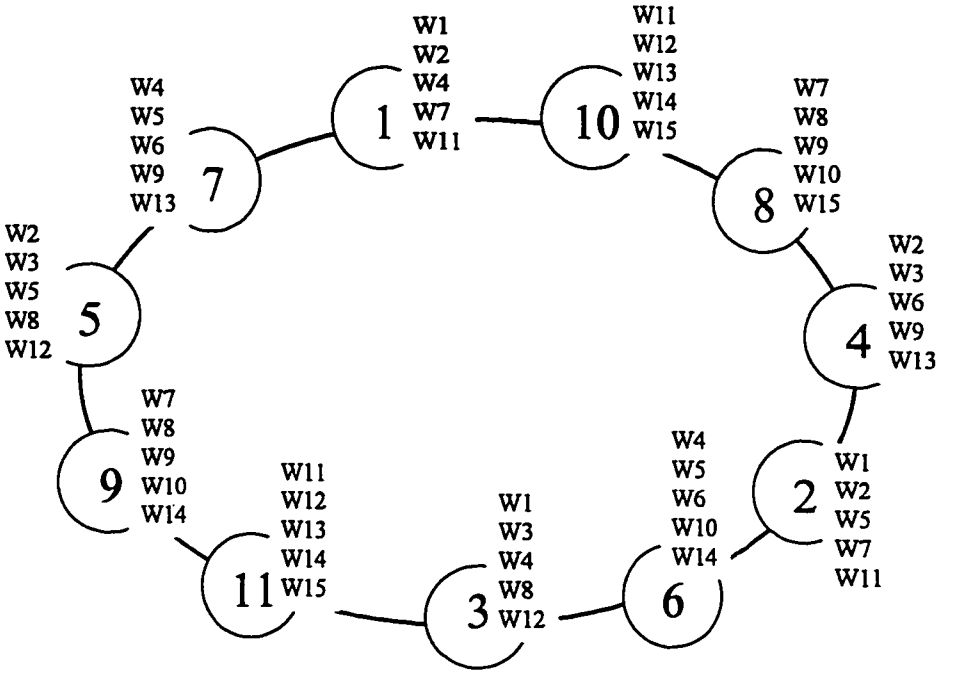

Figure 5.24, Wavelength add and drop Plan of 11 nodes mesh ring, the number indicating the adding sequence

Node	1	2(10)	3(8)*	4 (4)	5 (2)	6 (6)
A&D	W1,W2, W4,W7 W11	W11,W12 W13,W14, W15	W7,W8, W9,W10 W15	W2,W3, W6,W9 W13	W1,W2, W5,W7 W11	W4,W5, W6,W10 W14
Node	7 (3)	8(11)	9 (9)	10 (5)	11 (7)	
A&D	W1,W3, W4,W8 W12	W11,W12 W13,W14, W15	W7,W8, W9,W10 W14	W2,W3, W5,W8 W12	W4,W5, W6,W9 W13	

Table 5.3 Wavelength Add and Drop Plan for A 11-Node Mesh Ring

*The number in parentheses indicates the sequence of ring growth as shown in the Figure 5.23.

same wavelength will be added in this node. To have a flat gain profile, one of the key issues is to balance the added signals level with the passing signals, to

balance the amplifier's gain with loss of fiber transmission and losses of De/Mux filters, etc.

The major effect factor to SNR in the ring network is the accumulation of the ASE. It is not severe on the working path because the signal will not traveling a long chain EDFA (the signals are dropped and added frequently according to the mesh connection plan). The ASE accumulation comes mainly from the protection path where the signals passed cascaded EDFAs without any adding and dropping. The accumulation of the ASE along the EDFA chain will degrade the SNR, increase the signal level differences, which will limit the size of the ring.

The computer simulation has shown that the 11-node mesh ring can be designed for for 10 Gbit/s or higher transmissions if all the EDFAs are optimized, the adding signals and passing signals in each node are well balanced as well as the signals gain and their losses. The signals have 19 dB gain, a 7 dB insertion loss is assumed for combined loss of Demux and Mux, and the transmission loss is 12 dB for the working path. The average level of 5 dBm for each signal is got from the output of the EDFA. The inserted signal level has to match the level of bypassing signal. Therefore a 1.5 dBm of inserted signal level is used in the simulation, where -3.5 dB of Mux loss is assumed and another 12 dB of transmission will bring down the signal to -14 dBm level at the input of the next EDFA.

Figure 5.25 shows the signal profile in the node 11 before dropping some of the signals, where the worst SNR is better than 35 dB and the gain variation is less than 4 dB. After dropping wavelength W4, W5, W6, W9 and W13, the traffic is routed to the protection path, assuming the fiber cut is happened in between node 11 and node 1. Figure 5.26 shows the signals profile after first EDFA in the protection path. It shows all the signals have good SNRs and signal gain profile is almost flat.

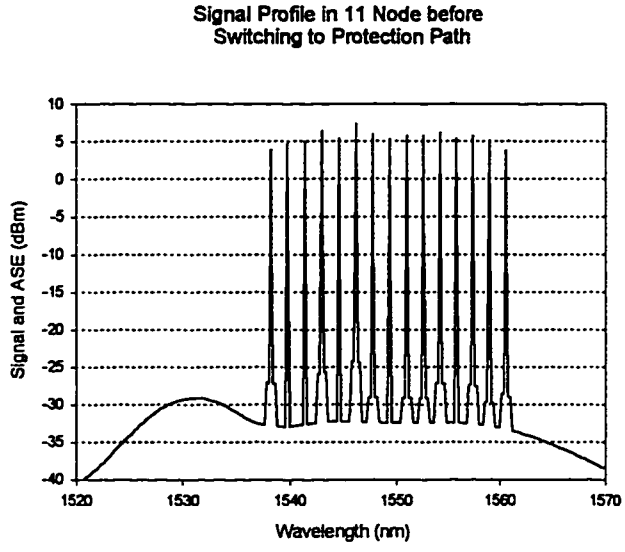

Figure 5.25, Signal Profile in Node 11

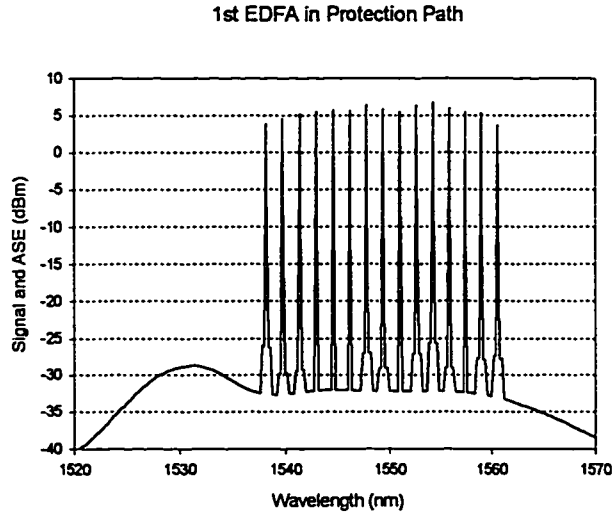

Figure 5.26, Signal Profile after 1st EDFA in Protection Path

When the signal pass the cascade of EDFA on the protection path, the signal quality is degraded by the accumulation of ASE and gain unflatness. Figure 5.27

shows the signal profile after last EDFA of the cascade on the protection before dropping into node 1.

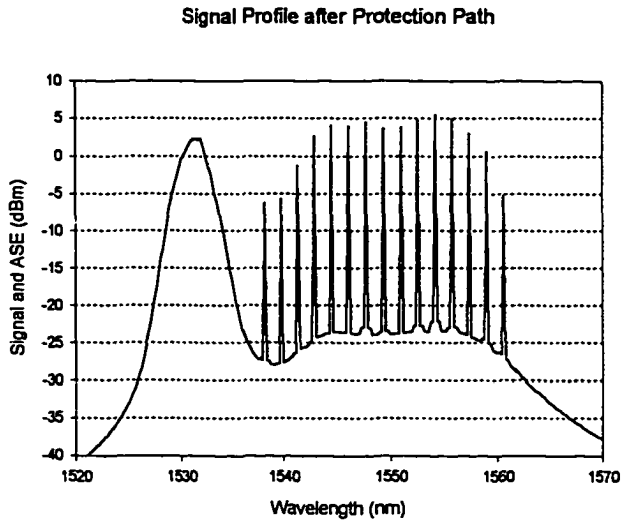

Figure 5.27, Signal Profile After Last EDFA in Protection Path

If the ASE is not filter out in the EDFA, the ASE is accumulatied to very high level which will saturate the amplifier and degraded the SNR. The wavelength W1, W2, W4, W7 and W11 in Figure 5.27 will be dropped in the node 1 when the signal is switched back to the working path from the protection path. The signal level of W1 W2 is about -6 dBm and the signal level of W7 is about 5 dBm, which has about 11 dB difference. This dynamic range is usually acceptable by most of the receivers. The worst SNR among these five signal is about 20 dB (W1) which is adequate for 2.5 Gbit/s or higher transmission. Other worst possible cases is in the node 3 and node 5 where the wavelength W3 and W5 which have worst SNR is going to be dropped after passing cascaded EDFAs in the working path respectively. Figure 5.28 shows the signal profile in node 3 where the W3 has the worst SNR. Figure 5.29 shows the signal profile in node 5 where the W5 is going to be dropped. Both worst

SNRd (W3 in Figure 5.28 and W5 in Figure 5.29) are showing better than 22 dB.

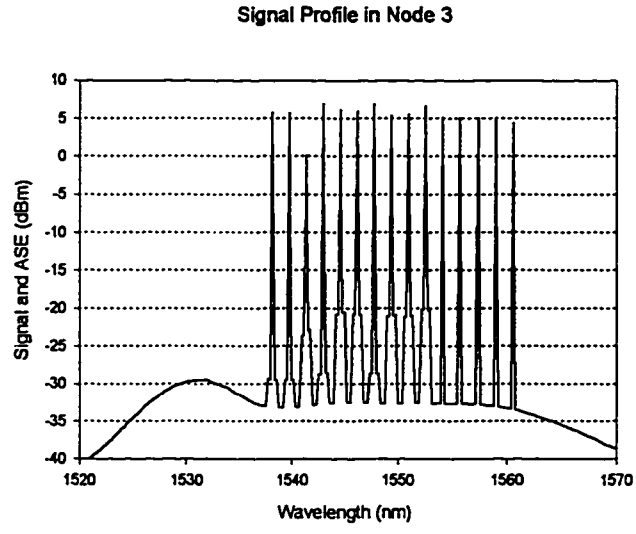

Figure 5.28, Signal Profile in Node 3 Before Dropping

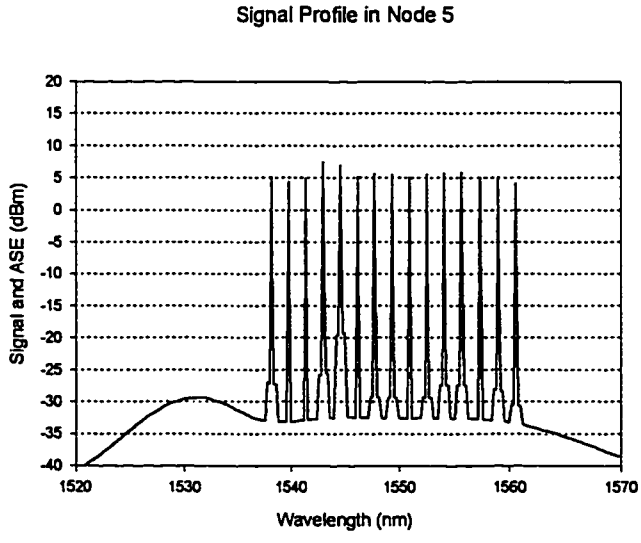

Figure 5.29, Signal Profile in Node 5 Before Dropping

By simply insert a notch filter in the EDFA of the protection path, we can filter out the 1530-nm ASE peak and improve the signal SNR and average signal gain. Figure 5.29 shows the signal profile after last EDFA on the protection path. Comparing Figure 5.27 and Figure 5.30, we can see that the average signal level increased about 3 dB and SNR increased about 5 dB when the ASE is filter out of the EDFAs in the protection path.

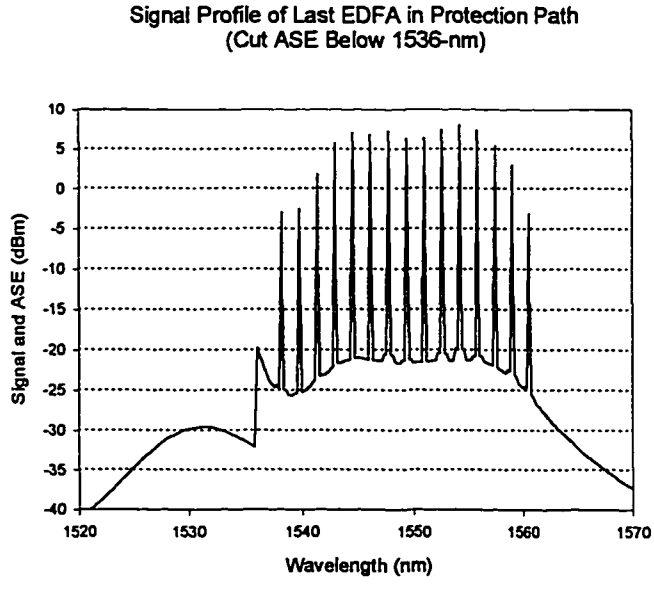

Figure 5.30, Signal Profile after Last EDFA in Protection
With ASE Cut Below 1536-nm

Figure 5.31 and Figure 5.32 show the signal profile in the node 3 and node 5 respectively. The worst SNR, W3 and W5 in node 3 and node 5 respectively, shows a 3 dB improvement of SNR comparing to the same wavelengths in Figure 5.29 and Figure 5.30. The SNR of W3 in node 3 is better than 25 dB and the SNR of W5 in node 5 is better than 31 dB. Both SNRs are more than enough for the 10 Gbit/s transmission.

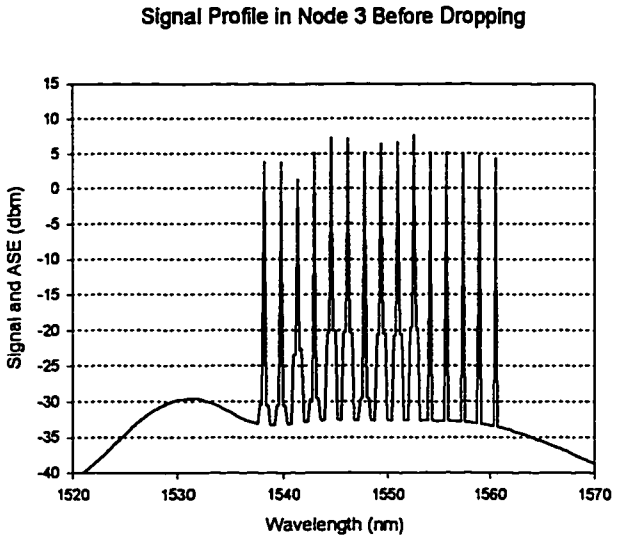

Figure 5.31, Signal Profile in Node 3 Before Dropping
Wavelength W3 shows a 25 dB of SNR

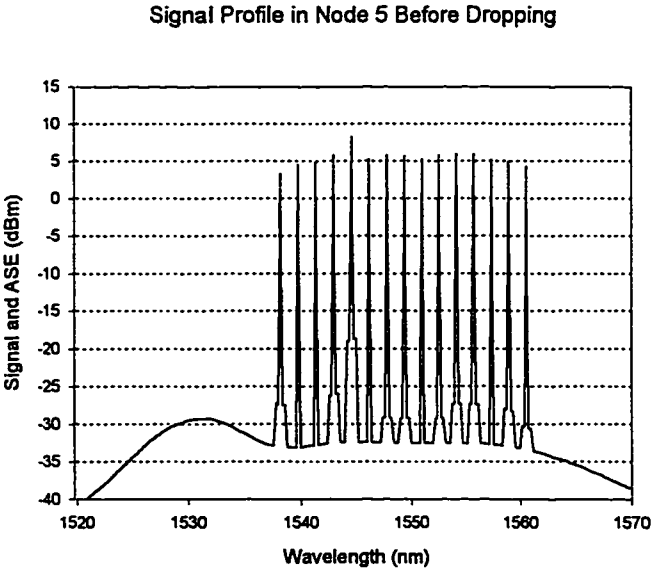

Figure 5.32, Signal and Profile in Node 5 Before Dropping
Wavelength W5 shows a 31 dB of SNR

Chapter 6

SUMMARY

This thesis investigates self-healing ring networks that utilize WDM technology, all-optical Add-and-Drop Multiplexers (ADMs) and all-optical protection ring using EDFAs and optical switches, to provide survivable transport in the local-exchange network layer. Specifically, we have analyzed and assessed two WDM schemes of self-healing ring architectures: 2-fiber uni-directional line path switched and line switched rings and 4-fiber bi-directional line switched rings. Both types of WDM ring can be designed to be consistent with present SONET standards, allowing graceful upgrades from electronic SONET rings to WDM SONET rings.

Through computer simulation and modeling, the performance of optimized EDFA and their applications in the 2-fiber and 4-fiber ring networks have been studied. A flexible, powerful computer modeling tool for design, optimizing and evaluating the end-and-end performance of ring architectures has been developed.

The general network design is given by this thesis research work and the network design, implementation and performance analysis are discussed in detail. It has shown that the erbium-doped fiber amplifier (EDFA) is the most important device to achieve the overall network performance such as signal gain variation, signal to noise ratio, etc. It has been demonstrated that by the EDFA optimization one can obviate or simplify the use of external gain equalization. A completed method for the EDFA design, optimization for the application in the ring network is developed.

Different node size of self-healing ring using EDFA and optical Add and Drop multiplexers are assessed. The most challenging issue is for a large size ring network, which not only the number of wavelength required for connection the ring is increased, therefore, occupying a wider bandwidth, but also the number of cascaded EDFA are increased for the self-healing protection path.

A 21-node uni-directional path switched self-healing ring with an aggregate capacity of 210 Gbit/s (assuming 10 G/s SONET ADMs are used) has been designed without using any external device to balance the gain flatness. An 11-node full mesh connection bi-directional line switched self-healing ring with an aggregate capacity of 825 Gbit/s has also been designed and assessed. The signals quality has also been assessed in each node for either drop and pass according to the unique wavelength assignment. The average signal to noise ratio of better than 25 dB with a gain variation less than 5 dB have been achieved without use any external gain variation devices.

This work has also provided the guidelines and benchmark for the telecommunication industry to design and deploy next generation of WDM ring networks for the emerging local exchange high-capacity broadband services.

References:

1. G. R. Hill, et al., " A Transport Network Layer Based on Optical Network Elements", J. of Lightwave Techno. 11, pp. 667, 1993.
2. C. A. Brackett, A. S. Acampora, J. Sweitzer, G. Tangonan, M. T. Smith, W. Lennon, K. C. Wang and R. H. Hobbs, "A scalable multiwavelength multihop optical network: A proposal for research on all-optical network," J. Lightwave Tech. , Vol. 11, pp. 736-753, May/June 1993
3. Stephen B. Alexander, "A Precompetitive Consortium on Wide-Band All Optical Networks", J. Lightwave Techno. Vol. 11, No. 5/6, May/June 1993.
4. R. E. Wagner, R. C. Alferness, A. A. M. Saleh, and M. S. Goodman, "MONET: Multiwavelength Optical Networking," J. Lightwave Tech. Vol. 14, No. 6, June, 1996, pp. 1349
5. G. K. Chang, et al. "Multiwavelength Recofigurable WDM/ATM/ SONET Network Testbed", J. Lightwave Techno. ,Vol. 14. No. 6, June 1996
6. T. Koai, ICC '94, Paper 331.4, New Orleans, May 1-3, 1994A.
7. W. J. Tomlinson and R. E. Wagner, NFOEC '93, paper 19.4 San Antonio, June 13-17, 1994.F.
8. R. J. Mears, L. Reekie, I. M. Jauncey, and D. N. Payne, "Low-threshold, tunable cw and Q-switched fiber laser operating at 1.55 mm," Electron. Lett., vol 22, no 3, 159, 1986
9. Elrefaie, ICC '93, paper 48.7, Geneva, May 23-26 1993.K.
10. E. Almston, et al., "A Uni-Directional Self-Healing Ring Using WDM Technique", 5th OEC '94, invited paper 13C1-4.
11. R. E. Wagner, et al., "Survivable WDM Rings for Interoffice Networks", 5th OEC '94, invited paper 14C3-1.

12. Charles A. Brackett, "Dense Wavelength Division Multiplexing Networks: Principles and Applications," IEEE J. SAC, vol. 8, no. 6, August 1990

13. Charles A. Brackett, ed., "Special Issue on Lightwave Systems and Components," IEEE Commun. Mag., vol. 27, no. 10, October 1989

14. A. F. Elrefaie, "Self-Healing WDM Ring Network with an All -Optical Protection Path," OFC '92, ThL3

15. S. S. Wagner and T. E. Chapuran, "Multiwavelength Ring Network for Switch Consolidation and Interconnection," IEEE ICC 92

16. M. S. Goodman, H. Kobrinski, and K. W. Lo. "The LAMBDANET Multiwavelength Network: Architecture, Applications and Demonstrations." IEEE Journal on Selected Area in Communications, 8(6), August 1990

17. N. Dono, P. E. Green, et al, "A Wavelength Division Multiple Access Network for Computer Communication." IEEE J. of Selected Area in Communications, 8(6), August 1990

18. S. B. Alexander et al. "A Precompetitive Consortium on Wide-band All Optical Networks." IEEE/OSA J. of Lightwave Techno. 11 (5/6), May/June 1993

19. Curtis A. Siller, M. Shafi, editor, "Synchronous Optical Network/Synchronous Dignal Hierachy: An Overview of Synchrouns Networking," pp. 1-16, IEEE Press, 1996.

20. T.-H. Wu, D. J. Kolar, R. H. Cardwell, "Survi[illegible]e Network Architectures for Broadband Fiber Optical Netwo[illegible]s: Model ad Performance Comparison," J. of Lightwave Techno., Vol. 6, No. 11, pp. 1698-1709, Nov. 1988

21. T.-H. Wu, D. J. Kolar, R. H. Cardwell, "High-speed self-healing ring architecture for future interoffice networks," IEEE GLOBECOM '89, Nov. 1989, pp. 23.1.1-23.1.7

22. Emmanuel Desurvire, "Erbium-Doped Fiber Amplifers, Principles and Applications," John Wiley & Sons, Inc. 1994

23. Anders Bjarklev, "Rare-Earth-Doped Fiber Amplifier for Optical Communication System," thesis for the degree of Doctor Technices, Technical University of Demark, 1995

24. C. Randy Giles, Emmanuel Desurvire, "Modeling Erbium-Doped Fiber Amplifiers", JLT, Vol. 9, No. 2, Feb. 1991

25. P. R. Morkel and R. I. Laming, "Theoretical modeling of erbium-doped fiber amplifiers with excited-state absorption," Opt. Lett., 14, 99. 1062-1064, 1989

26. Emmanuel Desurvire, J. R. Simpson, "Amplification of spontaneous emssion in erbium-doped single-mode fibers," IEEE J. Lightwave Techno., 7, pp. 835-845, 1989

27. C. R. Giles, C. A. Burrus, D. J. DiGiovanni, N. K. Dutta, and G. Raybon, "Characterization of Erbium-Doped Fibers and Application to Modeling 980-nm and 1480-nm Pumped Amplifers," IEEE, Photon. Techno. Lett. Vol. 3, No. 4, April, 1991

28. C. R. Giles, E. Desurvire, and J. R. Simpson, "Transient gain and cross talk in erbium-doped fiber amplifiers," Opt. Lett. Vol. 14, pp. 880-882, 1989

29. R. I. Laming, L. Reekie, P. R. Morkel, and D. N. Payne, "Multichannel crosstalk and pump noise characterization of Er^{3+}-doped fiber amplifier pumped at 980 nm," Electron. Lett., Vol. 25, pp. 455-456, 1989

30. A. A. M. Saleh, R. M. Jopson, J. D. Evankow, and J. Aspell, "Modeling of gian in erbium-doped fiber amplification," IEEE Photon. Technol. Lett., Oct. 1990

31. E. L. Goldstein, "Multiwavelength Fiber-Amplifier cascade for Networks," OFC' 94, TuI 4, pp. 39.

32. Tien-Pei Lee, Chung E. Zah, R. Bhat, W. C. Young, B. Pathak, F. Favire, Paul S. D. Lin, Nicholas C. Andreadakis, C. Canueau, Andrew W. Rahjel, et al, "Multiwavelength DFB Laser Array Transmitters for ONTC Reconfigurable Optical Network Testbed," J. of Lightwave Tech. Vol. 14, No. 6, June 1996

33. M. A. Ali, A. F. Elrefaie, R. E. Wagner, F. Mendez, Jin-Yi Pan, S. A. Ahmed, "Optimized Performance of Erbium-Doped Fiber Amplifiers in Multiwavelength Lightwave System," IEEE Photon. Techno. Lett. Vol. 6, No. 8, August 1994

34. Same as [22], pp. 207-303, 343-354

35. Same as [22], pp. 346

36. W. Rahjel, et al, "Multiwavelength DFB Laser Array Transmitter for ONTC Reconfigurable Optical Testbed," J. of Lightwave Tech. Vol. 14, No. 6, June 1996

37. Chung E. Zah, B. Pathak, M. R. Amersfoort, F. Favire, P. S. d. Lin, N. C. Andreadakis, A. Rajhel, R. Bhat, C. Caneau, and M. A. Koza, L. Cutis, "High Power 10-wavelength DFB Laser Arrays with Integrated Combiner and Optical Amplifier," 15th IEEE International Semiconductor Laser Conference, Haifa, Israel, October, 13-18, 1996

38. F. Shehadeh, R. Vodhanel, C. Gibbson, R. E. Wagner, and M. A. Ali, "Gain Equalized, eight wavelength WDM optical Add-Drop

Multiplexer with 8 dB dynamic range," OFC 95, Technical digest series, Vol. 8, paper TuH2, PP. 29-30.

39. M. A. Scobey, d. E. Spock, "Passive DWDM components using MicroPlasm® optical Interference filters," OFC '96, ThK1

40. Same as [22], pp. 354

41. J. L. Zyskind, R. G. Smart, D. J. DiGiovanni, "Two-stage EDFAs with Counterpumped First Stage Suitable for Long-Haul Soliton System," OFC '94, paper WK8, Feb. 1994

42. R. Welter, R. Laming, W. Sessa, R. Vodhanel, and R. E. Wagner, "Performance of EDFA in 16-channel coherent broadcast Network," Electron. Lett., vol. 25, pp. 1333-1335, 1989.

43. Dietrich Marcuse, "Derivation of analytical expressions for the bit-error probability in lightwave systems with optical amplifiers," J. Lightwave Technol., Vol. 8, No, 12, pp. 1816-1823, 1990.

44. M. A. Ali, A. Elrefaie, R. Wagner, and S. Ahmed,"Performance of EDFA Cascades in WDM Multiple access Lightwave Networks," IEEE, Phot. Tech. Lett., Vol. 6, PP. 1142-1145, Sep. 1994.

45. D. Bayart, B. Clesca, L. Hamon, and J. L. Beylat, "Experimental investigation of the gain flatness characteristics for 1.55 mm Erbium-doped Fluoride fiber amplifiers," IEEE, Phot. Tech. Lett., Vol. 6, No. 5, PP. 613-615, May 1994.

46. E. L. Goldstein, L. Eskildsen, C. Lin, and R. E. Tench "Multiwavelength propagation in lightwave systems with strongly inverted fiber amplifiers," IEEE, Phot. Tech. Lett., Vol. 6, No. 2, PP. 266-2269, Feb. 1994.

47. B. Clesca, D. Bayart, and J. L. Beylat, "1.5-mm Fluoride fiber amplifiers for wideband multichannel transport networks," Optical Fiber Technology, Vol. 1, no. 2, pp. 135-157, 1995.

48. Jin-Yi Pan, A. Elrefaie, R. E. Wagner, and M. A. Ali,"Fiber-amplifier cascades with Equalization employing Mach-Zehnder optical filters in multiwavelength Systems," Topical Meeting in Optical Amplifiers and their applications, Brecknridghe, Colorado, paper FA3 PP. 114-116, 1994.

49. K. Inoue, T. Kominato, and H. Toba, "Tunable Gain Equalization Using a Mach-Zehnder Optical Filter in Multistage Fiber Amplifiers," IEEE Photon. Tech. Lett., vol 3, no. 8, pp. 718-720, 1991.

50. S. -K Liaw, and Y. -K. Chen, "Passive Gain-Equalized Wide-Band Erbium-Doped Fiber Amplifier Using Samarium-Doped Fiber," IEEE Photo. Tech. Lett. Vol. 8, No. 7, July 1996

51. B. Clesca, D. Bayart, C. Caurjolly, L. Berthelon, L. Hamon, J. L. Beylet, "Over 25-nm, 16 Wavelength-Multiplexed Signal Transmission Through Four Fluride-Based Fiber-Amplifier Cascade and 440 km Standard Fiber," OFC '94, PD20-1

52. Jin-Yi Pan, et al, "Multiwavelength Fiber-Amplifier Cascades with Equalization Employing Mach-Zehnder Optical Filter," IEEE PTL., Vol 7, No. 12, Dec. 1995

53. A. F. Elrefaie, E. L. Goldstein, S. Zaidi, " Fiber-Amplifier Cascades with gain equalization in multiwavelength unidirectional inter-office ring Networks." IEEE PTL., Vol. 5, PP. 1026 -1028, 1993.

54. A. Elrefaie, M. A. Ali, R. E. Wagner, J. Pan, and F. Mendez, "Fiber-amplifier cascades in 4-fiber multiwavelength Interoffice Ring Networks," LEOS Summer Topical Meeting Digest on Optical

Networks and their enabling technologies, T1.3, PP. 31-32, Lake Tahoe, NV, 1994